HYDROGEOLOGY AND FLOW OF WATER IN A SAND AND GRAVEL AQUIFER CONTAMINATED BY WOOD-PRESERVING COMPOUNDS, PENSACOLA, FLORIDA

By Bernard J. Franks

U.S. GEOLOGICAL SURVEY

Water-Resources Investigations Report 87-4260

Tallahassee, Florida

1988

DEPARTMENT OF THE INTERIOR
DONALD PAUL HODEL, Secretary

U.S. GEOLOGICAL SURVEY
Dallas L. Peck, Director

For additional information write to:

District Chief
U.S. Geological Survey
Suite 3015
227 North Bronough Street
Tallahassee, Florida 32301

Copies of this report can be purchased from:

U.S. Geological Survey
Books and Open-File Reports Section
Federal Center, Bldg. 810
Box 25425
Denver, Colorado 80225

CONTENTS

ILLUSTRATIONS

TABLES

CONVERSION FACTORS AND ABBREVIATIONS

For use of readers who prefer to use inch-pound units, conversion factors for metric (International System) units used in this report are listed below:

Multiply metric unit	By	To obtain inch-pound unit
centimeter (cm)	0.3937	inch (in.)
meter (m)	3.281	foot(ft)
square meter (m^2)	10.764	square foot (ft^2)
hectare (ha)	2.469	acre
cubic meter (m^3)	0.0008107	acre-foot (acre-ft)
	264.2	gallon (gal)
liter (L)	0.2642	gallon (gal)
kilometer (km)	0.6214	mile (mi)
gram	0.0022	pound (lb)
meter per meter (m/m)	1.0	foot per foot (ft/ft)
milligram per liter (mg/L)	1.0	parts per milliom (ppm)
centimeter per year (cm/yr)	0.0328	inch per year (in/yr)
meter per day (m/d)	3.281	foot per day (ft/d)
square meter per day (m^2/d)	10.764	square foot per day (ft^2/d)
cubic meter per second (m^3/s)	35.31	cubic foot per second (ft^3/s)
cubic meter per day (m^3/d)	264.2	gallon per day (gal/d)
meter per day per meter ((m/d)/m)	1.0000	foot per day per foot ((ft/d)/ft)

Temperatures are converted from degrees Celsius (°C) to degrees Fahrenheit (°F) by the formula °F = 1.8x°C + 32.

ADDITIONAL ABBREVIATIONS

PCP	pentachlorophenol
USEPA	U.S. Environmental Protection Agency
FDER	Florida Department of Environmental Regulation
ROD	Record of Decision
GPR	ground-penetrating radar

Sea level: In this report "sea level" refers to the National Geodetic Vertical Datum of 1929 (NGVD of 1929) – A geodetic datum derived from a general adjustment of the first-order level nets of both the United States and Canada, formerly called "Mean Sea Level of 1929."

HYDROGEOLOGY AND FLOW OF WATER IN A SAND AND GRAVEL AQUIFER CONTAMINATED BY WOOD-PRESERVING COMPOUNDS, PENSACOLA, FLORIDA

By Bernard J. Franks

ABSTRACT

The sand and gravel aquifer in southern Escambia County, Florida, is a typical surficial aquifer composed of quartz sands and gravels interbedded locally with silts and clays. Problems of ground-water contamination from leaking surface impoundments are common in surficial aquifers and are a subject of increasing concern and attention. A potentially widespread contamination problem involves organic chemicals from wood-preserving processes. Because creosote is the most extensively used industrial preservative in the United States, an abandoned wood-treatment plant near Pensacola was chosen for investigation.

This report describes the hydrogeology and ground-water flow system of the sand and gravel aquifer near the plant. Recharge occurs predominantly in the northern part of the study area, while discharge occurs along the coast and to Pensacola Bay. The movement of water is generally from north to south. In the study area, the sand and gravel aquifer, about 100 meters thick, consists of three permeable zones separated by confining units. A three-dimensional simulation of ground-water flow in the aquifer was evaluated under steady-state conditions. The aquifer was treated as multilayered and horizontally isotropic, with water moving only horizontally within layers, and only vertically between layers. Input to the model consisted of recharge (28 centimeters per year), hydraulic conductivity (0.3–23 meters per day), vertical hydraulic conductivity between layers ($1x10^{-3}$–$9x10^{-3}$ meters per day), and boundary inflow ($2.6x10^4$ cubic meters per day total) from north of the model area. Model outflows include discharge to constant head boundaries and to active municipal wells. The model was calibrated for assumed steady-state conditions on the basis of water levels measured in January 1986. Calibration criteria included reproducing all water levels within the accuracy of the data – to within one-half contour interval in most cases. Sensitivity analysis showed that the simulations were most sensitive to recharge and vertical leakance of the confining units between layers 1 and 2, and relatively insensitive to changes in hydraulic conductivity and transmissivity and to other changes in vertical leakance. Applications of the results of the calibrated flow model in evaluation of solute transport may require further discretization of the contaminated area, including more sublayers, than were needed for calibration of the ground-water flow system itself.

INTRODUCTION

Ground-water contamination has been the focus of increasing public attention during the past decade. Contaminants in ground water are frequently associated with adverse environmental and health effects, as well as social and economic effects. Although contaminants can enter ground-water systems along diverse and complex pathways (production, transport, storage, disposal), one common source of ground-water contamination is a leaking surface impoundment.

Contaminants commonly stored in potentially leaky impoundments include organic chemicals from wood-preservative processes. Creosote, a complex distillate of coal tar, is the most extensively used industrial wood preservative in the United States (von Rumker and others, 1975). It is estimated that there are more than 400 commercial wood-preserving plants in the United States, many of which discharge their wastes to onsite impoundments, which in turn discharge into an underlying surficial aquifer. Because of its complex chemical composition, which consists of some 200 "major" constituents and several thousand "minor" components (U.S. Department of Agriculture, 1981), creosote is difficult to characterize chemically. It is heavier than water and has a continuous boiling range of at least 125 °C, beginning at about 200 °C. It is, by weight, composed of about 85 percent polynuclear aromatic compounds, 12 percent phenolic compounds, and 3 percent heterocyclic nitrogen, oxygen, and sulfur compounds.

Because of the increasing need to quantify the potential effects of toxic compounds on ground-water systems, the U.S. Geological Survey began the Toxic Waste – Ground-Water Contamination Program in 1983. One of the primary components of this program consists of an interdisciplinary investigation of the physical, chemical, and microbiological processes that affect contaminant transport in the subsurface environment (Ragone, in press). The wide distribution of the wood-preserving industry led to the selection of a wood-preserving operation as one of the initial sites in the Toxic Waste – Ground-Water Contamination Program.

In 1983, a site near Pensacola, Fla., was selected as one of three national research demonstration areas to enhance our understanding of hydrologic processes affecting the distributions of contaminants in ground water. The site was selected because of its long, uninterrupted history (1902–81) of discharging wastewaters to unlined surface impoundments, availability of a preliminary data base (Troutman and others, 1984), and the probability of transferring useful technology from an investigation of organic compounds associated with wood-preserving wastewaters.

Purpose and Scope

The purpose of this report is to describe the hydrogeology and the ground-water flow system of the sand and gravel aquifer in the vicinity of the site area. This knowledge is needed to evaluate geochemical and microbial data in relation to solute transport in the aquifer. The scope of this report includes:

- a site description and history,
- a review of existing hydrogeologic data from the site and the surrounding area,
- a documentation of hydrogeologic data collected during this investigation, and
- a presentation of a synthesis of the above data through documentation of a three-dimensional simulation of ground-water flow in the sand and gravel aquifer.

This report does not discuss contaminant plume definitions or other geochemical data collected during investigations of the site. Preliminary assessments of the initial geochemical data have been discussed in Mattraw and Franks (1986), Franks, (1987), and Ragone (in press). Ongoing investigations are evaluating the geochemistry of the site and relating the hydrogeology and ground-water flow system to the geochemistry.

Area of Investigation

The large study area used by Trapp and Geiger (1986) and referred to later in this report is shown in figure 1. Within that large study area is the area of investigation of this report. It is located in southern Escambia County, Fla., in and adjacent to the city of Pensacola (fig. 1) and contains a subarea of about 1,200 m (meters) by 1,000 m (fig. 2), including the former wood-preserving plant property and the adjoining area of contamination, referred to as the "site" in this report. To adequately simulate ground-water flow in and near the site, it was necessary to evaluate the hydrogeology of the entire area of investigation of this report in order to account for significant geologic variations and hydrologic boundaries.

Site Description and History

Between 1902 and 1981, a wood-preserving plant was operated on a 7.3 ha (hectares) site in a moderately dense, commercial and residential area of Pensacola. The area of the former plant is located about 500 m north of Pensacola Bay and Bayou Chico and is bounded on the east and west, respectively, by "F" and "L" Streets. The wood-treatment process used throughout plant history included mechanical debarking of logs (feeding the bark to a boiler for steam production), air drying, and then steam-heating the poles to burst the wood cells. A vacuum was then applied to remove the remaining cellular moisture. The pressure cylinder was then filled with preservative and the poles treated for several hours. Pressure was released, excess liquid pumped from the chamber, and the poles removed to an outside area for storage.

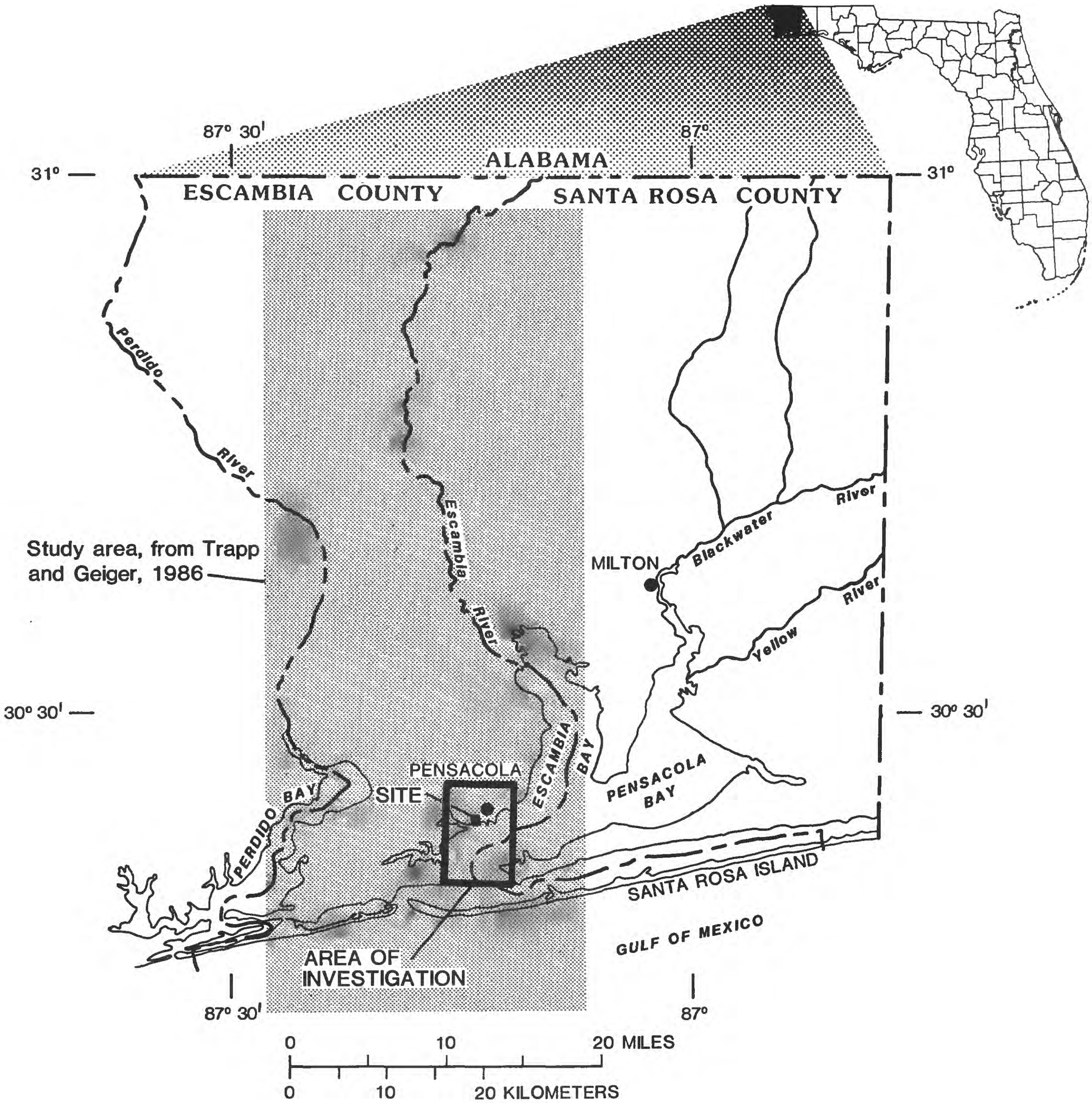

Figure 1.–Location of area of investigation.

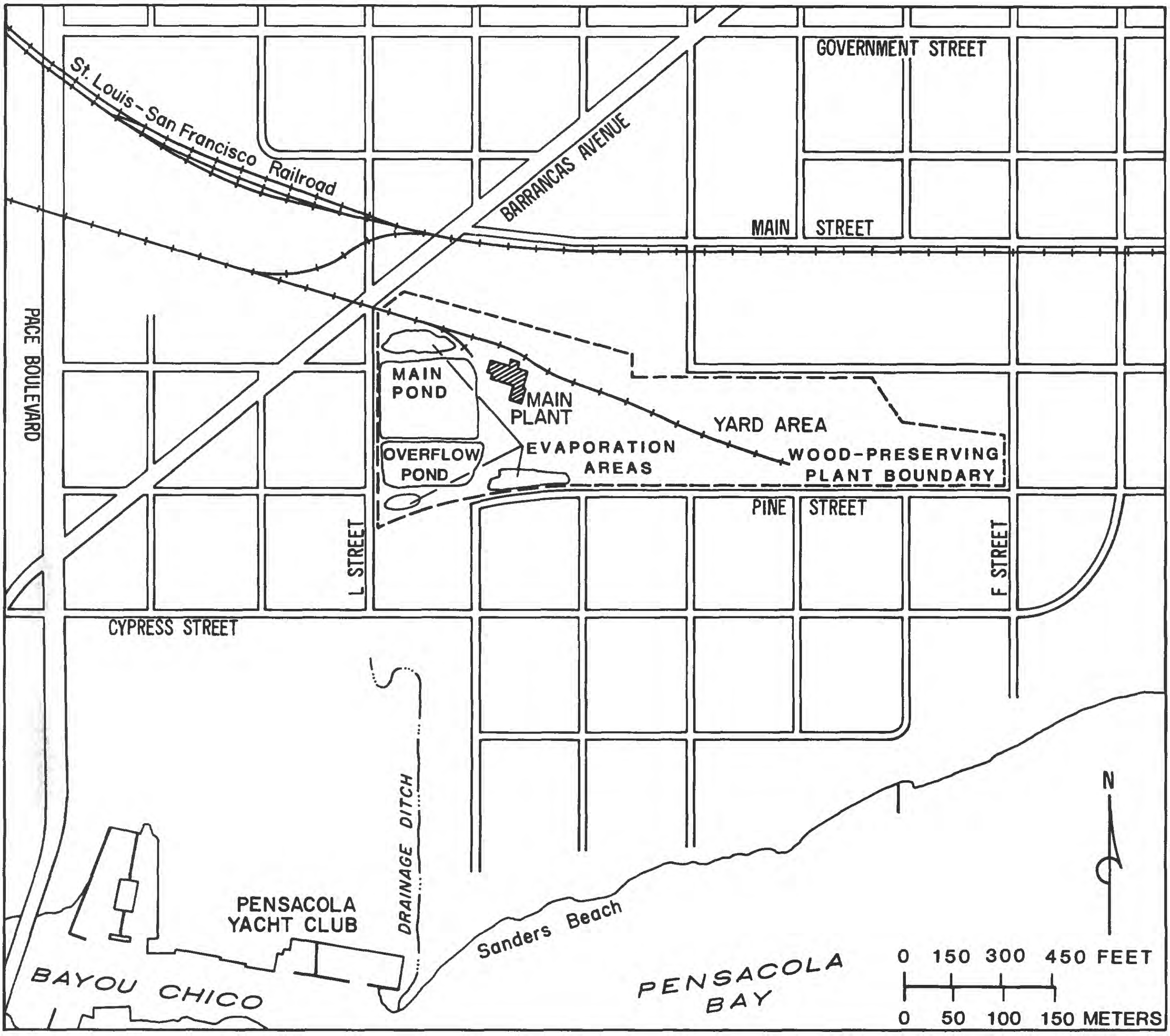

Figure 2.—Location of wood-preserving plant and site area.

The history of disposal practices of the residual liquid ("blowdown") is unclear. Figure 3 presents selected aerial photographs that were used in an attempt to partially reconstruct plant disposal history. The earliest available information is from 1940 (fig. 3a), at which time the site was relatively undeveloped, and there was no indication of a surface impoundment for disposal of residual creosote. During World War II, an extender (diesel fuel?) was added to the creosote, which was in short supply. After the war, production increased, the main pond was developed, and PCP (pentachlorophenol) began to be used as an alternate preservative, varying between 25 and 40 percent of the total preservative. The PCP solution consisted of 5 percent PCP and 95 percent diesel

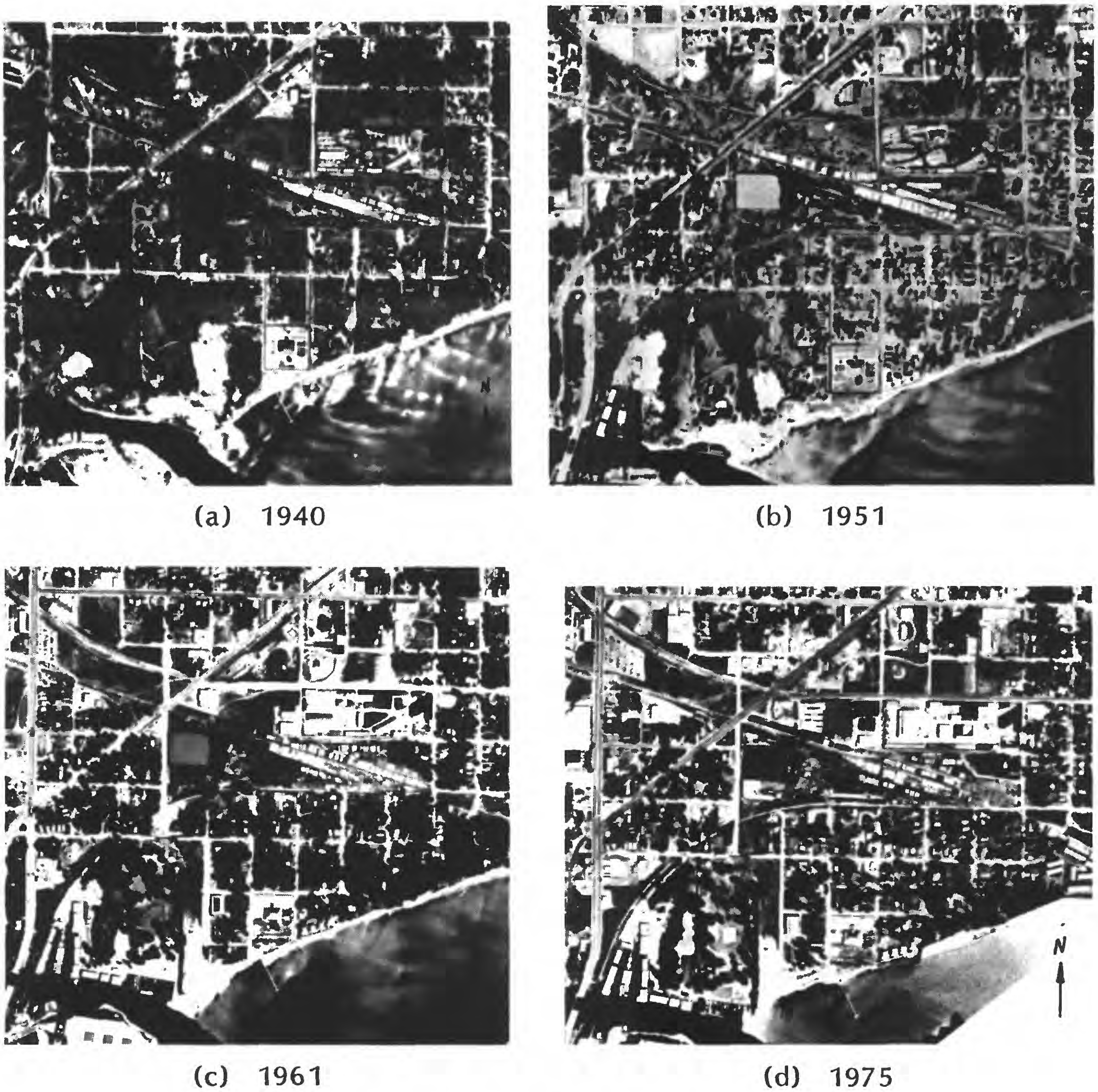

Figure 3.—Photographic history of site development.

fuel, which acted as a "carrier" to increase the penetration of the preservative into the wood fiber. By 1951, the main impoundment was fully developed (fig. 3b). It is estimated that, since 1951, approximately 13,200 L (liters) of blowdown were discharged to the impoundment each week (C.E. Brown, American Creosote Works, written commun., 1984).

During the early years of plant operation, wastewaters were allowed to discharge naturally through a spillway and to follow natural drainage into Pensacola Bay and Bayou Chico. Throughout the 1950's and 1960's, water in the impoundments would overtop the containment dikes during periods of heavy rainfall and follow these same natural drains. In an attempt to eliminate overland flow, wastewaters were periodically drawn from the ponds during times of high water level and discharged to three designated "evaporation areas" on the plant property (fig. 2). Excess water was also allowed to flow from the main pond to an "overflow" pond, constructed sometime prior to 1961 (fig. 3c). Also during this period, the natural drainage was partially modified by construction of a stormwater outfall and dredging of a drainage ditch about 180 m south of the overflow pond.

Figure 3d shows the site as it appeared in 1975 and for most of the period between 1962 and 1981. The main pond occupied 7,700 m^2 (square meters) and held 9,400 m^3 (cubic meters) of liquid on average. The overflow pond occupied 3,200 m^2 and held 4,000 m^3 of liquid. Both impoundments were built up with clay embankments about 1.2 m high. The bottoms of the ponds were filled with 0.6 to 1.2 m of oils and sludge, including materials scraped from the pressure cylinder walls and disposed of in the ponds. Although construction data for the ponds are limited, it is believed that the ponds were dug only slightly (0.3–0.6 m) below land surface, with most of the liquid held above land surface by the embankments.

Despite periodic buildup of the clay embankments, overtopping of the ponds has occurred occasionally during the past 20 years. Several such events have been recorded in the files of the Florida Department of Environmental Regulation (FDER), one each in the summer of 1978, March 1979, and March 1980 (Camp, Dresser, and McKee, Inc., 1983). As a result, in March 1981, the FDER entered into a Consent Order with the company. Unable to meet the requirements of the Consent Order, the plant ceased operating in late 1981 and the company filed for reorganizational bankruptcy in May 1982.

In 1982, the site was included on the Federal "Superfund" list of hazardous waste sites. The U.S. Environmental Protection Agency (USEPA) completed an initial field investigation (U.S. Environmental Protection Agency, 1983) and contracted a Remedial Investigation and Feasibility Study to determine the possible impact of the site on the environment and on public health, and to develop a series of viable remedial action alternatives (NUS Corporation, 1984; 1985). Because of the public health threat from overtopping of the ponds, the USEPA Region IV Emergency Response Team performed an emergency cleanup at the site in September 1983. The two onsite impoundments were drained and the liquids treated by a portable treatment facility set up adjacent to the site. The remaining sludges in the bottoms of the ponds were then flocculated with a mixture of "fly ash" and limedust and covered with a temporary clay cap, which has since been sodded and planted with grass seed. A fence and warning signs were also installed to restrict access to the site.

As of June 1986, a formal Record of Decision (ROD) had not yet been signed. The ROD will propose the preferred remedial alternative, as agreed on by the USEPA and the FDER. Because all available technologies have not yet been fully evaluated, no decision is expected until the screening process is completed (Ecology and Environment, Inc., 1986).

Ackowledgments

The continuing assistance and cooperation of many individuals and organizations has greatly assisted this investigation. Thanks are due to all the owners of property near the plant site, with special thanks to the members of the Pensacola Yacht Club for their frequent assistance and interest throughout this investigation. Also, numerous personnel of the Florida Department of Environmental Regulation, including Richard Singer and William Kellenberger, have contributed to discussions regarding the site. James Barksdale and John Mann of the U.S. Environmental Protection Agency, and personnel of the NUS Corporation (especially Robert Marks), have been instrumental in planning and coordinating our investigations of the site. Ken Evans of the Escambia County Utilities Authority made available lithologic and water-use data on the sand and gravel aquifer. Keith Wilkins and Jeffry Wagner of the Northwest Florida Water Management District provided access to relevant wells and hydrogeologic data. Most of the wells and test holes were constructed by a drilling team led by Lewis Burgess, which included Thomas Turner, Michael Orr, Barry Levine, Richard Orr, and Paul Messer. Computer assistance has been provided by Rene Barker, Stan Leake, and Donald Foose. Particular thanks are due Richard Milner, David Hunn, and J.B. Martin for their major contributions to the project, including assistance in the preparation of this report.

HYDROGEOLOGY

Geologic Framework

The site is underlain to about 90 m by surficial deposits ranging in age from middle Miocene through Holocene (fig. 4). These deposits constitute the sand and gravel aquifer, the source of water supply for the city of Pensacola and the westernmost Florida Panhandle. The geology of these deposits was initially characterized by Matson and Sanford (1913). Marsh (1966) and Barraclough (1967) further detailed the geology of the western panhandle.

The sand and gravel aquifer consists of nonhomogeneous fine-to-coarse grained, locally well-sorted fluvial and deltaic sediments. The dominantly quartz sands and gravels are interbedded locally with discontinuous silt and clay lenses. As reported by Musgrove and others (1961) and Barraclough and Marsh (1962), abrupt facies changes are characteristic of the aquifer.

The top of the sand and gravel aquifer is coincident with land surface, with altitudes ranging from sea level near the coast to about 60 m above sea level in northern Escambia County. In the area of investigation, the top of the aquifer ranges from sea level to about 30 m above sea level. The base of the aquifer in northern Escambia County is coincident with the underlying Floridan aquifer system at an altitude of about 150 m below sea level; in the area of investigation, the base is defined by the top of the Pensacola Clay at an altitude of about 90 m below sea level.

Table 1 summarizes all the well construction data, including comments on available hydrologic and geophysical data. All wells are identified, as appropriate, in either a site map (fig. 5) or an area of investigation map (fig. 6), or in figure 7 which includes locations of five geologic cross sections. The cross sections are presented in figures 8–12. The sections show an assemblage of nonhomogeneous sedimentary deposits. The north-

Series	Stratigraphic unit		Lithology	Principal hydrogeologic units		Thickness (meters)	Equivalent units in digital model
Holocene and Pleistocene	Alluvium and terrace deposits.		Undifferentiated silt, sand, and gravel, with some clay.	Water-table zone	Sand and gravel aquifer	6-15	Layer 1
Pliocene	Citronelle Formation		Sand, very fine to very coarse and poorly sorted. Hardpan layers in upper part. Fossils scarce.	Discontinuous semiconfining unit		0-6	
Miocene	Unnamed coarse clastics	Choctawhatchee Formation	Sand, shell, and marl. Fossil-bearing.	Intermediate zone		18-27	Layer 2
		Alum Bluff Group (Shoal River Formation and Chipola Formation)	Fossiliferous sand with lenses of silt, clay, and gravel (includes unnamed coarse clastics and Alum Bluff Group). The clay is extensive in the southern part of Escambia County, acting as a semiconfining unit above the main producing zone.	Confining clay unit		0-9	
				Main producing zone		30-50	Layer 3
	Pensacola Clay		Dark-to-light gray sandy clay. Pensacola Clay stratigraphic unit is the base of water-bearing zone in area of investigation.	Confining unit		75-100	Lower boundary
	Tampa Limestone and equivalents		Limestone and dolomite	Top of the Floridan aquifer system			

Figure 4.—Generalized hydrogeologic column for the sand and gravel aquifer in southern Escambia County, Florida.

ernmost section, Z–Z', located slightly north of the area of investigation, most clearly suggests the subdivision of the aquifer into three, or perhaps even four, permeable layers. Section Y–Y', on the northern border of the area, is less detailed, but indicates a heterogeneous mixture of sediments, with significantly thicker shallow clay deposits in the east. Section W–W', intersecting the site area, indicates the presence of a shallow clay layer in the aquifer parallel to the coastline. The two north-south sections indicate the presence of a discontinuous, interbedded, shallow clay, as well as a fairly continuous clay 20 to 30 m below local land surface. Data on the shallow clay lens were useful in locally modifying hydraulic conductivity in the shallow layer. The deeper, continuous clay has a slight regional dip to the south, approximating the local land surface.

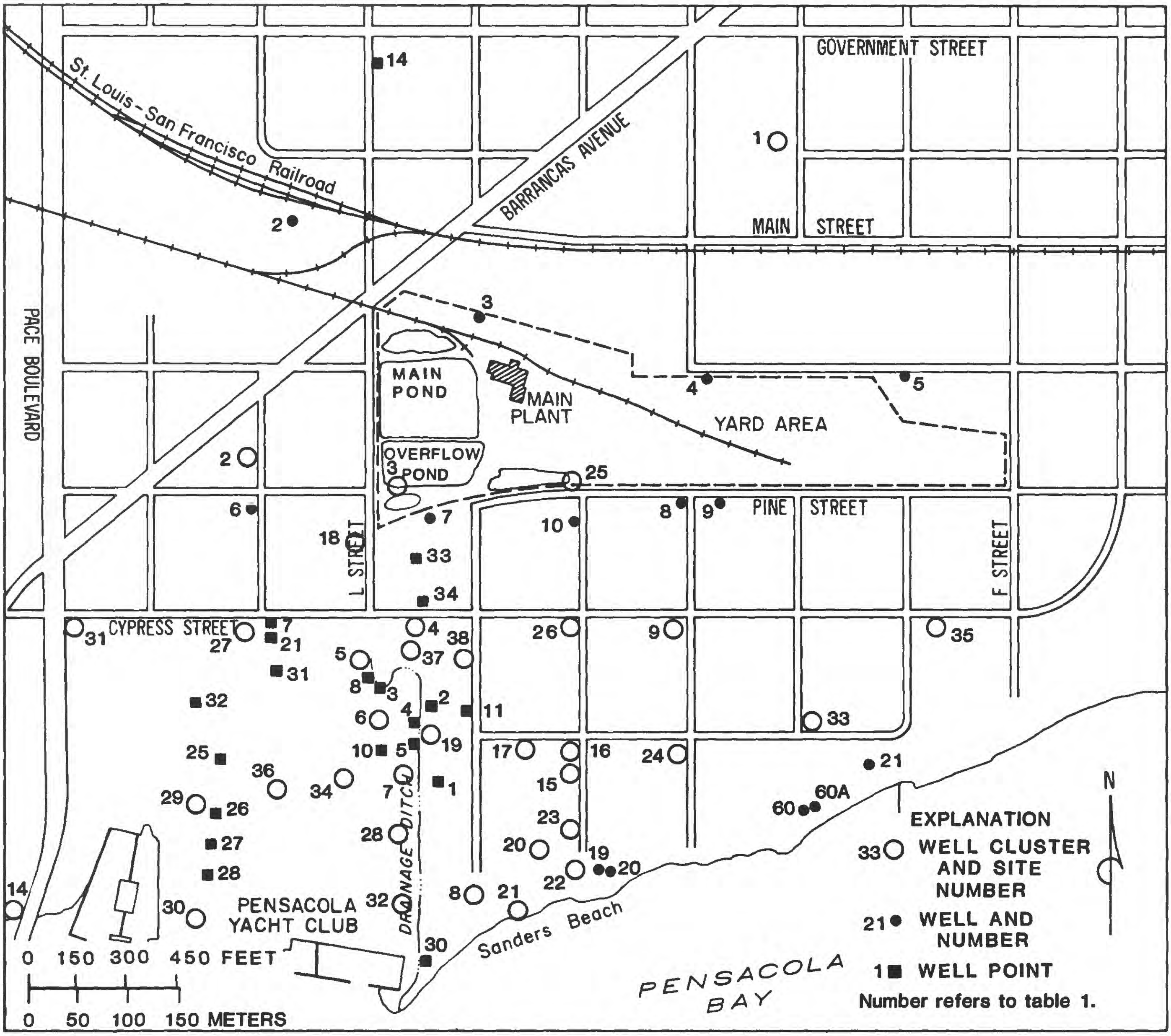

Figure 5.—Location of site, clusters of wells, wells, and well points.

Table 1.—*Well construction data, including availability of geophysical and hydrologic data*

Station ID: First six digits are latitude of well location in degrees, minutes, and seconds; next seven digits are longitude in degrees, minutes, seconds; last two digits are arbitrarily assigned to distinguish wells within a 1-second square area.

Site number: Where available, unique designation assigned to a cluster of wells.

Well number: Unique designation assigned to each well. For sites 1 through 38, the leading one or two digits refer to the site number, the last two digits refer to the approximate well depth (in feet). Well 120 is a 20-foot deep well at site 1. Well 300 is a 100-foot deep well at site 3. Wells that exceed 100 feet in depth are assigned a sequence number. Well 1402 is a 200-foot well at site 14. WP prefix = well point. Other listed designations are described in the text.

Geophysical data: G, natural gamma log; N, neutron log; D, gamma-gamma (density) log; A, acoustic velocity log; E, electric; and S, spontaneous potential.

Water-level measurement frequency: C, continuous record available; P, at least periodic (monthly) measurements; and M, less than six measurements.

Site (well cluster) No.	Well or well point (WP) No.	Station ID	Well depth, in meters	Casing diameter, in centimeters	Screen length, in meters	Land surface altitude, in meters	Geophysical data	Water-level measurements
1	100	302423087140400	30.1	5.1	1.5	4.05	G,N,D	P
1	160	302423087140401	17.7	5.1	.9	4.08		P
1	120	302423087140402	6.3	5.1	.9	4.18		P
1	199(03)	302423087140403	7.0	1.6	.15	4.13		P
1	199(04)	302423087140404	11.0	1.6	.15	4.13		P
1	199(05)	302423087140405	17.0	1.6	.15	4.13		P
1	199(06)	302423087140406	21.6	1.6	.15	4.13		P
1	199(07)	302423087140407	29.9	1.6	.15	4.13		P
1	199(08)	302423087140408	29.9	2.5	1.5	4.13		P
2	200	302415087142500	30.4	5.1	.9	3.89	G,N,D	P
2	220	302415087142501	6.5	5.1	.9	3.82		P
2	[1]260G	302415087142502	19.6	5.1	.9	3.88		P
2	260P	302415087142503	18.4	5.1	1.5	3.88		P
2	[1]260S	302415087142504	18.4	5.1	.9	3.85		P
3	300	302413087141902	29.8	2.5	.9	3.36		P
3	320	302413087141903	6.1	2.5	.9	3.44		P
3	340	302413087141904	12.1	2.5	.9	3.46		P
3	360	302413087141905	18.3	2.5	.9	3.52		P
3	380	302413087141906	23.6	2.5	.9	3.42		P
3	321	302413087141921	6.1	2.5	.3	[2]3.35		—

[1]Well permanently sealed or destroyed.

[2]Estimated from topographic map.

Table 1.—*Well construction data, including availability of geophysical and hydrologic data*—Continued

Site (well cluster) No.	Well or well point (WP) No.	Station ID	Well depth, in meters	Casing diameter, in centimeters	Screen length, in meters	Land surface altitude, in meters	Geophysical data	Water-level measurements
4	12	302408087141701	2.7	10.2	1.5	2.33		C,P
4	440	302408087141703	12.2	2.5	.9	2.36		P
4	420	302408087141704	6.3	2.5	.9	2.37		P
4	400	302408087141705	31.0	2.5	.9	2.33		P
4	480	302408087141707	24.2	2.5	.9	2.27		P
4	415	302408087141715	3.8	2.5	.3	[2]2.29		—
5	500	302407087142000	30.5	5.1	.9	2.37	G,N,D	P
5	520	302407087142001	4.6	5.1	.9	2.24		P
5	540	302407087142002	11.5	5.1	.9	2.23		P
5	560	302407087142003	18.2	5.1	.9	2.33		P
5	580	302407087142004	23.8	5.1	.9	2.36		P
6	WP8	302407087141901	2.1	2.5	.3	2.25		P
6	600	302405087142000	30.3	5.1	.9	2.49	G,N,D	P
6	620	302405087142001	6.5	5.1	.9	2.48		P
6	660	302405087142002	17.8	5.1	.9	2.44		C,P
7	700	302404087142000	30.5	5.1	.9	2.07	G,N,D	P
7	720	302404087142001	5.9	5.1	.9	2.10		P
7	760	302404087142002	19.6	5.1	.9	2.07		C,P
8	800	302400087141600	30.4	2.5	.9	1.49	G,N,D	P
8	820	302400087141601	6.6	5.1	.9	1.49		P
9	900	302407087140900	30.2	10.2	.9	3.12	G,N,D	C,P
9	920	302407087140901	6.8	2.5	.9	3.08		P
9	960	302407087140902	18.0	2.5	.9	3.09		P
10	1000	302420087144800	26.5	5.1	1.5	3.17	G,N,D	M
10	1030	302420087144801	9.1	5.1	1.5	3.75		M
11	1100	302438087135300	18.4	5.1	1.5	4.79	G,N,D	M
11	1120	302438087135301	8.5	5.1	1.5	4.85		M
12	TH104	302435087141601	62.2	5.1	1.2	6.91		P
12	1200	302435087141700	28.0	5.1	1.5	6.98	G,N,D	M
12	[1]WP13	302435087141703	3.7	2.5	.3	6.91		M
12	[1]WP19	302435087141704	5.5	2.5	.3	6.91		M
13	1380	302451087142900	24.0	5.1	1.5	6.71	G,N,D	M
13	1320	302451087142901	11.1	5.1	1.5	6.71		M
14	1400	302401087143400	33.5	5.1	1.5	.64		P
14	1420	302401087143401	7.0	5.1	1.5	.55		P

[1]Well permanently sealed or destroyed.

[2]Estimated from topographic map.

Table 1.—*Well construction data, including availability of geophysical and hydrologic data*—Continued

Site (well cluster) No.	Well or well point (WP) No.	Station ID	Well depth, in meters	Casing diameter, in centimeters	Screen length, in meters	Land surface altitude, in meters	Geophysical data	Water-level measurements
14	1402	302401087143402	62.9	5.1	1.5	0.82	G,N,D	P
15	[1]1500	302404087141300	33.1	10.2	12.2	2.44	G,N,D	C,P
15	[1]1530	302404087141301	8.7	10.2	3.0	2.68		C,P
15	[1]1580	302404087141303	20.4	10.2	9.1	2.50		M
16	1600	302405087141300	28.1	5.1	6.1	2.39	G,N,D	C,P
16	1620	302405087141301	6.6	5.1	4.1	2.47		P
17	1700	302404087141500	30.0	5.1	5.5	1.92		P
17	1730	302404087141501	8.6	5.1	2.4	1.95		P
18	1800	302411087142100	29.1	5.1	1.5	2.83		P
18	MW6	302411087142101	30.5	10.2	3.0	2.84		P
18	WP12	302411087142107	2.3	2.5	.3	2.81		M
18	1860	302411087142102	17.9	5.1	.9	2.87		P
18	1830	302411087142103	8.7	5.1	.9	2.96		P
18	MW5	302411087142115	45.7	10.2	3.0	2.83		P
18	MW4	302411087142120	61.0	10.2	3.0	2.83	G,N,D,A	P
19	1970	302408087141800	21.8	5.1	1.5	1.80		P
19	1930	302408087141801	9.0	5.1	1.5	1.89		P
19	1902	302408087141802	.6	2.5	.1	[3]1.90		M
19	1904	302408087141804	1.2	2.5	.1	[3]1.97		M
19	1906	302408087141806	1.8	2.5	.1	[3]1.97		M
19	1908	302408087141808	2.4	2.5	.1	[3]1.97		M
19	1910	302408087141810	3.0	2.5	.1	[3]2.02		M
19	1915	302408087141812	4.6	2.5	.1	[3]2.01		M
19	MW2	302408087141815	45.7	10.2	3.0	1.84		P
19	1917	302408087141817	5.2	2.5	.1	[3]2.47		M
19	1901	302408087141820	61.0	10.2	3.0	1.85	G,N,D,A	C,P
19	MW3	302408087141830	30.5	10.2	3.0	1.85		P
20	[4]2020	302402087141501	6.7	5.1	3.0	[2].9		—
20	[4]2080	302402087141502	23.8	5.1	—	[2].9		—
21	[4]2120	302359087141501	4.6	5.1	3.0	[2].9		—
21	[4]2180	302359087141502	22.3	—	—	[2].9		—
22	[4]2220	302400087141301	4.6	5.1	3.0	[2].9		—
22	[4]2280	302400087141302	22.3	—	—	[2].9		—
23	[4]2320	302401087141301	6.1	5.1	3.0	[2].9		—
23	[4]2380	302401087141302	23.8	—	—	[2].9		—

[1]Well permanently sealed or destroyed.

[2]Estimated from topographic map.

[3]Measuring point elevation.

[4]Test hole only (no permanent well).

Table 1.—*Well construction data, including availability of geophysical and hydrologic data*—Continued

Site (well cluster) No.	Well or well point (WP) No.	Station ID	Well depth, in meters	Casing diameter, in centimeters	Screen length, in meters	Land surface altitude, in meters	Geophysical data	Water-level measurements
24	[4]2420	302405087140901	7.6	5.1	3.0	[2]1.8		—
24	[4]2480	302405087140902	23.8	—	—	[2]1.8		—
25	[4]2520	302412087141301	6.7	5.1	3.0	[2]4.0		—
25	[4]2580	302412087141301	26.8	—	—	[2]4.0		—
26	2620	302408087141320	7.5	5.1	3.0	3.11		M
26	2680	302408087141380	26.9	5.1	1.5	3.13		M
27	2702	302409087142602	.6	2.5	.15	[3]3.67		M
27	2704	302409087142604	1.2	2.5	.15	[3]3.64		M
27	2706	302409087142606	1.8	2.5	.15	[3]3.51		M
27	2708	302409087142608	2.4	2.5	.15	[3]3.57		M
27	2710	302409087142610	3.0	2.5	.15	[3]3.56		M
27	2713	302409087142613	4.0	2.5	.15	[3]3.66		M
27	2715	302409087142615	4.6	2.5	.15	[3]3.90		M
27	2718	302409087142618	5.5	2.5	.15	[3]3.55		M
27	2720	302409087142620	6.0	5.1	1.5	3.38		M
27	2780	302409087142680	25.5	5.1	1.5	3.40		M
28	2820	302403087142020	5.9	5.1	1.5	2.67		M
28	2880	302403087142080	27.5	5.1	1.5	2.68		M
29	2920	302404087142620	6.2	5.1	1.5	2.76		M
29	2980	302404087142680	27.8	5.1	1.5	2.76		M
30	WP29	302400087142718	5.4	2.5	.3	1.90		M
30	3020	302400087142720	6.6	5.1	1.5	2.36		M
30	3080	302400087142780	27.6	5.1	1.5	2.37		M
31	3120	302409087143020	6.2	5.1	1.5	3.36		M
31	3180	302409087143080	27.1	5.1	1.5	3.33		M
32	3220	302400087142020	6.4	5.1	1.1	2.47		M
33	3320	302405087140420	6.2	5.1	1.5	3.27		M
34	3420	302404087142220	4.4	5.1	1.5	2.97		M
35	3520	302407087135801	5.9	2.5	.3	[2]3.20		
35	3527	302407087135802	8.2	2.5	.3	[2]3.20		
36	WP6	302403087142501	2.4	2.5	.3	3.03		P
36	3602	302403087142502	.61	2.5	.15	[3]3.20		M
36	3604	302403087142504	1.2	2.5	.15	[3]3.18		M
36	3606	302403087142506	1.8	2.5	.15	[3]3.20		M
36	3608	302403087142508	2.4	2.5	.15	[3]3.16		M

[2]Estimated from topographic map.

[3]Measuring point elevation.

[4]Test hole only (no permanent well).

Table 1.—*Well construction data, including availability of geophysical and hydrologic data*—Continued

Site (well cluster) No.	Well or well point (WP) No.	Station ID	Well depth, in meters	Casing diameter, in centimeters	Screen length, in meters	Land surface altitude, in meters	Geophysical data	Water-level measurements
36	3610	302403087142510	3.0	2.5	0.15	[3]3.22		M
36	3615	302403087142515	4.6	2.5	.15	[3]3.24		M
36	3620	302403087142525	6.1	2.5	.15	[3]3.21		M
37	3702	302407087141802	.6	2.5	.15	[3]1.87		M
37	3704	302407087141804	1.2	2.5	.15	[3]1.90		M
37	3706	302407087141806	1.8	2.5	.15	[3]1.95		M
37	3708	302407087141808	2.4	2.5	.15	[3]2.00		M
38	3802	302407087141702	.6	2.5	.15	[3]2.11		M
38	3804	302407087141704	1.2	2.5	.15	[3]2.11		M
38	3806	302407087141706	1.8	2.5	.15	[3]2.20		M
38	3808	302407087141708	2.4	2.5	.15	[3]2.20		M
38	3810	302407087141710	3.0	2.5	.15	[3]2.21		M
38	3815	302407087141715	4.6	2.5	.15	[3]2.21		M
38	38CP	302407087141725	7.5	2.5	.3	[2]2.1		M
38	3830	302407087141730	9.5	2.5	.15	[2]1.5		
	[1]2	302421087142101	14.9	10.2	.9			
	3	302419087141501	2.7	10.2	1.5	3.77		P
	4	302416087140701	4.3	10.2	1.5	3.92		P
	5	302417087140001	2.7	10.2	1.5	3.73		P
	6	302412087142501	14.9	10.2	.9			M
	7	302413087141701	27.1	10.2	.9			M
	8	302412087140801	2.7	10.2	.9	3.37		P
	9	302412087140701	24.1	5.1	.9	3.69	G,N,D	P
	10	302412087141201	3.4	10.2	1.5	3.40		C,P
	[1]13	302408087141702	18.3	5.1	.9	2.23		C,P
	18	302411087142001	4.9	5.1	1.5	2.61		C,P
	19	302402087141102	8.5	5.1	.9	1.83		C,P
	[1]20	302402087141101	21.0	5.1	.9	1.83		M
	[1]21	302404087140101	13.4	5.1	.9		G	M
	[1]39	302308087163501	74.7	7.6	—	3.02		
	60	302402087140501	46.3	10.2	—	2.12	GN	P
	60A	302408087140502	5.5	10.2	—	2.19		P
	[1]62	302432087151701	43.3	15.2	—	4.25		
	[1]62A	302432087151701	5.5	10.2	—	4.25		
ES41	[5]NWF41–1	302644087122501	57.9	5.1	6.1	[2]25.0		M

[1]Well permanently sealed or destroyed.

[2]Estimated from topographic map.

[3]Measuring point elevation.

[5]Written commun., Northwest Florida Water Management District (1985).

Table 1.—*Well construction data, including availability of geophysical and hydrologic data*—Continued

Site (well cluster) No.	Well or well point (WP) No.	Station ID	Well depth, in meters	Casing diameter, in centimeters	Screen length, in meters	Land surface altitude, in meters	Geophysical data	Water-level measurements
ES41	[5]NWF41–2	302644087122502	30.5	5.1	3.0	[2]25.0		M
ES41	[5]NWF41–3	302644087122503	16.8	5.1	1.5	[2]25.0	E	M
ES42	[5]NWF42–1	302543087105601	45.7	5.1	3.0	[2]13.1		M
ES42	[5]NWF42–2	302543087105602	24.4	5.1	3.0	[2]13.1		M
ES42	[5]NWF42–3	302543087105603	13.7	5.1	1.5	[2]13.1	D,E	M
ES47	[5]NWF47–1	302656087161001	57.9	5.1	3.0	[2]10.7		M
ES47	[5]NWF47–2	302656087161002	18.3	5.1	3.0	[2]10.7		M
ES47	[5]NWF47–3	302656087161003	6.1	5.1	1.5	[2]10.7	D,N,S	M
ES49	[5]NWF49–1	302704087134101	54.9	5.1	3.0	[2]25.6		M
ES49	[5]NWF49–2	302704087134102	15.2	5.1	3.0	[2]25.6	D	M
	[6]W223	302307087162601	94	29	–	3.3	–	–
	[6]Peoples 4A	302332087154101	27	91	–	7.0	–	–
	[6]Weiss-Fricker	302400087145103	18	52	18.3	1.2	–	–
	[6]Tool and Supply	302408087142601	18.9	25.4	2.7	10.6	–	–
	[4]B–1	302418087141901	61.0	–	–			
	[6]Joe Patti	302416087133901	58	–	–			
	[6]Owsley	302420087140301	7.5	7.6	4.6	4.3	–	–
	[7]Crystal Ice	302427087140601	4.9	22.8	–	3.9	G	M
	[8]TH–1D	302457087144601	40	5.1	–	[2]7	G	–
	[9]City 7	302534087160301	81	66	–	21.3	–	–
	[7]TH1	302541087114501	18.8	5.1	.9	18.9	G,N	M
	City 4	302555087122701	67.1	66.0	30.0	[2]24.4		M
	City 5	302514087160301	71.6	66.0	30.0	[2]12.2		M
	City 8	302553087145701	76.5	66.0	24.4	[2]25.9		M
	[9]City 3	302602087130701	77	66	30.5	15.8	–	–

[2]Estimated from topographic map.

[4]Test hole only (no permanent well).

[5]Written commun., Northwest Florida Water Management District (1985).

[6]U.S. Geological Survey file data.

[7]Trapp (1972).

[8]Written commun., Post, Buckley, Schuh, and Jernigan (1986).

[9]Written commun., Escambia County Utilities Authority (1985).

Table 1.—*Well construction data, including availability of geophysical and hydrologic data*—Continued

Site (well cluster) No.	Well or well point (WP) No.	Station ID	Well depth, in meters	Casing diameter, in centimeters	Screen length, in meters	Land surface altitude, in meters	Geophysical data	Water-level measurements
	[6]Catholic High School	302609087152401	13.0	15.2	3.0	23.8	–	–
	[9]City 9	302615087134401	74	66	30.5	18.9	–	–
	[10]TH100	302617087152401	13.9	5.1	.9	23.2	G	–
	County jail	302640087140801	15.1	10.2	4.3	22.2	–	–
	[10]TH2	302643087153601	16.6	5.1	.9	18.9	G,N	M
	Agrico	302703087133502	15.7	52	12.2	25.6	–	–
	[6]TH10	303204087213701	45	–	–	–	–	–
	[1]WP1	302401087141801	1.4	2.5	.3	1.79		P
	WP2	302406087141801	1.5	2.5	.3	1.55		P
	[1]WP3	302406087141901	1.2	2.5	.3	.26		M
	WP4	302405087141901	1.2	2.5	.3	1.57		P
	WP5	302404087142501	1.0	2.5	.3	.67		P
	[1]WP7	302408087142401	1.9	2.5	.3	3.43		M
	WP9	302405087142003	2.1	2.5	.3	2.47		M
	WP10	302404087142101	2.3	2.5	.3	2.14		P
	WP11	302405087141701	1.7	2.5	.3	1.57		M
	WP14	302427087142401	3.5	2.5	.3	5.72		M
	WP15	302427087140401	2.2	2.5	.3	3.35		M
	[1]WP16	302417087133801	–	2.5	.3	1.48		M
	WP17	302433087125901	1.4	2.5	.3	[2]3.0		M
	WP18	302409087143501	3.3	2.5	.3	3.88		M
	WP20	302456087141401	9.8	2.5	.3	12.48		M
	WP21	302408087142402	3.0	2.5	.3	3.41		M
	WP22	302435087134901	3.8	2.5	.3	4.18		M
	WP23	302455087134801	6.6	2.5	.3	8.44		M
	WP24	302410087143901	5.3	2.5	.3	7.31		M
	WP25	302405087142501	3.7	2.5	.3	2.39		M
	WP26	302404087142601	1.5	2.5	.3	2.23		M
	WP27	302403087142601	2.5	2.5	.3	2.00		M
	WP28	302402087142601	3.9	2.5	.3	1.92		M

[1]Well permanently sealed or destroyed.

[2]Estimated from topographic map.

[6]U.S. Geological Survey file data.

[9]Written commun., Escambia County Utilities Authority (1985).

[10]Trapp and Geiger (1986).

Table 1.—*Well construction data, including availability of geophysical and hydrologic data*—Continued

Site (well cluster) No.	Well or well point (WP) No.	Station ID	Well depth, in meters	Casing diameter, in centimeters	Screen length, in meters	Land surface altitude, in meters	Geophysical data	Water-level measurements
	WP30	302380087141801	2.2	2.5	0.3	1.15		M
	WP31	302408087142401	3.2	2.5	.3	2.91		M
	[4]WP32	302407087142601	5.5					
	[4]WP33	302411087141701	6.1					
	[4]WP34	302410087141701	6.1					
	[4]WP35	302511087151201	11.1			[2]24.4		
	[4]WP36	302622087151001	11.1					
	WP37	302558087134701	11.1	2.5	.3	[2]18.0		M
	[4]WP38	302603087131401	11.1					
	[4]WP39	302650087141101	11.1			[2]22.9		

[2]Estimated from topographic map.

[4]Test hole only (no permanent well).

Lithologic Data

About 200 split-spoon samples were collected throughout the course of this investigation. Laboratory analyses include X-ray diffraction on selected clay samples, grain size and porosity determinations, and hydraulic conductivity measurements on selected sands and clays. The clay assemblages are typical of Cenozoic fluvial and marine clays of the southeastern United States. Dioctahedral clays, including kaolinite, aluminous smectite, and illite dominate over trioctahedral varieties. The kaolinite-dominant assemblages reflect detrital fluvial input, and the smectite-rich assemblages are assumed to be mixtures of Gulf Coast marine muds with locally derived detritus (Bodine, in press).

Table 2 summarizes porosity, grain size, and hydraulic conductivity determinations on selected samples from a single test hole. The data are representative of the range of values measured. Porosity was determined by calculating the volume of saturated material in a permeameter, extruding the materials and determining the weight loss after oven drying at 110 °C. The volume loss computed from the weight loss in grams divided by the volume of sediment in cubic centimeters yielded the porosity (Richard Strom, University of South Florida, written commun., 1984). Size analyses consisted of settling tube determinations on the sand-size fractions combined with pipette analyses on the finer fractions. Hydraulic conductivities were run on a constant head permeameter after extrusion of the sample from the core tube. These data are summarized in tables 2 and 3. Comparable data also used in this report were collected by NUS Corporation (1985, Volume II). The data show that permeability in the aquifer is vertically stratified, dependent primarily on grain size and packing characteristics of the sediments.

Maps of the base of the permeable zone in layer 1 and the top of layer 2 are presented in figures 13 and 14 for the site area. Distributions of these features for the entire area of investigation are presented in figures 15 and 16. The linearity of contours on these two maps, particularly along the coastline, is a result of the sparse data base combined with the large grid block size, particularly in the east-west direction.

Table 2.—*Porosity, grain-size, and hydraulic conductivity determinations on selected sand samples from well 1901*
[Analyses by the Department of Geology, University of South Florida]

Depth, meters	Lithology	Porosity, percent	Grain size, percent			Hydraulic conductivity, meters per day
			Sand	Silt	Clay	
6	Coarse quartz sand	33.1	97.7	.5	1.8	21
8	Coarse quartz sand	36.7	97.6	1.2	1.2	27
13	Medium quartz sand	31.1	96.5	1.9	1.6	6.1
20	Medium well-rounded quartz sand Some iron cement.	32.0	91.2	.8	7.8	.3
22	Medium well-rounded quartz sand	38.1	97.8	.7	.6	31
27	Medium-fine well-rounded clay-cemented quartz sand	35.9	88.3	1.3	10.4	.06
30	Coarse-to-medium iron mineral and clay-cemented quartz sand.	32.9	89.1	1.9	8.9	≤.03
44	Coarse-to-medium quartz sand	37.6	97.1	.6	2.2	22
57	Coarse quartz sand	35.4	97.1	.8	2.2	31

Table 3.—*Cation-exchange capacities and hydraulic conductivities on selected clay samples*
[Analyses by the Department of Geology, University of South Florida]

Well	Depth, in meters	Lithology	Cation-exchange capacity, milliequivalents per 100 grams at pH = 7	Hydraulic conductivity, in meters per day
1901	10	Sandy clay, smectite with accessory kaolinite.	9.7	—
1901	12	......do................................	16.3	—
1901	15	......do................................	12.7	$6x10^{-5}$
1901	19	......do................................	—	$2x10^{-5}$
MW–4	33	Sandy clay, kaolinite with accessory smectite.	10.4	$9x10^{-6}$

The thickness of the confining bed between layers 1 and 2 is also shown (fig. 17). The wedge of clay due south of the impoundments, and thickest near the middle of the drainage ditch, is perhaps the most significant shallow lithologic feature. The location and shape of the clay complicates the local flow system, effectively separating the upper 40 m of sediments into two permeable hydrogeologic units. Because of a paucity of data at depth in the aquifer, the thickness and hydraulic conductivity of the confining bed between layers 2 and 3 are simulated by using uniform values in the model.

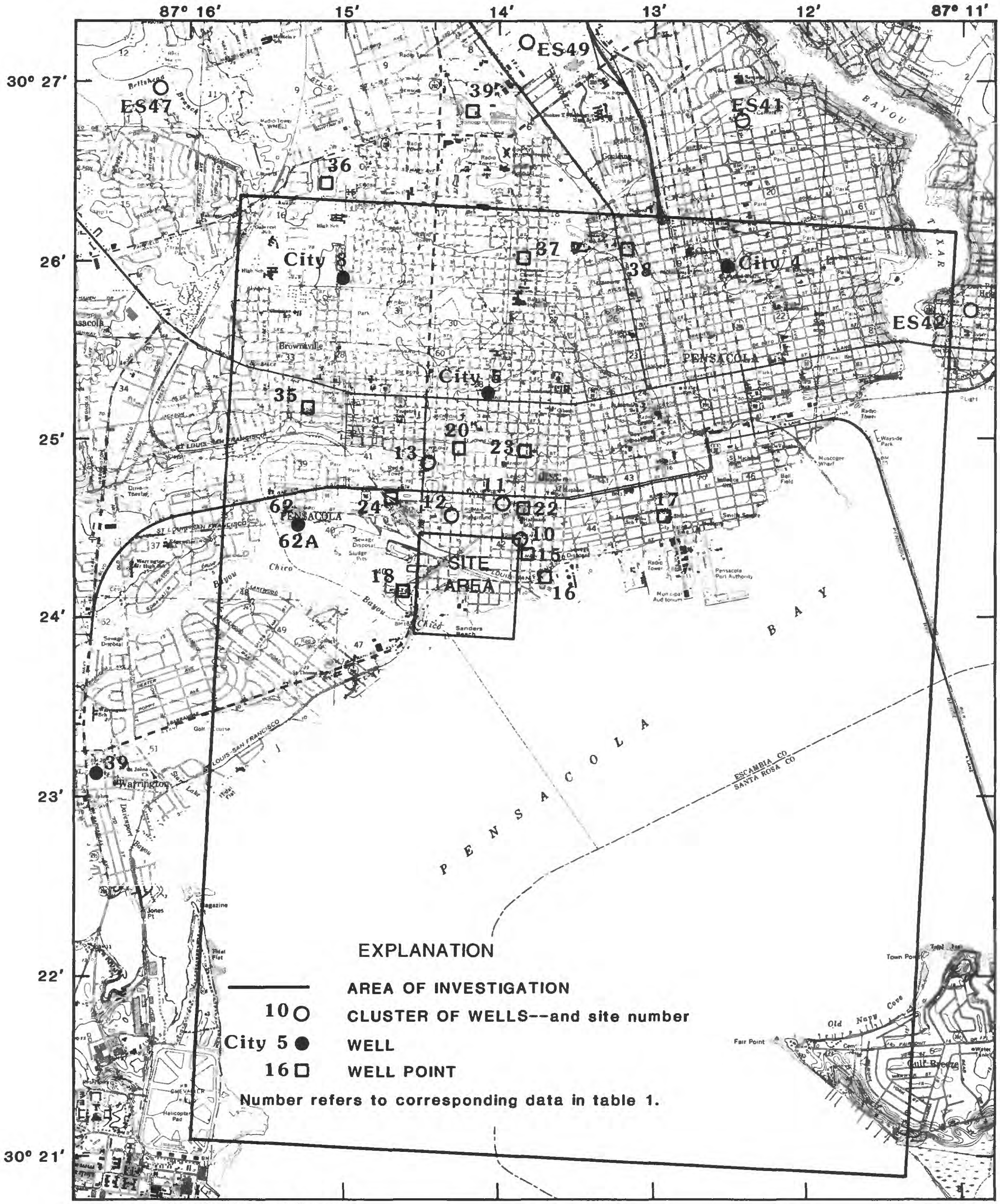

Base from U.S. Geological Survey
Pensacola 1:24,000, 1970, West Pensacola 1:24,000, 1970,
Gulf Breeze 1:24,000, 1969, Fort Barrancas 1:24,000, 1970

0 1 2 MILES
0 1 2 KILOMETERS

Figure 6.—Location of site, clusters of wells, wells, and well points in and near the area of investigation.

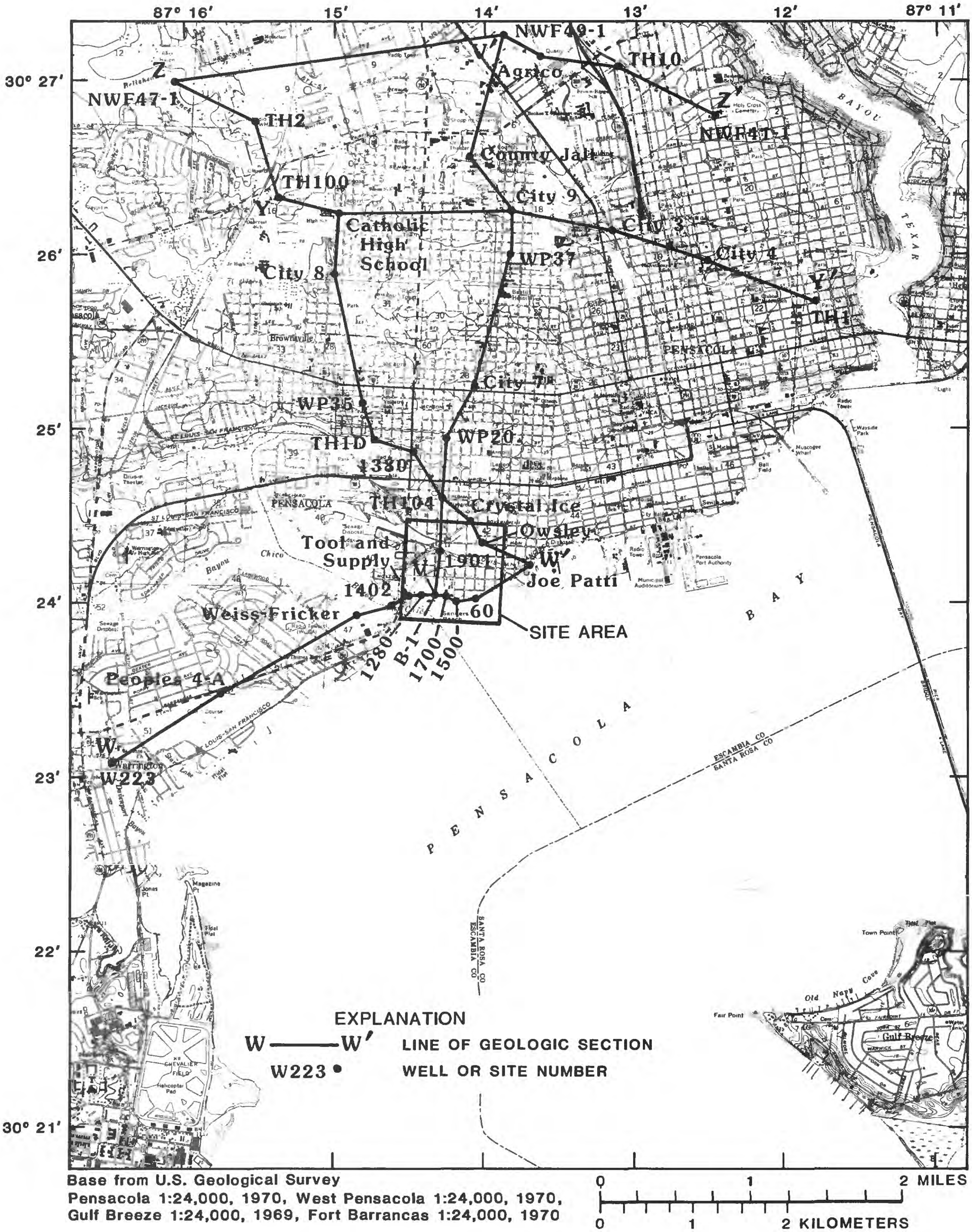

Base from U.S. Geological Survey
Pensacola 1:24,000, 1970, West Pensacola 1:24,000, 1970,
Gulf Breeze 1:24,000, 1969, Fort Barrancas 1:24,000, 1970

Figure 7.—Location of selected geologic cross sections.

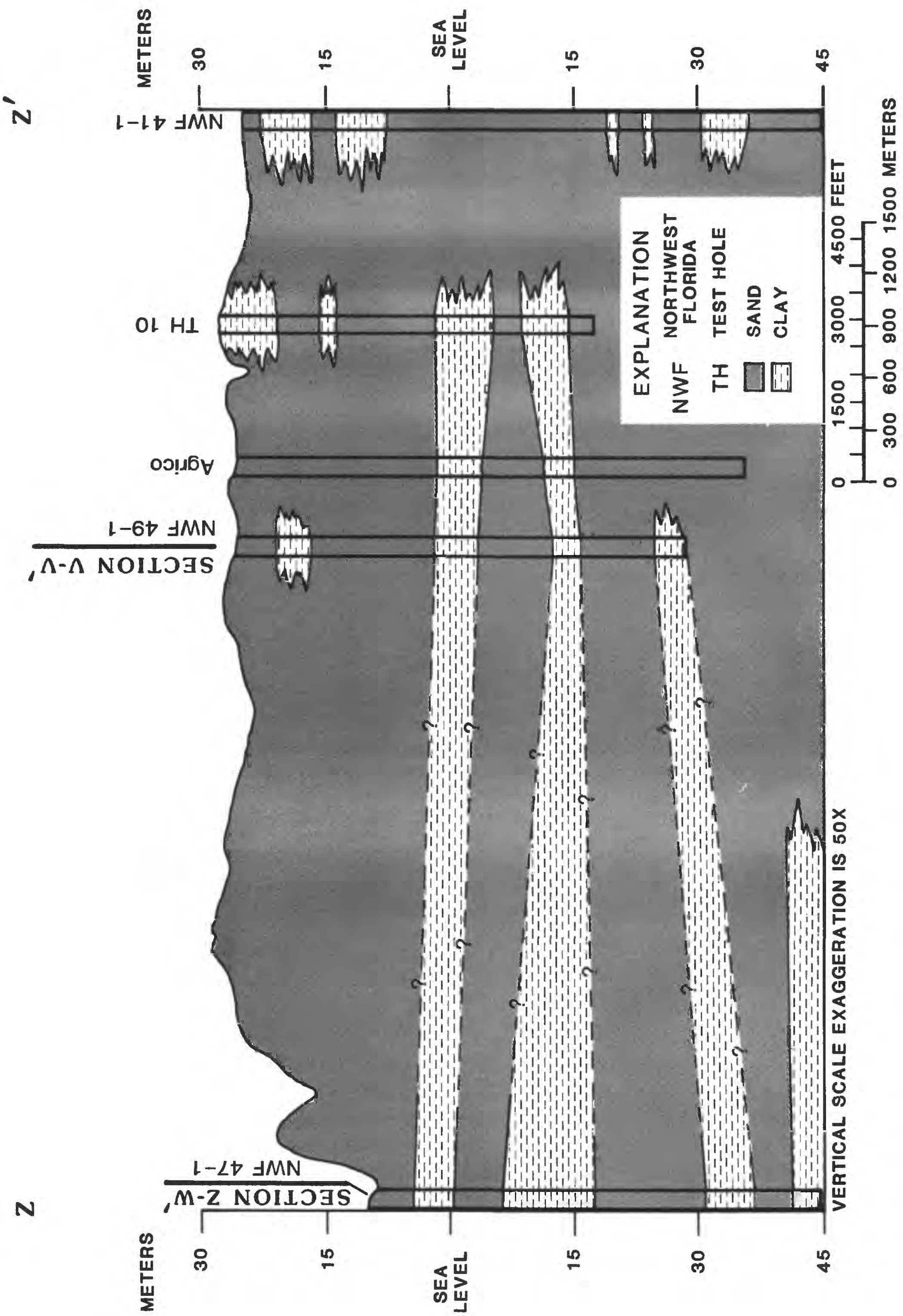

Figure 8.—Geologic section Z–Z'.

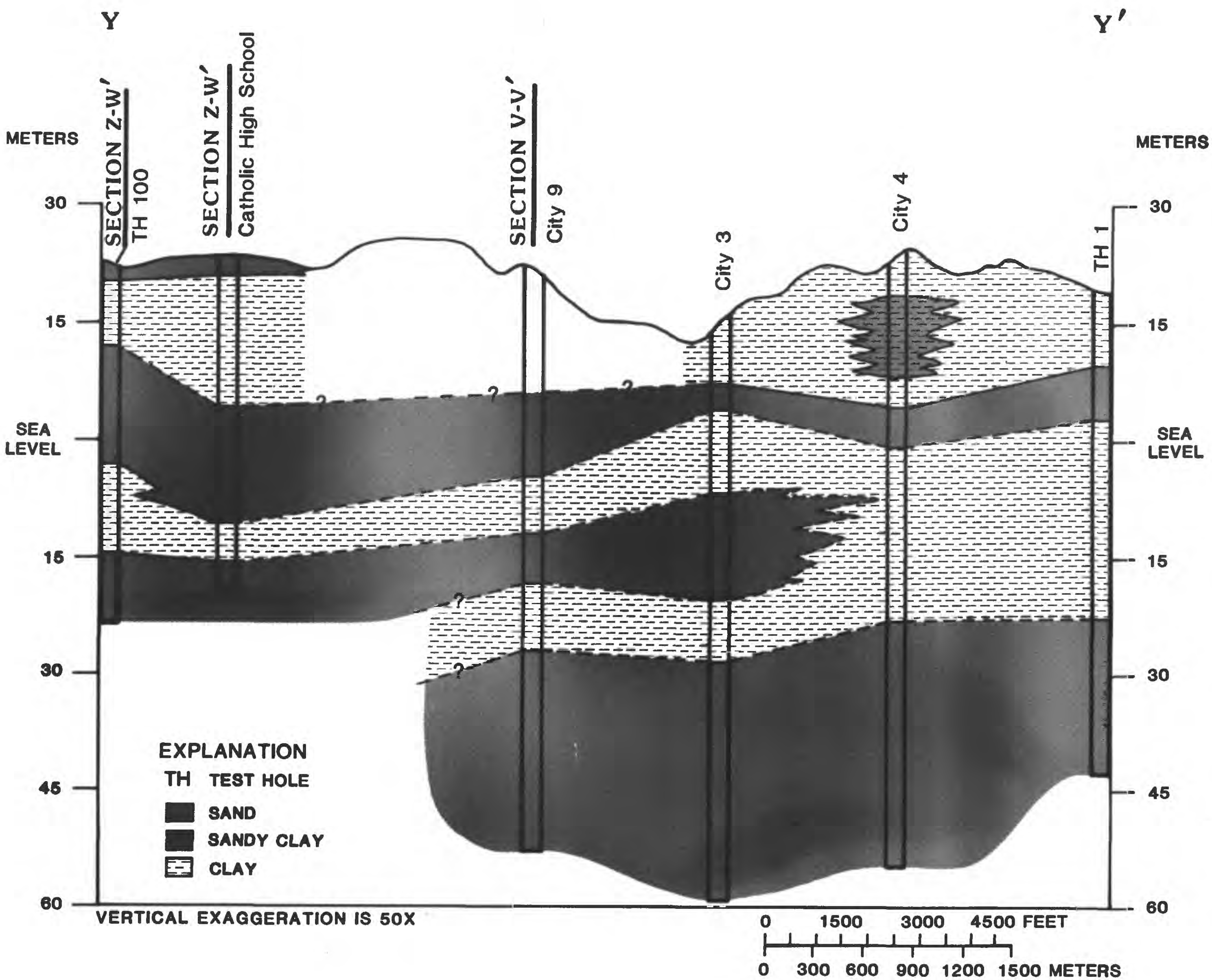

Figure 9.—Geologic section Y–Y'.

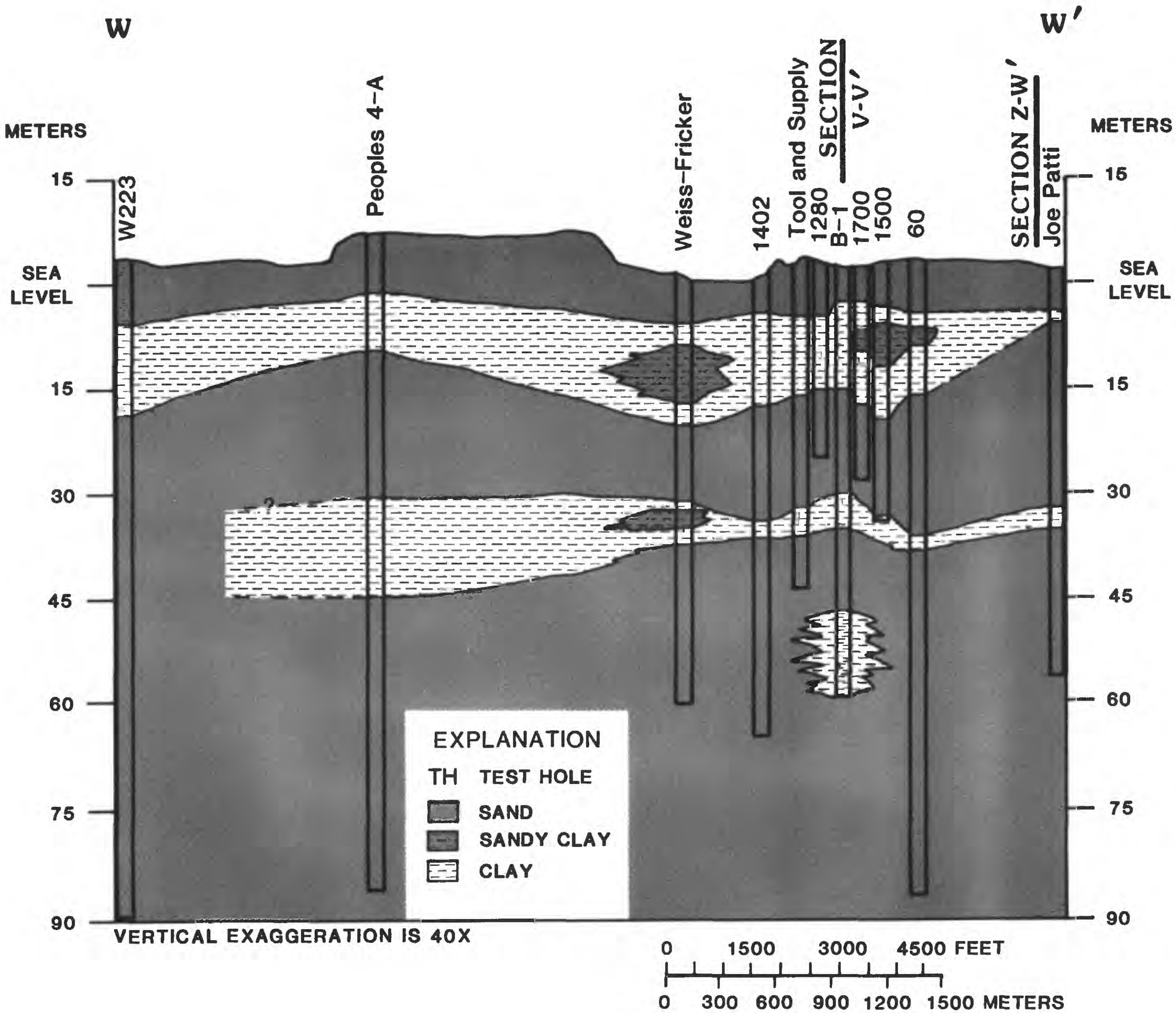

Figure 10.—Geologic section W–W'.

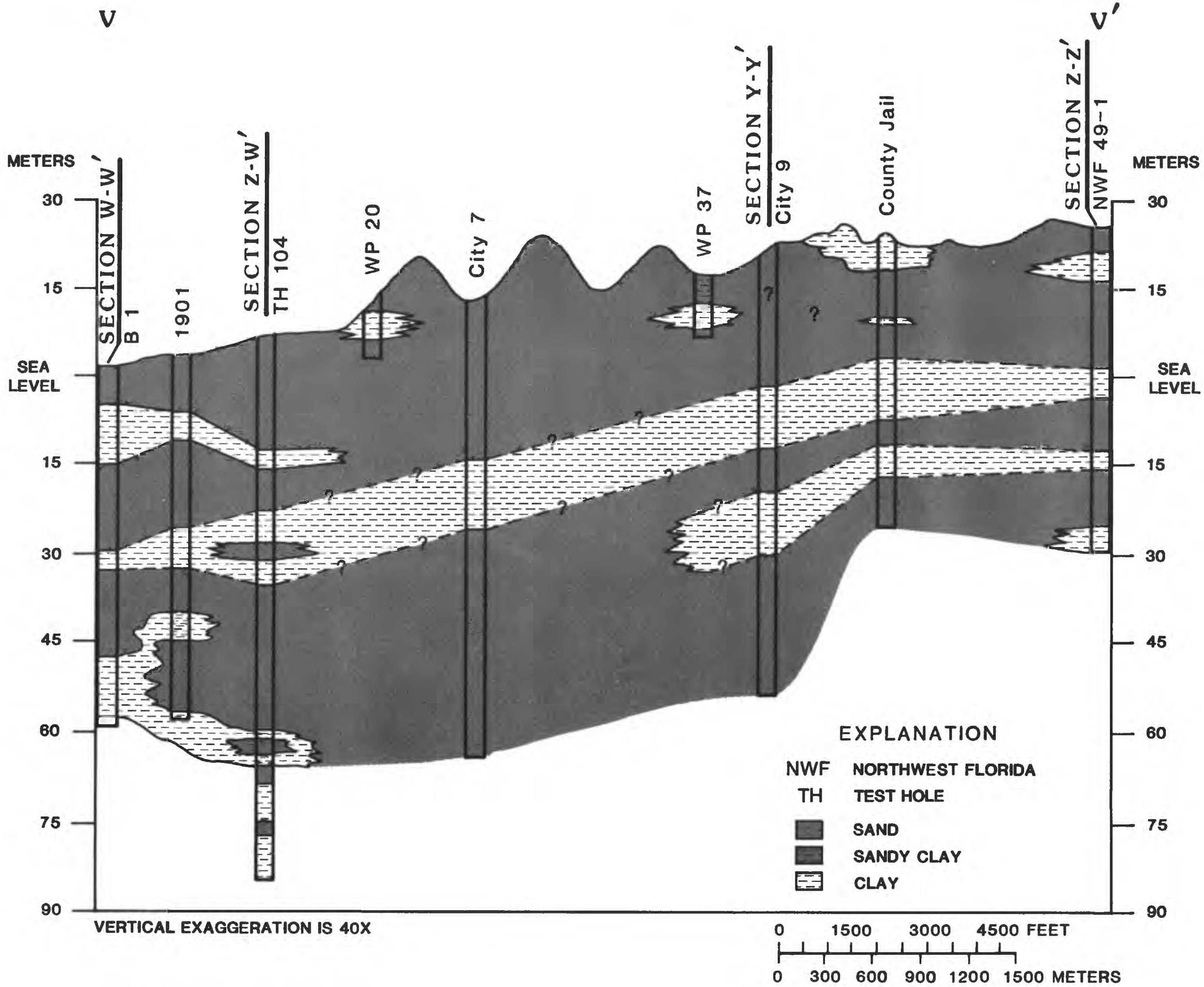

Figure 11.—Geologic section V–V'.

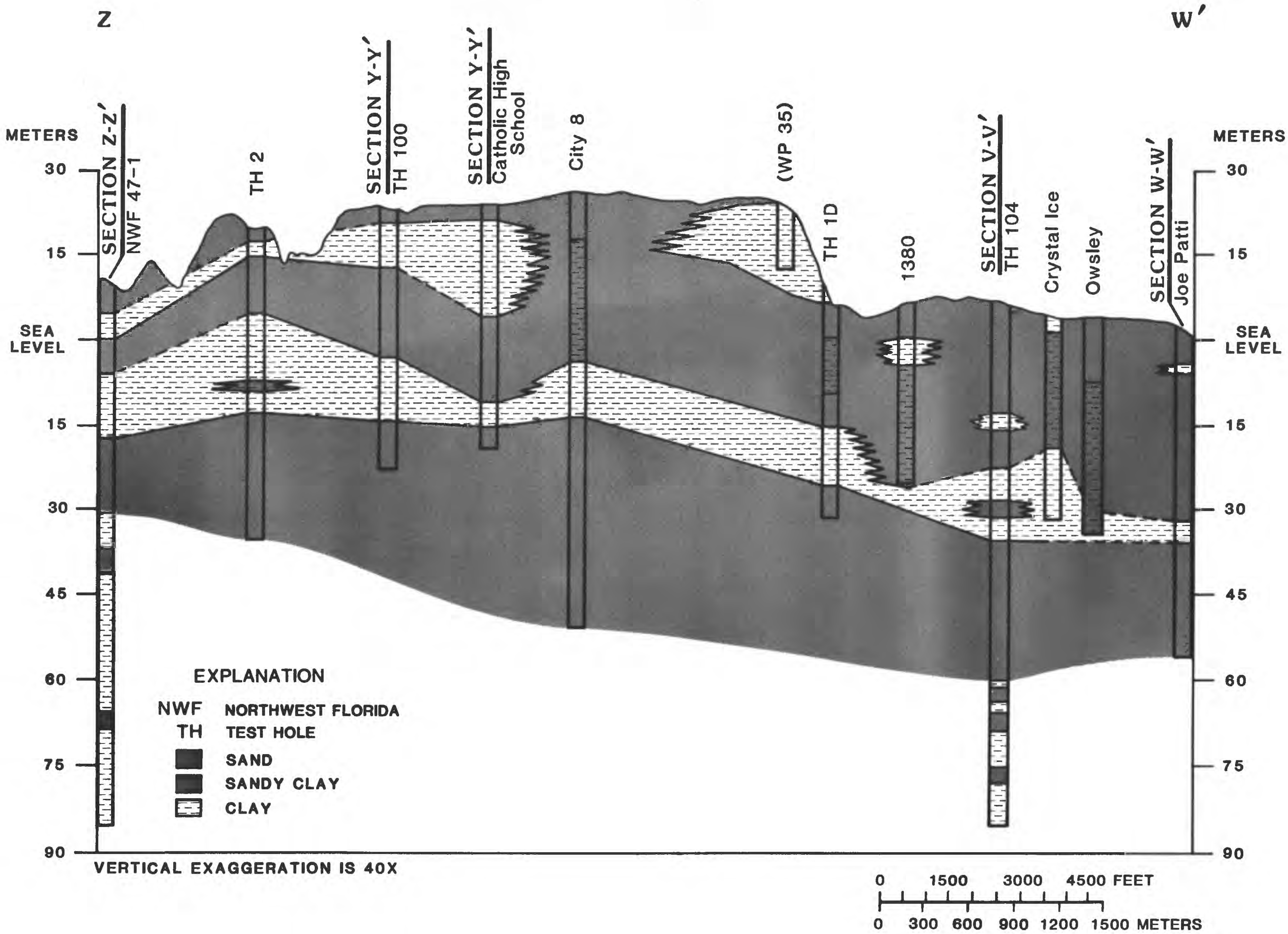

Figure 12.—Geologic section Z–W'.

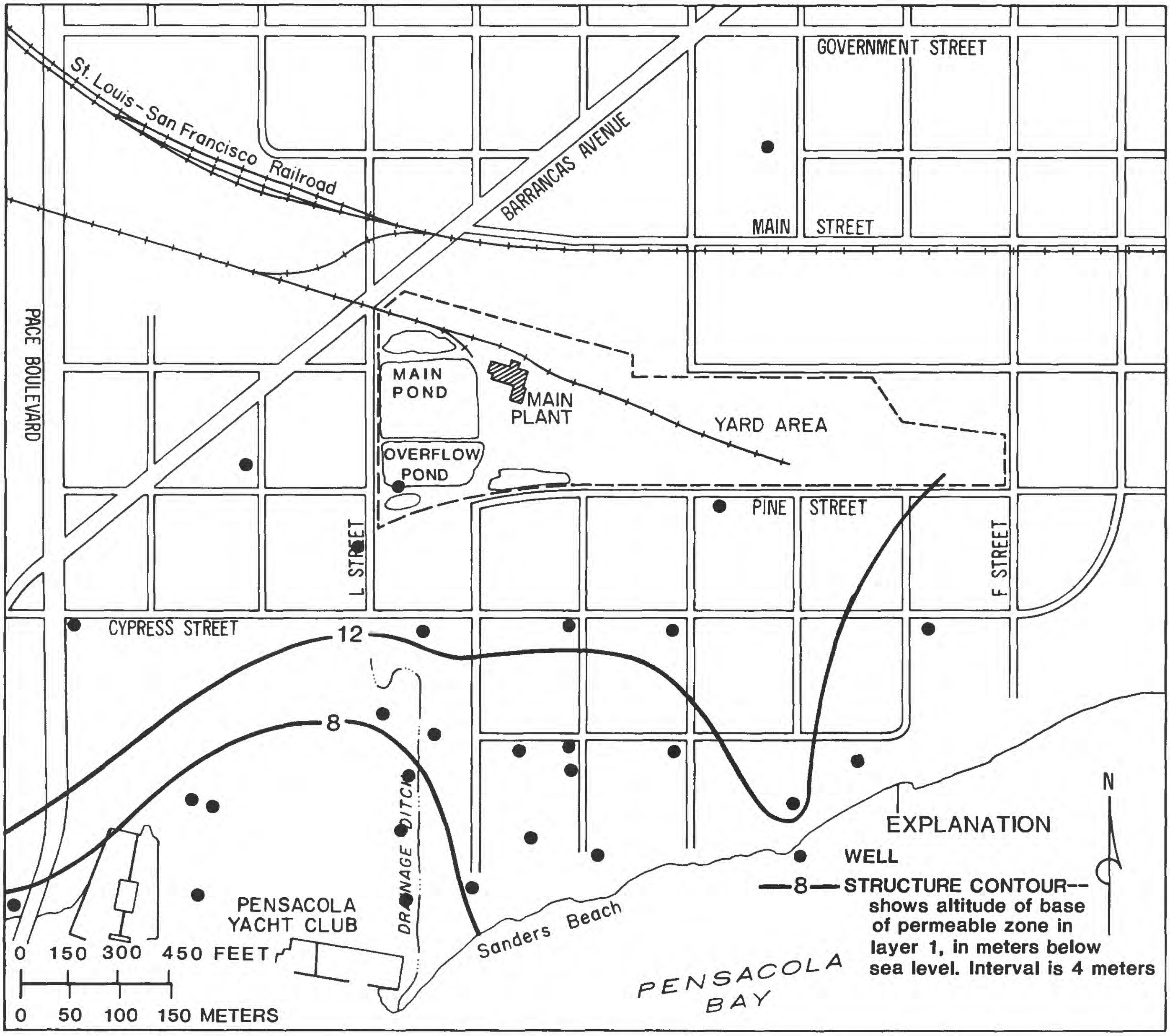

Figure 13. – Contours for the base of permeable zone in layer 1.

Geophysical Data

Natural gamma, gamma-gamma, neutron, and acoustic velocity borehole logs were run in selected wells during this investigation (table 1). Electric and spontaneous potential logs are also available on some older wells used in this study. These logs confirmed the heterogeneity of the surficial aquifer in the site area. Results of these data have been incorporated with other geologic data and presented in figures 8–17.

Several surface geophysical techniques were also applied at the site. Electromagnetic induction was not practical because of interference from city utilities and the masking effect of the saline water in Pensacola Bay. Other techniques, including ground-penetrating radar (GPR), complex resistivity, and seismic reflection, were hindered by the complex lithology in the surficial aquifer, with its large electrical and seismic attenuation in the surficial sands and sporadic clay lenses. Although each of these techniques has proved successful at other sites, only GPR may prove useful at this site. GPR produces higher resolution data than any other technique, but is severely limited in depth penetration in soils with a large clay content, such as those that occur discontinuously at the site. Olhoeft (1986) discusses preliminary applications of the GPR data at the site, including the possibilities of using GPR to delineate effects of the contaminant plume on the aquifer materials.

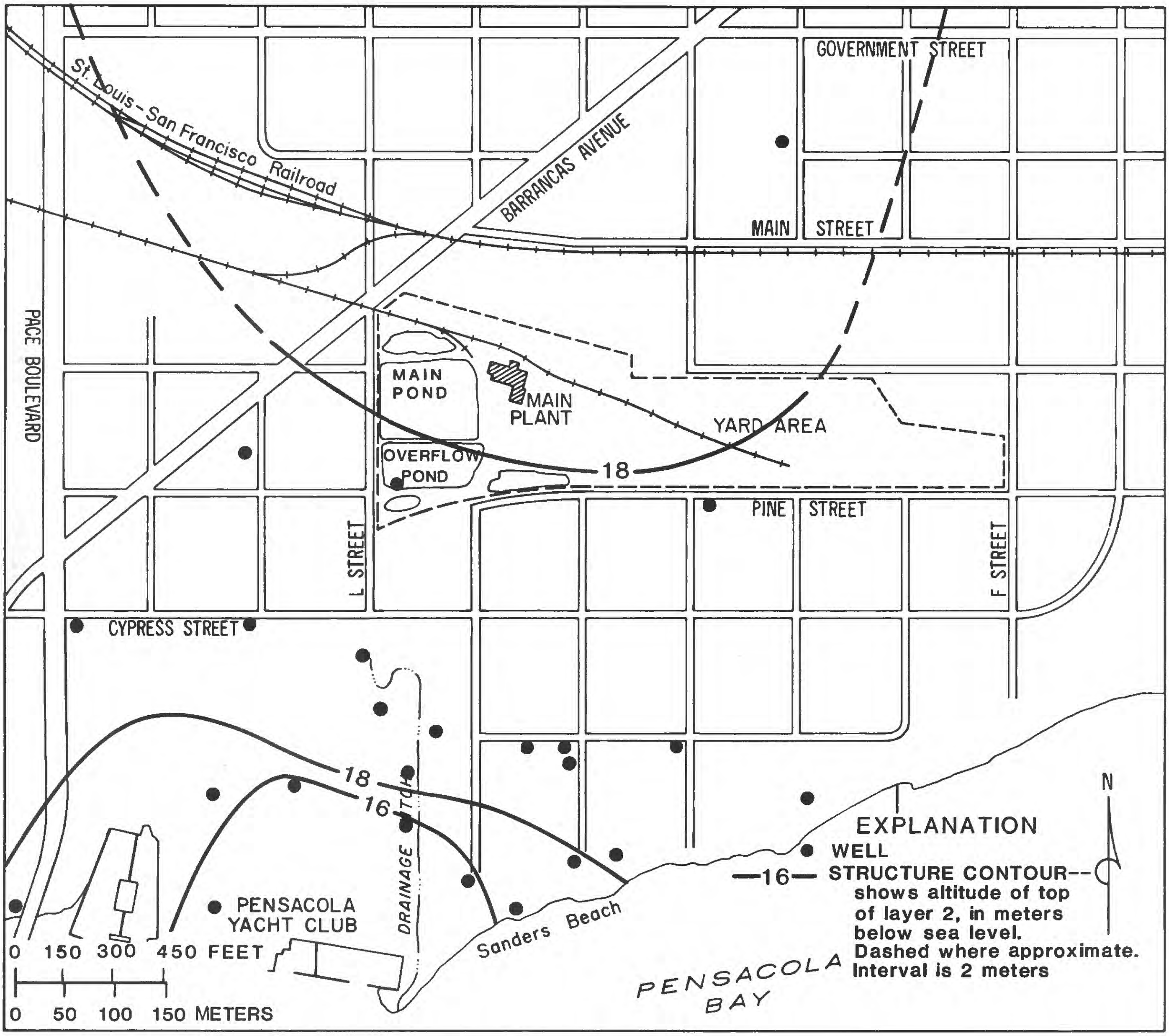

Figure 14.—Contours for the top of layer 2.

Hydrologic Framework

The earliest compilations of hydrologic data in the area are reported in Musgrove, Barraclough, and Marsh (1961) and Musgrove, Barraclough, and Grantham (1965, 1966). They point out that movement of water in the surficial parts of the sand and gravel aquifer is controlled principally by local topographic variations. Trapp (1972, 1973, 1975) presents extensive geohydrologic data including water-table maps. The complexity of water levels resulting from combinations of a true water table and local perched water tables is further discussed in Dysart and others (1977). A

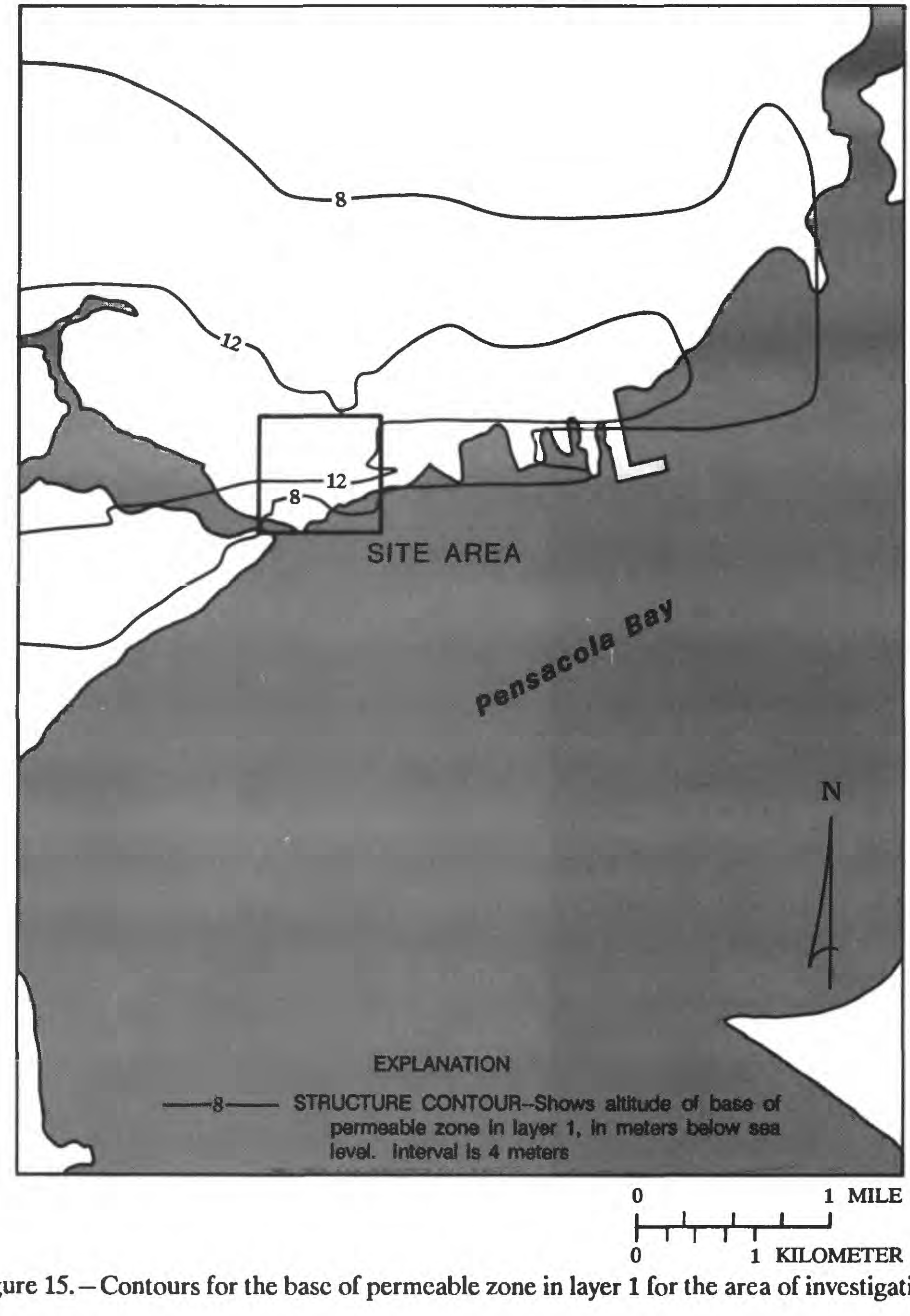

Figure 15.—Contours for the base of permeable zone in layer 1 for the area of investigation.

synopsis of all the above data is provided in Cushman-Roisin and Franks (1982). Wilkins and others (1985) present lithologic and hydrologic data from an ongoing investigation of the sand and gravel aquifer in southern Escambia County.

Barr and others (1981) divide the aquifer into three permeable zones: a surficial (water-table) zone, a low-permeability intermediate zone, and a main producing zone. The surficial zone ranges in depth from land surface to a maximum thick-

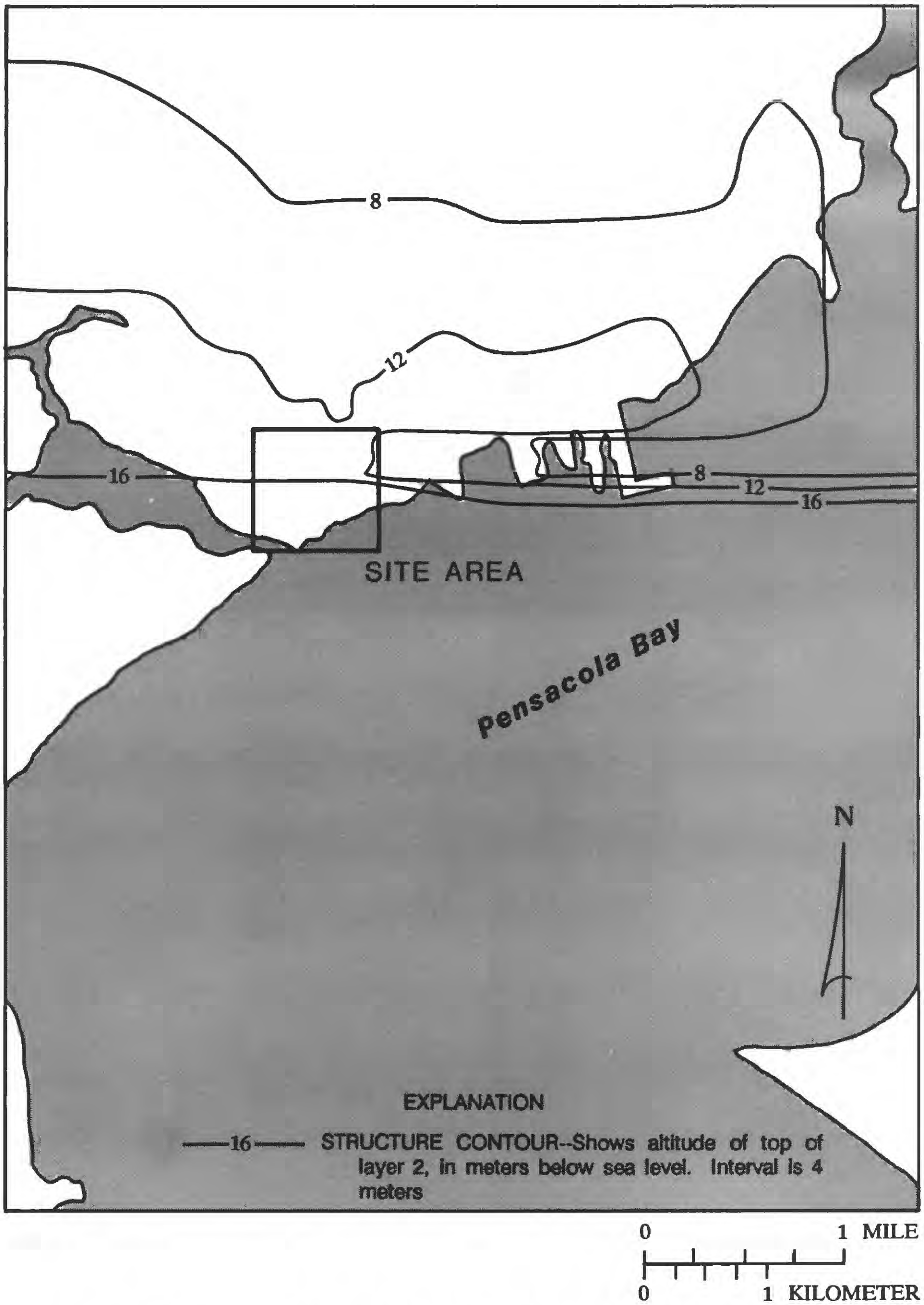

Figure 16.—Contours for the top of layer 2 for the area of investigation.

ness of 60 m. The intermediate zone, where present, is generally thin, typically between 18 and 27 m. The main producing zone may be up to 60 m thick. In the area of investigation for this study (fig. 1), the water-table zone and underlying discontinuous semiconfining unit are about 15 m thick and comprise the surficial zone; the intermediate zone and underlying confining clay unit are about 27 m thick; and the main producing zone, corresponding to the lower zone, is about 20

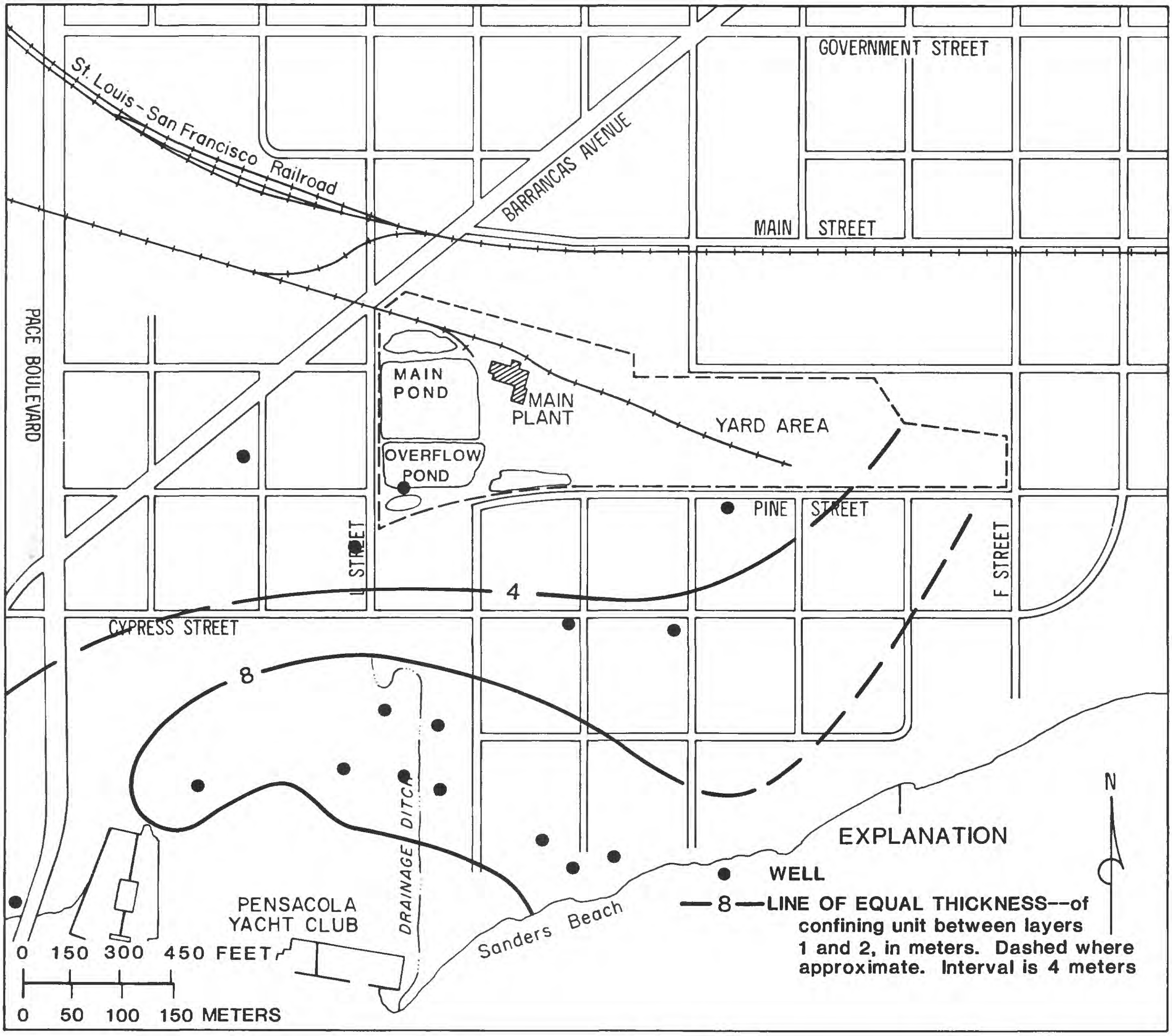

Figure 17.—Contours for the thickness of the confining unit between layers 1 and 2 in the site area.

m thick. These distinct lithologic zones are designated, respectively, as layers 1, 2, and 3 in this report (fig. 4).

Water-Level Data

There are three wells with long-term water-level records in the area of investigation (fig. 18). Well 62A (8.5 m deep) has data from 1940 to 1973. Set in the water-table zone, this well shows an annual range of 0.3 to 1.5 m, related to local recharge events. The adjacent well 62 (43 m deep) has a similar period of record. Water levels range more than about 5 m, with the lowest levels occurring in the mid-1950's when pumping at a nearby chemical plant was at a maximum, reducing heads about 3 m below normal. Well 39 (74 m deep) has record from 1940 to 1980. The total range for the period of record is about 3.6 m. During the period of this investigation, fluctuations have been minimal (less than 1.5 m).

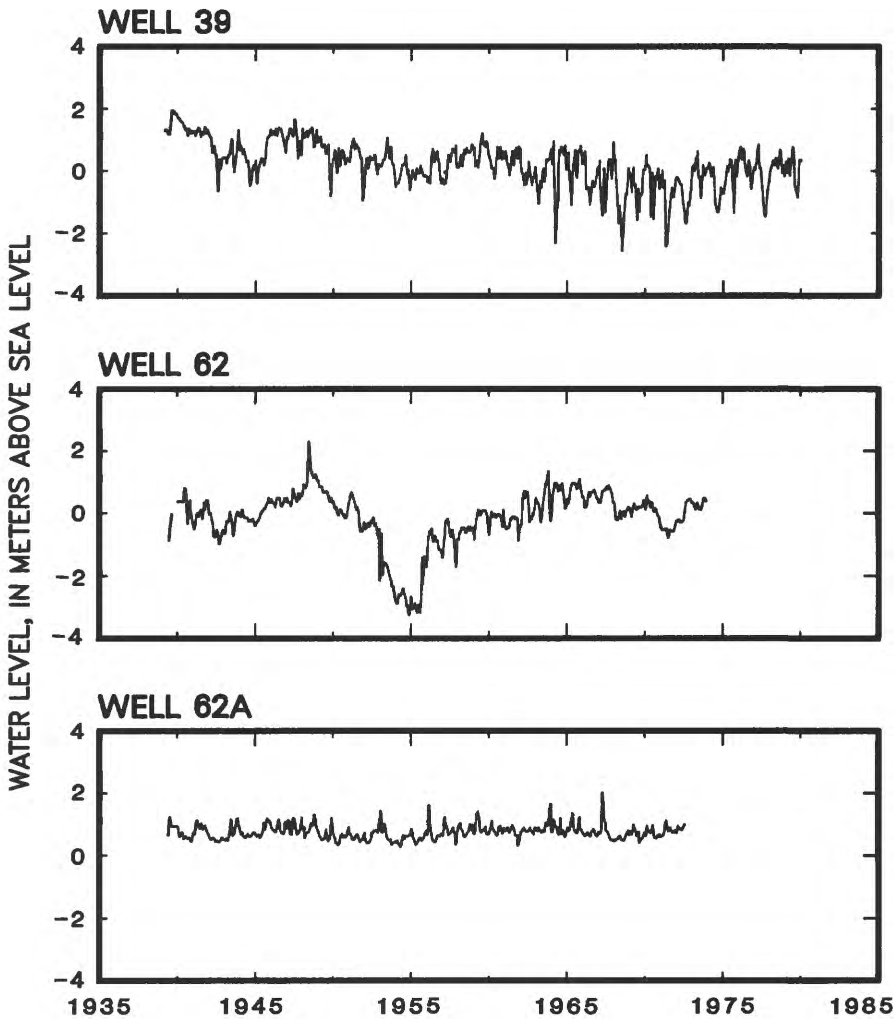

Figure 18.—Long-term hydrographs of wells 39, 62, and 62A.

Water-level measurements were made periodically in selected wells in the area of investigation. A summary of the frequency of measurements is presented in table 1. Figures 19–23 present the January 1986 potentiometric surfaces for the area.

The measured January 1986 water levels are equivalent to the median water levels observed in the long-term record (fig. 18). These data are considered representative of steady-state conditions because head measurements at that time

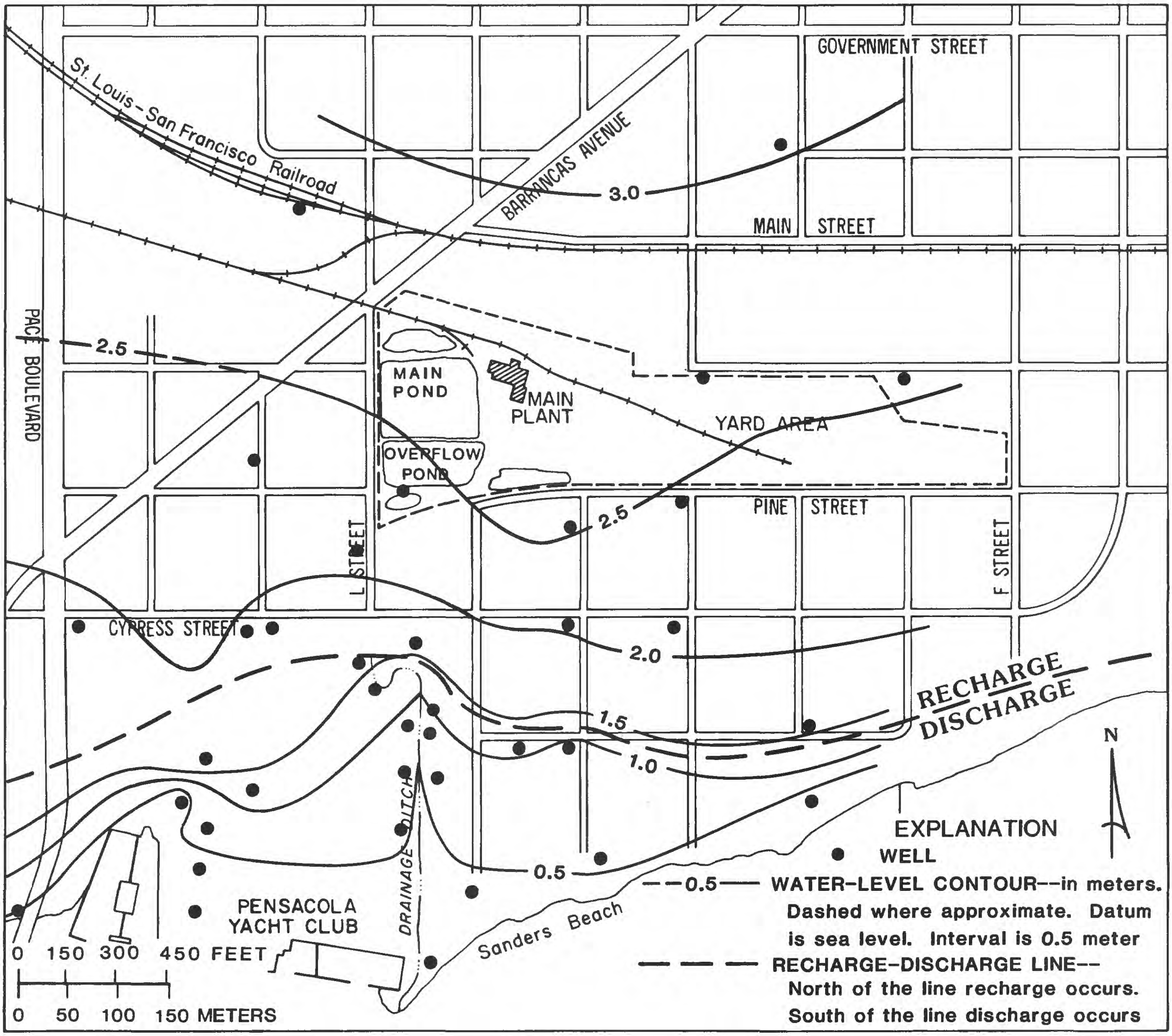

Figure 19.—Contours for the water-table configuration in layer 1 in the site area.

were representative of "average" conditions in the aquifer, both during the period of this investigation and over the much longer period of record. More importantly, the range of water-level variation is small, with little change over the period of record.

There are two maps for layer 1, one for the site area (fig. 19) and one for the area of investigation (fig. 20). The site water-table (layer 1) map is based on 37 data points. The water-table map for the area of investigation is based on an additional 11 water-level measurements, as indicated. Addi-

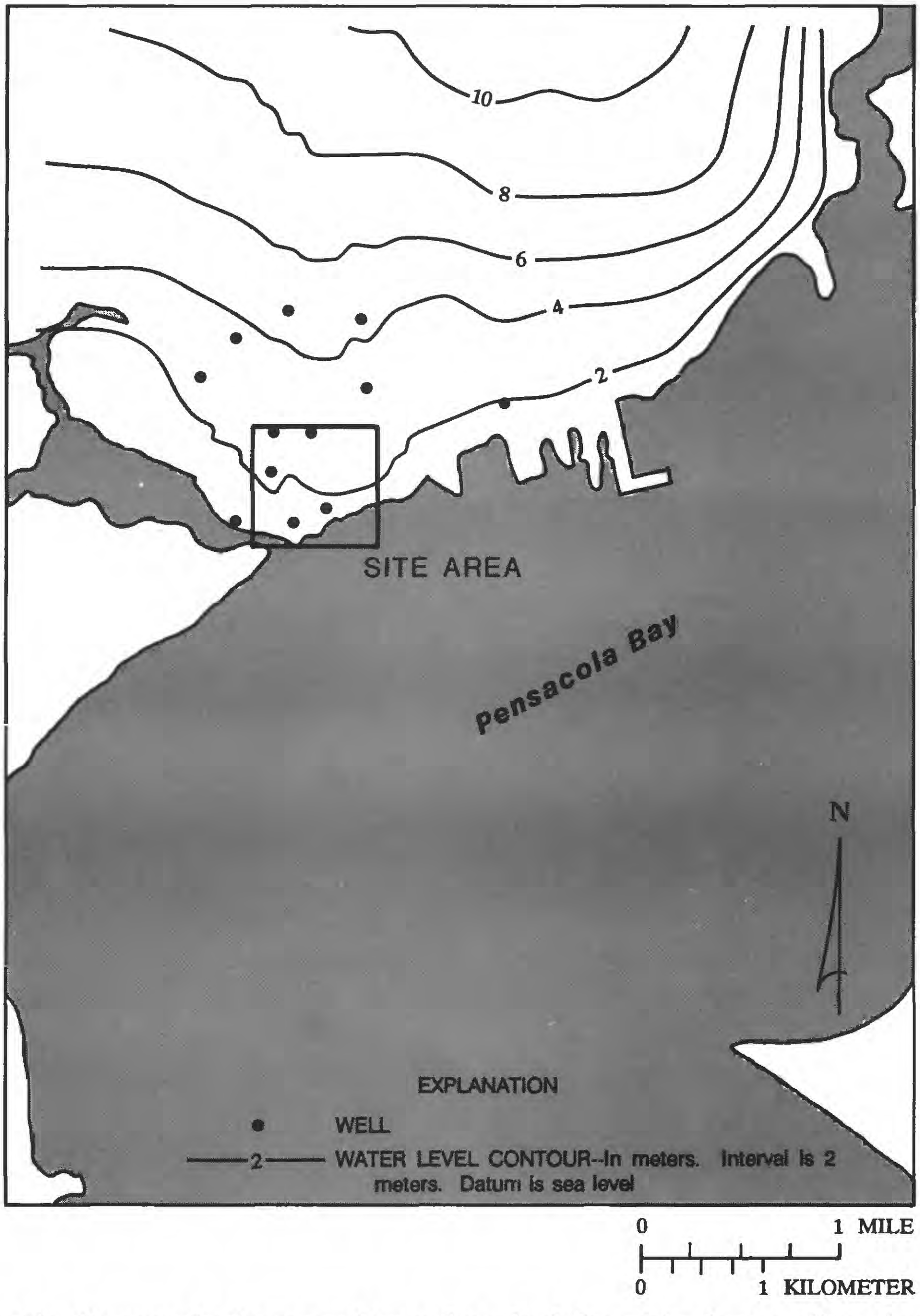

Figure 20.—Contours for the water-table configuration in layer 1 for the area of investigation.

tional control was provided by few surface-water features (swamps), although the area contains no natural lakes or rivers within it. The water-table surface is influenced by topographic features, especially the coastline of Pensacola Bay and the adjacent bayous. Figure 19 also indicates the influence of the small drainage ditch in layer 1 on flow south of the site. The flow in layer 1 is to the south-southeast. Near the coastline and offshore in Pensacola Bay the vertical hydraulic gradient is upward in layer 1; to the north of the coastline the gradient is downward toward layer 2.

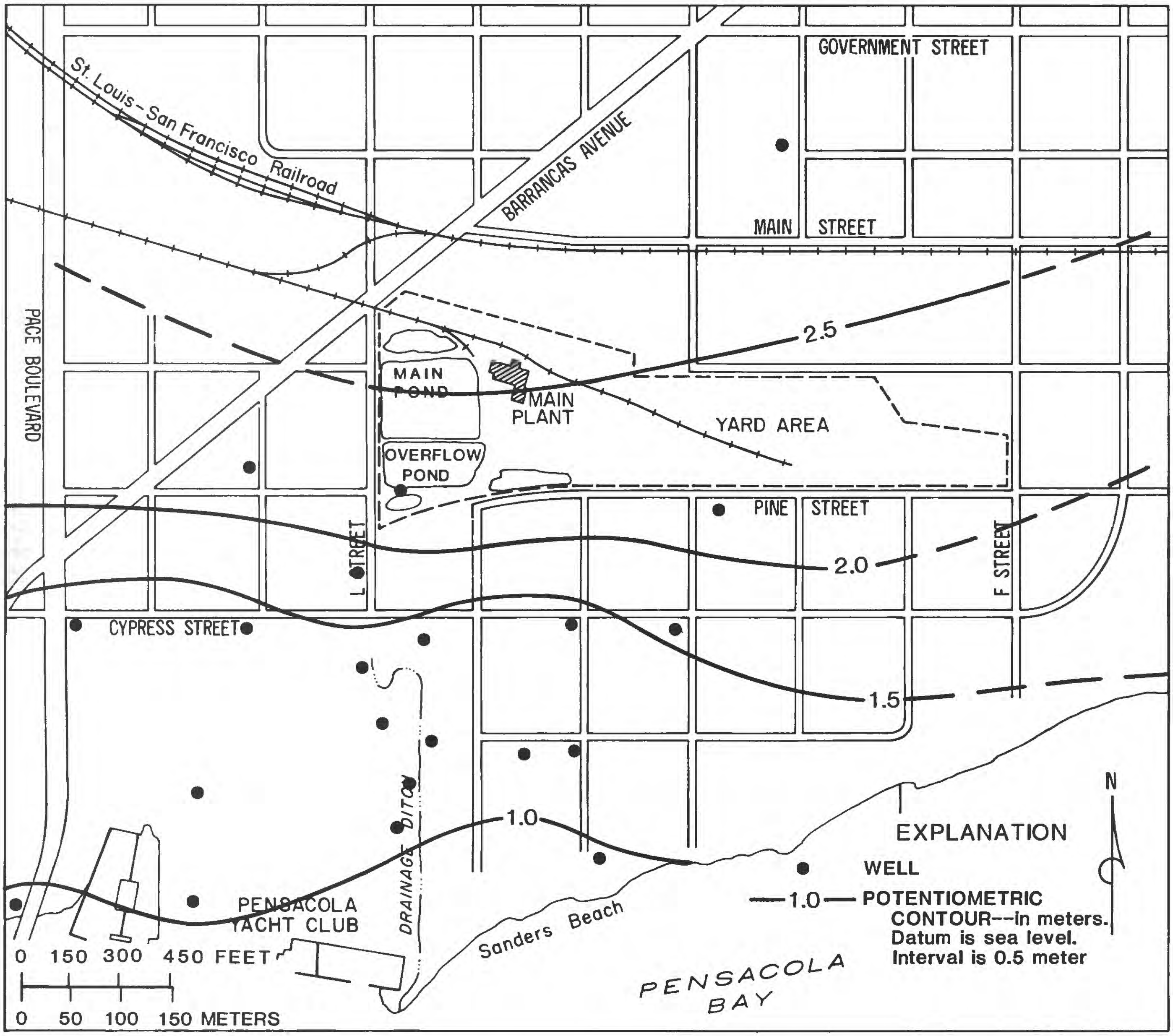

Figure 21.—Contours for the potentiometric surface for layer 2 in the site area.

The layer 2 potentiometric surface map for the site area was based on 21 data points (fig. 21). This surface parallels that for layer 1, except for the influence of the coastline and the drainage ditch on heads in layer 1. The potentiometric surface for the area of investigation is based on an additional six measurements shown outside the site area (fig. 22). Flow in layer 2 is also to the south-southeast. The vertical movement of water into and out of layer 2 is downward from layer 1 in the north and upward into layer 1 near the coastline and offshore Pensacola Bay. The only evidence of

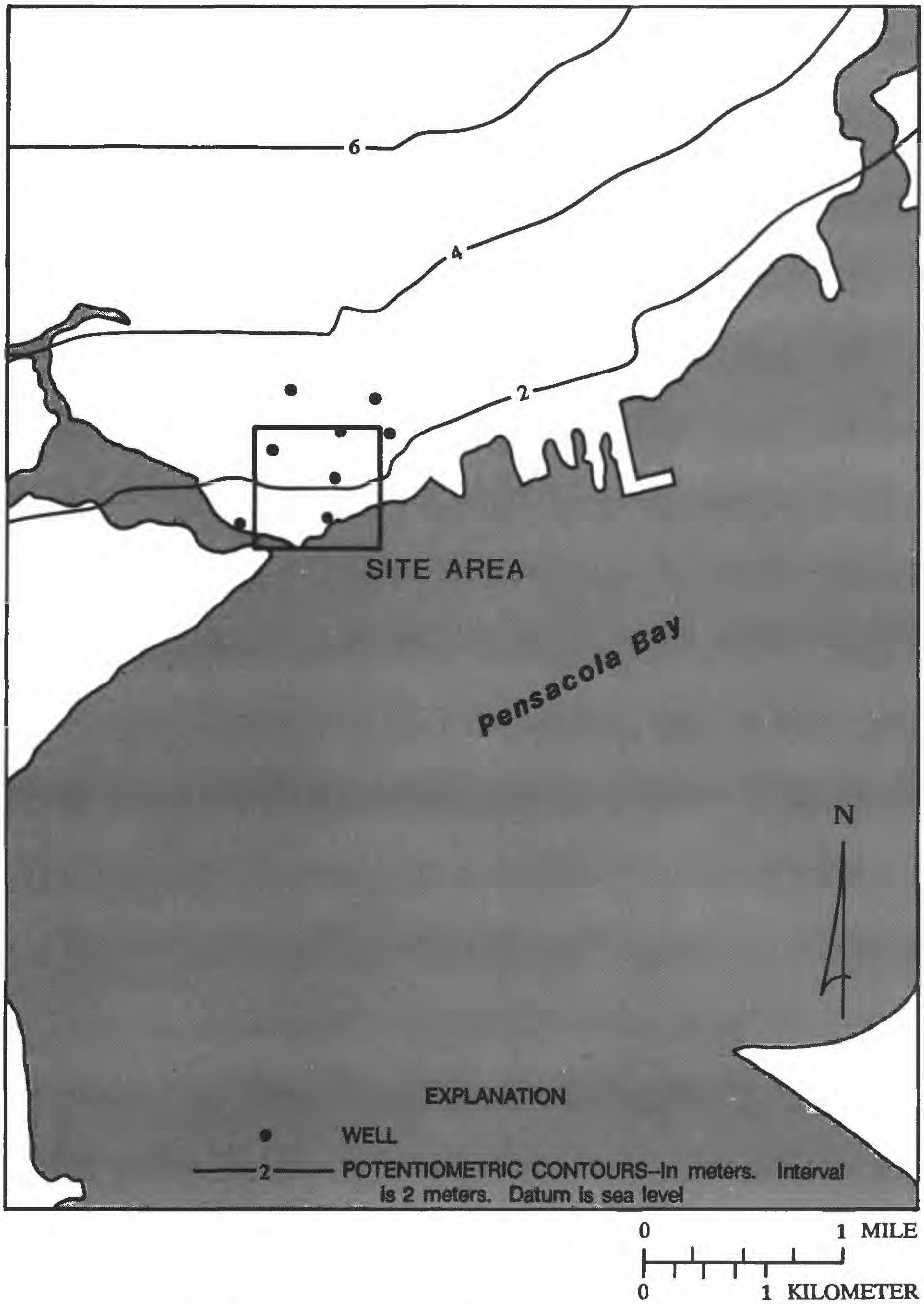

Figure 22.—Contours for the potentiometric surface for layer 2 for the area of investigation.

topographic influence on flow in layer 2 is the general similarity of the flow surface to that of layer 1, reflecting the subdued influence of topography at depth.

Vertical gradients between layers 1 and 2 can be seen by comparing figures 19 and 21, and figures 20 and 22. In the northern part of the area of investigation, there is an average of 0.1 m/m (meter per meter) gradient downward into layer 2. This relatively high gradient is in part a result of discontinuous but thick (up to 10 m) confining clays in layer 1 in the northern part of the area of

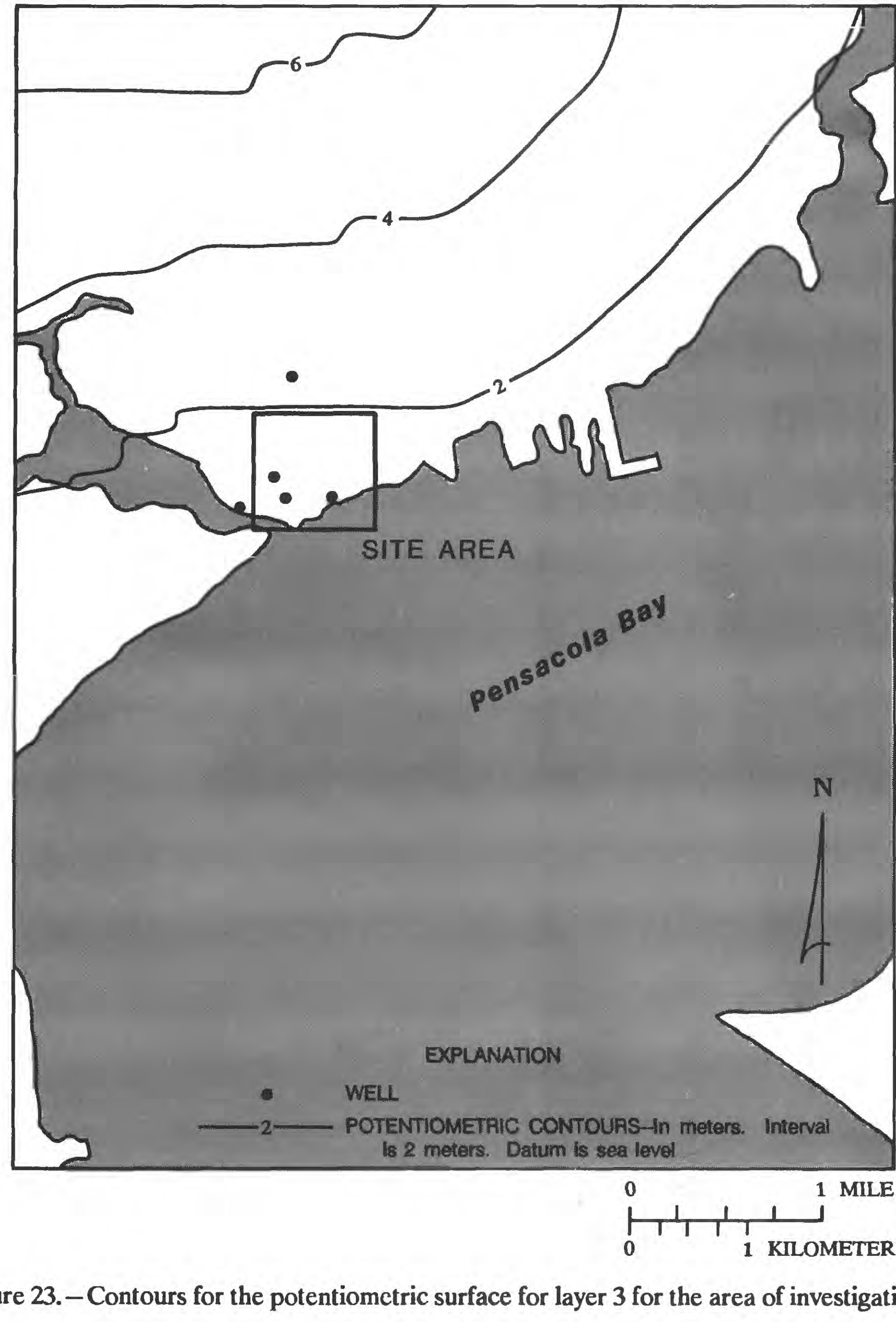

Figure 23.—Contours for the potentiometric surface for layer 3 for the area of investigation.

investigation. These clays significantly reduce vertical hydraulic conductivity where they are present. Moving south, the vertical gradient gradually decreases, reversing to an upward direction indicating discharge from layer 2 to layer 1 near the top of the drainage ditch in the site area. Discharge gradients are estimated to be about 0.02 m/m offshore in Pensacola Bay.

Layer 3, the main producing zone, has the least available data, but is the simplest flow regime. Water levels were obtained from eight wells, and the potentiometric surface is presented only at the scale of the area of investigation (fig. 23). Flow in layer 3 is to the south-southeast, approximately parallel to the coastline as in the upper two layers. As in the overlying layers, the general vertical movement of water is downward in the northern part of the area of investigation and upward in the southern, offshore areas. There appears to be little or no influence of topographic relief on the potentiometric surface of layer 3.

Vertical gradients between layers 2 and 3 are evident by comparing figures 22 and 23. The average vertical gradient in the northern part of the area of investigation is 0.02 m/m downward into layer 3. Moving south, the gradient gradually-decreases to an upward, discharge direction near the coastline. Discharge gradients are estimated to be about 0.01 m/m offshore in Pensacola Bay.

All three layers have similarly shaped potentiometric surfaces that indicate ground-water flow generally to the south, discharging into Pensacola Bay. Perturbations in water-level surfaces shown on the site maps of layers 1 and 2 are probably a function of the large amount of available data for the site rather than local anomalies of the flow system. A comparison of water-level surfaces among all three layers confirms that recharge is dominant over most of the area of investigation, with downward movement of water from layer 1 into layer 2 into layer 3. Within about 300 m of the coastline, this relationship is reversed, with upward movement of water (discharge) from layer 3 into layer 2 into layer 1.

During this study, continuous water-level records were collected from several wells, both to determine periodic (seasonal) variations during the study period and to document the effects of tidal fluctuations. The seasonal range was about 1 m during the period of record (1983–84), as measured at wells set in the water table (layer 1) and the intermediate zone (layer 2). Figure 24 presents hydrographs for wells 10 (layer 1), 13 (layer 2), and 900 (layer 2). These hydrographs are representative of water-level variations during the period of investigation. The January 1986 water levels in these wells are very close to the mean water levels during the period of record:

		Water levels (in meters above sea level)	
Well	Layer	January 1986	Mean (1983–84)
10	1	2.5	2.6
13	2	1.4	1.4
900	2	1.8	1.7

In order to determine diurnal (tidal) influences on head in the aquifer, water levels near the coast were determined (fig. 25), and two cross sections of water levels perpendicular to the coastline were developed. Wells 19 (layer 1) and 20 (layer 2), which are close to the coast, have the maximum amount of tidal influence. Tidal effects attenuate rapidly inland, particularly in layer 1, as illustrated in figures 26 and 27.

Tidal effects are one of the factors affecting head distributions in the water table (layer 1) near the small drainage ditch which nearly bisects the southern half of the site area (fig. 2). Flow in the ditch is influenced by stormwater influx, ground-water seepage, and tidal variations. Discharge measurements were made throughout a range of rainfall and tidal events. Inflow through a culvert at the head of the ditch was fairly uniform, about 0.001 to 0.002 m^3/s (cubic meter per second), except during very brief and intense rainfall events. Discharge along the entire reach of the ditch was generally uniform over a range of tidal conditions, varying from a minimum of about 0.002 m^3/s to about 0.009 m^3/s during this investigation. Although there were subtle differences in discharge between low and high tide conditions (probably because of greater inflow of bay water and increased bank storage during high tide), the overall small volume of flow in this drainage ditch did not justify more extensive investigation of the flow.

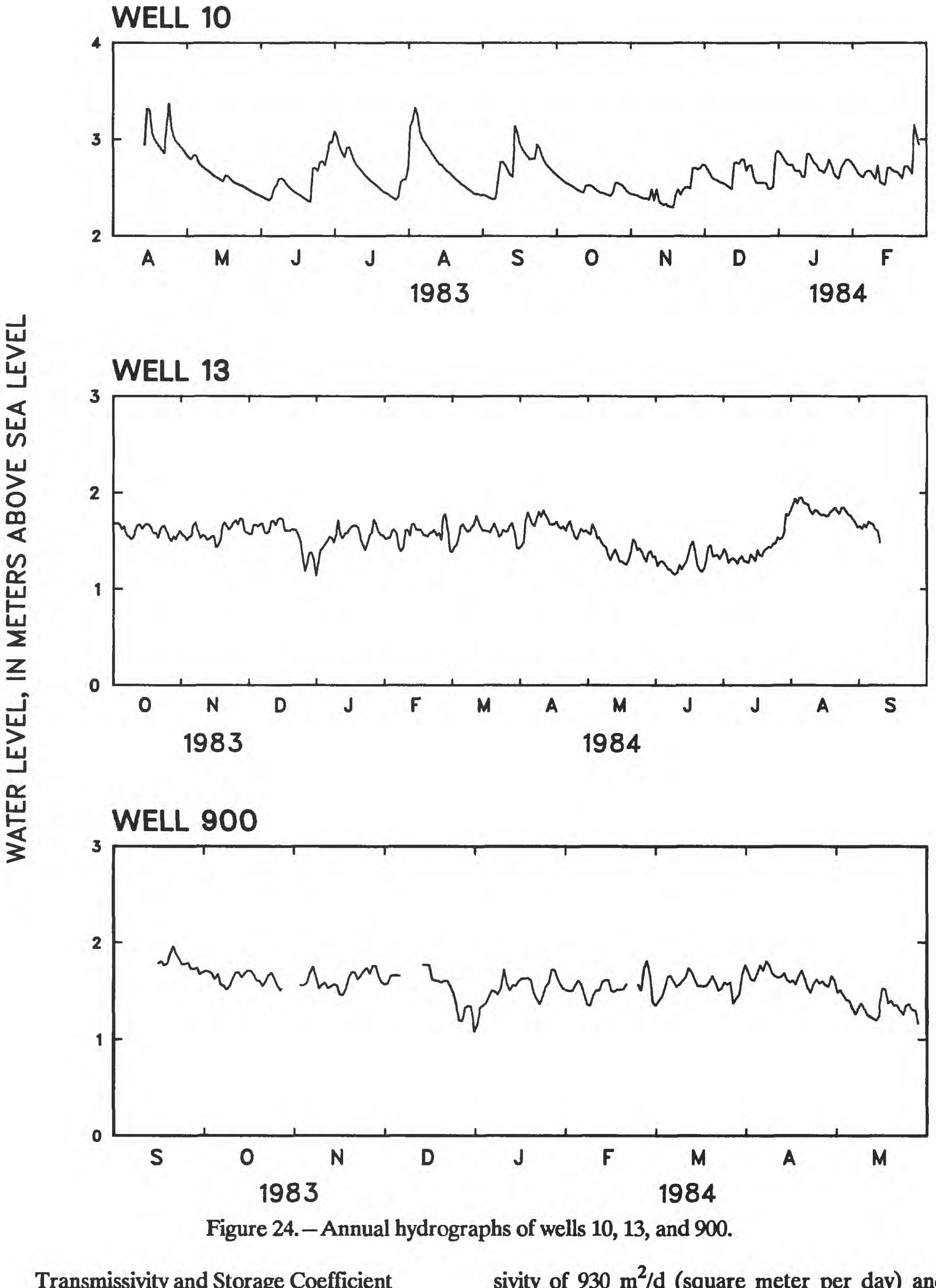

Figure 24.—Annual hydrographs of wells 10, 13, and 900.

Transmissivity and Storage Coefficient

Most of the available data on hydraulics of the sand and gravel aquifer are from analyses of aquifer tests in layer 3 by Jacob and Cooper (1940). They obtained average values of transmissivity of 930 m^2/d (square meter per day) and storage coefficient of $6x10^{-4}$, based on tests of nine large-capacity wells in Pensacola. These tests were all conducted on wells tapping the deepest layer of the aquifer, the main producing zone.

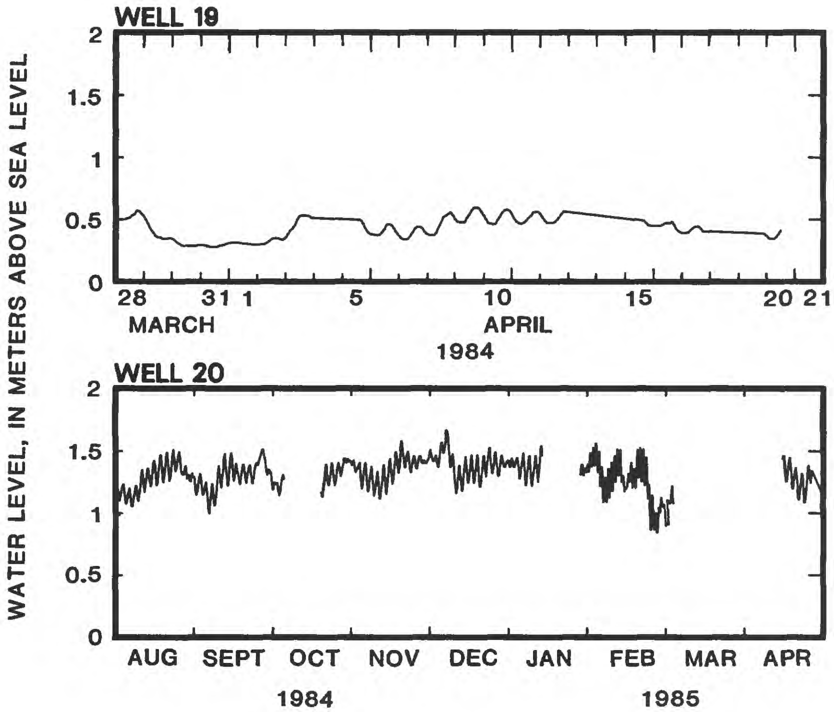

Figure 25. – Hydrographs of wells 19 and 20.

Trapp and Geiger (1986) report transmissivity values ranging from 500 to 3,500 m^2/d in southern Escambia County, based on specific-capacity data and estimates from geophysical and lithologic data from layer 3.

An aquifer test performed during this investigation tested the hydraulic properties of layer 2. Well 1500 was pumped, and water levels measured at wells at sites 15, 16, and 17. From this test, transmissivity was estimated to be 210 m^2/d, and the storage coefficient estimated to be $2x10^{-4}$. Based on an average aquifer thickness of 14 m in the test area, hydraulic conductivity of the tested aquifer is about 15 m/d (meters per day). The hydraulic conductivity was assumed to be representative of layer 2 throughout the area of investigation.

Hydraulic conductivity in layer 1 was initially estimated to be the same as in layer 2. Both layers were observed to have slightly higher silt and clay content and lower hydraulic conductivity than the more transmissive material in layer 3.

Recharge

The ground-water system in the area of investigation receives freshwater from two sources, rainfall and boundary inflow. Rainfall in the Pensacola area averages 155 cm/yr (centimeters per year) (National Oceanic and Atmospheric Administration, 1982). During the period June 1984 through June 1986, a rainfall gage in the site area measured an annual average of 147 cm/yr. The gage was located on "L" Street on the west berm of the main pond. Estimates of average annual evapotranspiration in the area range from a maximum evaporation of about 120 cm/yr (Visher and Hughes, 1975) to a minimum of about 75 cm/yr (Hughes, 1978). The latter value is a minimum based on subtracting Hughes estimate of maximum average annual runoff (75 cm/yr) from his estimate of average annual rainfall (150 cm/yr). Dohrenweld (1976) published a similar minimum value of 85 cm/yr evapotranspiration. Thus, between 35 and 79 cm/yr, on the average, is available for runoff and ground-water recharge. Of this total, based on

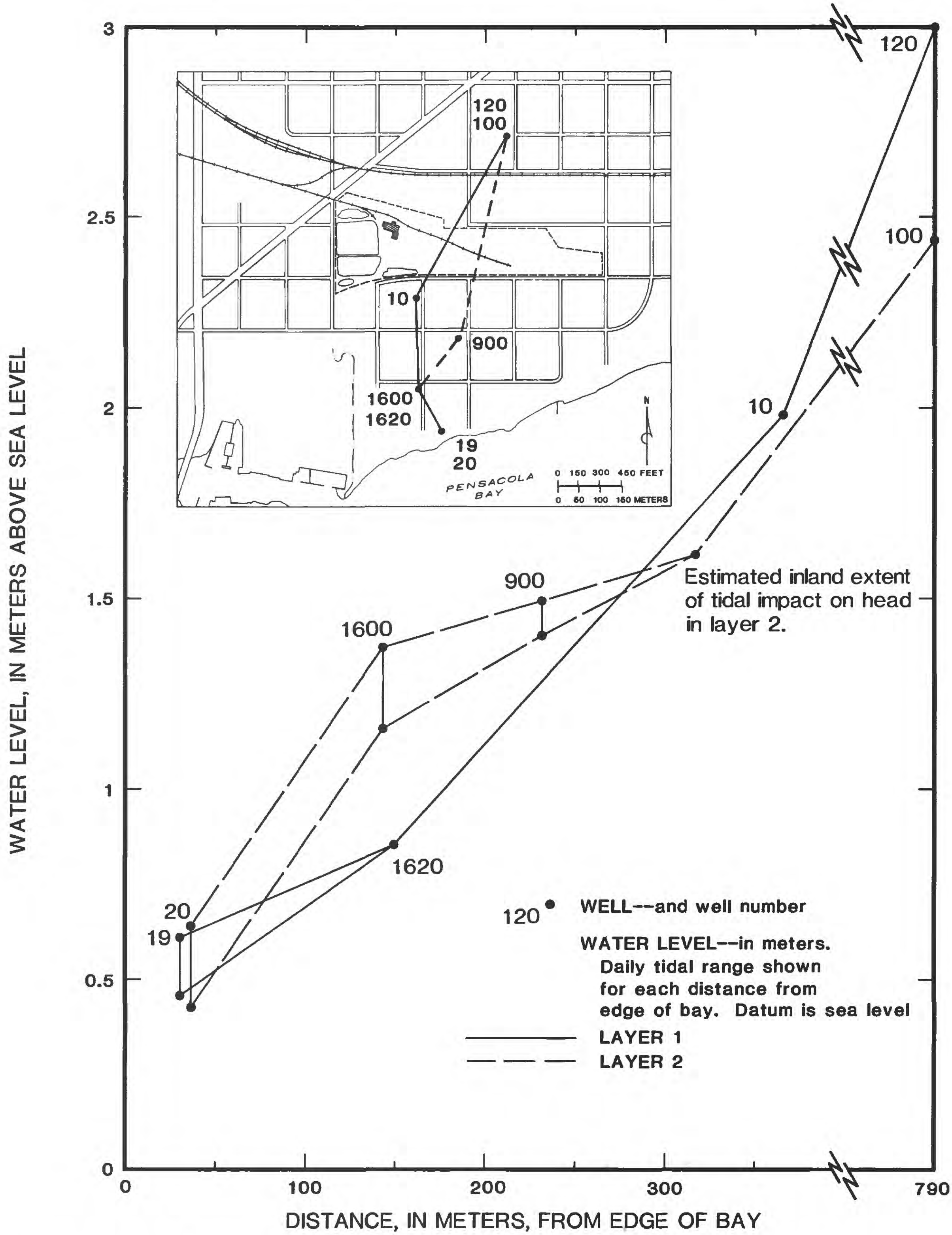

Figure 26.—Profiles of water-level ranges indicating tidal influence in layers 1 and 2 along the east edge of the site area.

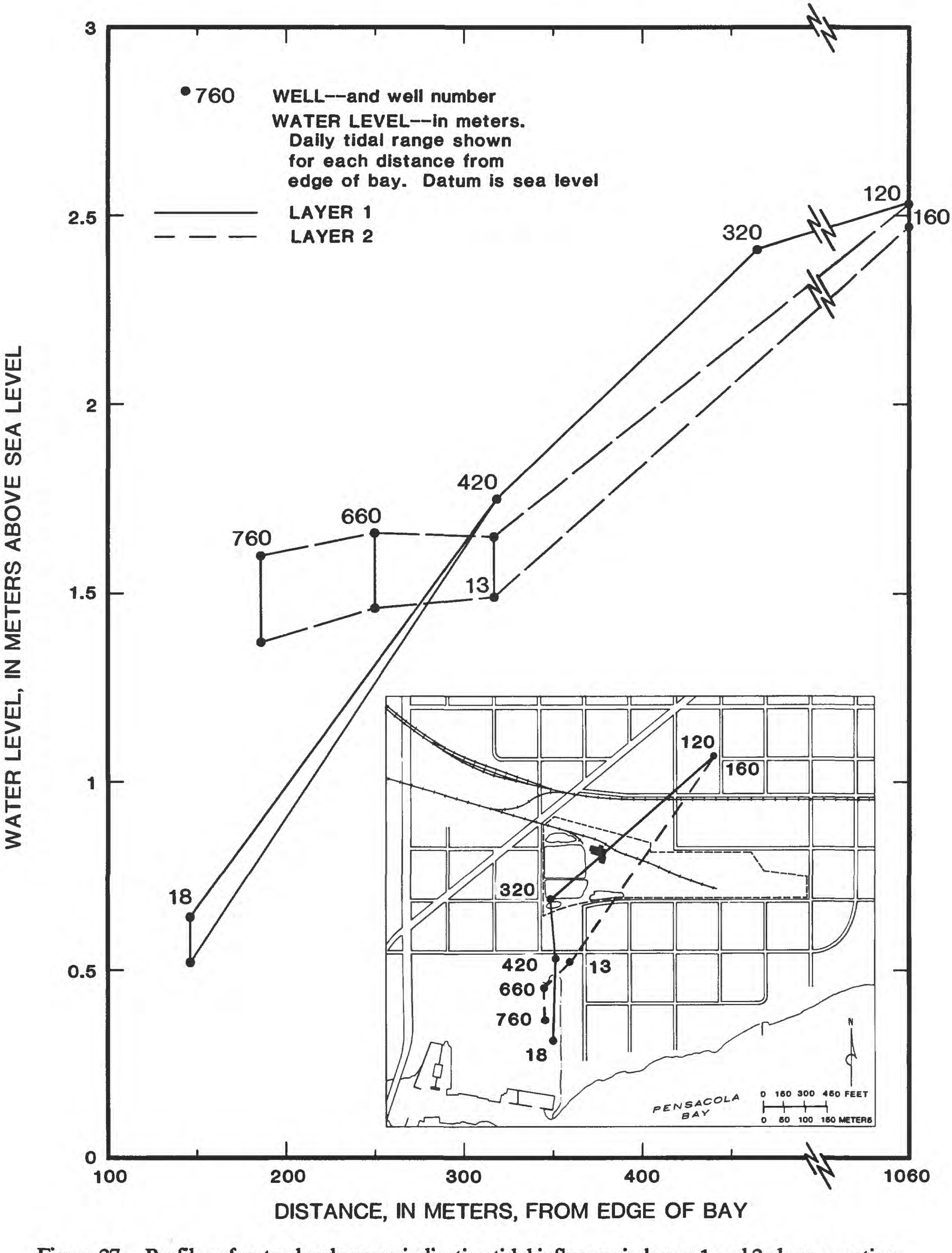

Figure 27.—Profiles of water-level ranges indicating tidal influence in layers 1 and 2 along a section affected by the drainage ditch.

estimates of land use and percent impervious cover over the entire area of investigation, about 50 percent is surface runoff to stormwater drains and 50 percent is recharge to the surficial aquifer. Estimated annual ground-water recharge over the area of investigation is, therefore, between 18 and 39 cm/yr. Because of a relatively large percentage of impervious cover in the site area, a value of recharge of 20 cm/yr, near the lower end of the estimated range, was considered most reasonable for the area. Although recharge in the northern part of the area of investigation is probably greater than elsewhere, because of the increased vertical gradient at the greater elevations a single value was chosen due to the sparse data.

Saltwater Interface

In the water-table zone, the saltwater interface is assumed to be nearly identical with the coastline. The difference between the saltwater head and the equivalent freshwater head is considered negligible because of the shallow water depth offshore, dilution and mixing, and the scale of the area of investigation.

The deeper parts of the aquifer (model layers 2 and 3) also contain an interface between the freshwater and saltwater somewhere to the south in Pensacola Bay or further out in the Gulf of Mexico, but its precise limits and position are uncertain.

The only available data at depth are for Santa Rosa Island, in the southeast part of the area of investigation, where the extent of freshwater in the deeper aquifer is defined based on chloride content of water samples collected during well construction. Heath and Clark (1951, p. 26) present the following data collected during the period February 21–March 11, 1940:

Depth of sample, in meters	Hydrogeologic unit in this report	Chloride concentration, in milligrams per liter
6.4	Layer 1	10
23	Layer 2	4,150
27	..do...	6,650
32	..do...	12,600
36	..do...	16,100
56–58	Layer 3	830
76–77	..do...	3,500
91	..do...	1,130

They point out that the last three samples may have been diluted with freshwater from drilling fluids. Another factor is that, below 52 m, the aquifer is fine grained, with clay and silt dominant. The lower chloride concentrations in these depths may represent fossil water not yet totally flushed from the less permeable parts of the aquifer. Consequently, the lower samples are not considered to be representative of the aquifer water under steady-state conditions.

The only other prior work on the deeper part of the sand and gravel aquifer near the saltwater interface is an analysis of freshwater found at Fort Pickens (just beyond the southwest corner of the area of investigation) at a depth of 90 m. Carbon-14 analyses of the water indicated an age of about 9,000 years, suggesting that its source may be an isolated lens of fossil freshwater that entered the aquifer when sea level was lower. Other wells on Santa Rosa island are reported to contain saline water at the same depth (U.S. Geological Survey, 1975, p. 91).

SIMULATION OF THE GROUND-WATER FLOW SYSTEM

Ground-water flow in the sand and gravel aquifer in southern Escambia County has been previously simulated. Trapp (1978) reported an investigation of the southern half of the county, including construction and calibration of a preliminary digital model of the aquifer. His principal assumption was that the main producing zone (layer 3, this report) could be treated as a discrete, leaky confined aquifer. He assumed constant head boundaries around most of the aquifer's borders and concluded that the two-dimensional treatment used was inadequate to realistically simulate flows in the aquifer.

Consequently, Trapp and Geiger (1986) applied a two-layer, three-dimensional digital model to the sand and gravel aquifer in southern Escambia County (see fig. 1 for their study area). One layer was the main producing zone, as before. An upper layer represented the overlying remainder of the aquifer (equivalent to layers 1 and 2, this report), including the heterogeneous, discontinuous unconfined, leaky confined, and perched zones found throughout the aquifer system. The two layers are coupled by a leakance matrix, with steady-state flow assumed throughout the aquifer. The model was calibrated for 1972 pumping, and tested by simulating pumpage during the periods 1939–40, 1958, and 1977. Sensitivity analyses showed that water levels in both model layers were most sensitive to variations in recharge and least sensitive to leakage along rivers in the area.

Most of the grid blocks in the Trapp and Geiger model are about 1,600 m by 1,600 m. The area simulated in this report represents about 4 percent of the Trapp and Geiger model area (fig. 1). Because of the significant scale difference between their regional model and the simulations discussed in this report, and the additional data collected during this investigation, direct comparisons of model input or simulations are not meaningful. Generalized comparisons of aquifer characteristics, water budget, and conclusions derived from each model are made, as appropriate, later in this report.

Three-Dimensional Flow

In order to synthesize the available hydrogeologic data, a three-dimensional ground-water flow model was used to simulate flow in the area of investigation. The simulation calculates the hydraulic head in the aquifer at specified locations under steady-flow conditions, based on available data on hydraulic properties, boundary conditions, and ground-water inflow and outflow for the modeled area. A block-centered finite-difference approach developed by McDonald and Harbaugh (1984) was used. The strongly implicit numerical procedure was used to solve the set of algebraic difference equations representing ground-water flow.

The differential equation describing three-dimensional movement of constant density fluid in a porous medium is

$$\frac{\partial}{\partial x} K_{xx} \frac{\partial h}{\partial x} + \frac{\partial}{\partial y} K_{yy} \frac{\partial h}{\partial y} + \frac{\partial}{\partial z} K_{zz} \frac{\partial h}{\partial z} - W(x,y,z) = S_s \frac{\partial h}{\partial t} \quad (1)$$

where K_{xx}, K_{yy}, and K_{zz} are the principal components of the hydraulic conductivity tensor aligned with the principal Cartesian coordinates x, y, and z; h is the hydraulic head in the aquifer; W(x,y,z) is a flux per unit volume and represents sources and sinks to the aquifer; S_s is the specific storage of the porous medium; and t is time. For this investigation, it is assumed that the simulations represent steady-state conditions, based on evaluation of the hydrologic data presented earlier in this report, and, therefore, that there is no observable change in head versus time. That is $\partial h/\partial t = 0$ and, therefore, $S_s \partial h/\partial t = 0$.

Assumptions and Limitations

Model analysis and results are subject to the following assumptions and limitations.

- Only the aqueous flow system is being simulated. Nonaqueous phase liquids (contaminant fluids) are not part of the aqueous flow system and are not considered here.
- The estimated saltwater-freshwater interface is at equilibrium. Its position is fixed and represents the southern extent of the freshwater flow system.
- The sand and gravel aquifer in the area of investigation can be treated as multilayered, with water moving in a horizontal plane in each layer, and water moving vertically through confining beds between layers.
- The aquifer is treated as three permeable layers, separated by less permeable confining units. The layers and confining units correspond to the lithologic stratification presented in figure 4.

Any model requires a series of simplifications to fit the real ground-water flow system into the idealized model simulation. Figure 28 shows the conceptual model of the aquifer in a typical cross section and the corresponding idealization of that section for modeling. The section includes areal recharge, boundary inflow from the north, leakage between layers, no flow beneath the aquifer, and freshwater-saltwater interfaces to the south. These features are also shown in areal view (figs. 28c and 28d) and discussed in detail in the following section.

Boundary Conditions and Finite-Difference Grid

The limits of the modeled area would ideally correspond to natural hydrologic boundaries of the system being simulated. Because the contaminated area is so small, it was not possible to simulate natural boundaries near the site. Use of artificial boundaries on such a small scale could totally constrain the simulations and produce reproducible, and meaningless, results. Thus the model area was chosen to correspond to the much larger scale of the area of investigation. On this scale, model boundaries were chosen to cor-

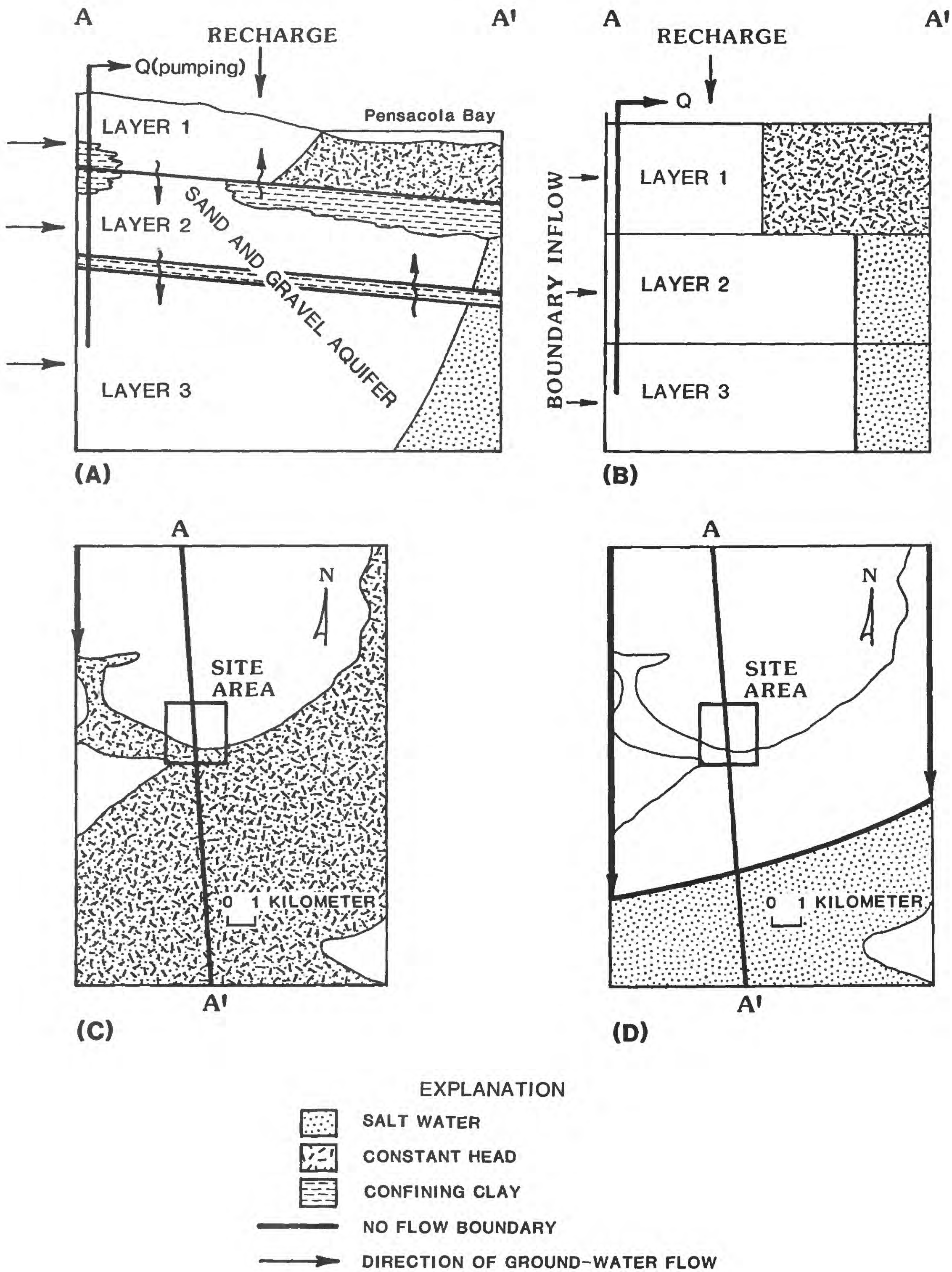

Figure 28. Conceptual representation of the aquifer, including boundary conditions in the area of investigation, and idealized representation in the model: (a) conceptual cross section, (b) idealized model cross section, (c) conceptual areal view of layer 1, and (d) conceptual areal view, layers 2 and 3.

respond to natural aquifer boundaries where possible and to areas likely to be beyond the effects of expected hydrologic stresses on the site area.

Each of the three layers in the sand and gravel aquifer has its own set of unique boundary conditions. The size of the area of investigation is based on an attempt to select the best boundary conditions for each layer. The types of boundary conditions used are specified flux and specified head. Their use in the model application is summarized in figure 28 and discussed below.

Uniform areal recharge into the system is an example of a specified (constant) flux boundary. Ground-water recharge is assumed uniform over the entire area of investigation.

A specified, and constant, head boundary is used when a part of the boundary of an aquifer system coincides with a surface of constant known head. About 40 percent of the nodes in layer 1 are treated as constant head, corresponding to the uniform head in Pensacola Bay to the south and in Bayou Chico and Bayou Texar on the west and east boundaries, respectively.

A no-flow boundary is a special case of a specified flux boundary with a flux of zero. There are several no-flow boundaries present in the model. The lower boundary of the modeled area is the Pensacola Clay, a thick, impermeable confining unit which is treated as a no-flow boundary. Flow velocity vectors drawn along the east and west boundaries of layers 2 and 3, and the north part of the west boundary of layer 1, are stream lines, and by definition no components of flow can cross stream lines. Water is moving parallel to the model borders in these areas, and a no-flow boundary may be used. Other no-flow boundaries include the southern border of layers 2 and 3 where the saltwater interface is encountered. The freshwater-saltwater boundary is assumed stationary, at equilibrium, and with no mixing zone.

The northern boundary in all three layers consists of a specified head. Because there are no nearby natural hydrologic boundaries to the north, it is necessary to estimate boundary inflow into each model layer of the aquifer based on the configuration of the potentiometric surface for that layer. The specified head boundary is actually a more general case of the constant head boundary condition, allowing head to be specified as a function of position and time over a part of the boundary surface of a ground-water system. Since this simulation is steady state, head does not change with time, and head can be specified as a function of position alone.

The variable finite difference grid chosen for this study consists of 38 rows by 32 columns. Rows are numbered from north to south, 1 through 38; columns from west to east, 1 through 32. Position of the grid for the area of investigation is shown in figure 29. Node dimensions vary from 460 m by 460 m to 60 m by 60 m. In the site area, which is the primary area of interest, the nodes are 60 m on each side immediately south of the impoundments, and gradually increase in length and width farther away from the contaminated area (fig. 30). Data input to the model and model results will be discussed throughout the remainder of this report for the area of investigation and for the more detailed site area, as appropriate.

Hydrogeologic Data

The model was constructed to evaluate steady-state conditions using data collected during January 1986. The starting head for each node in each of the three layers was obtained by superimposing the appropriate finite-difference grid (figs. 29 and 30) on the potentiometric surface maps for that layer and determining the average head for each node.

Types of data used in the model are summarized in table 4. These data are discussed, as appropriate, for both the site and the area of investigation, for layers 1, 2, and 3, in turn. Most of the data are concentrated in the site area, particularly for layers 1 and 2. Many parameters are regionalized (assumed constant) for the area of investigation.

Table 4.—*Lithologic and hydrologic model input data*

Lithologic or hydrologic parameter	Aquifer layer
Hydraulic conductivity	1, 2
Transmissivity	3
Base of permeable layer	1, 2
Top of permeable layer	2, 3
Leakance between layers	1/2, 2/3
Recharge	1
Pumping wells	3
Impoundments	1

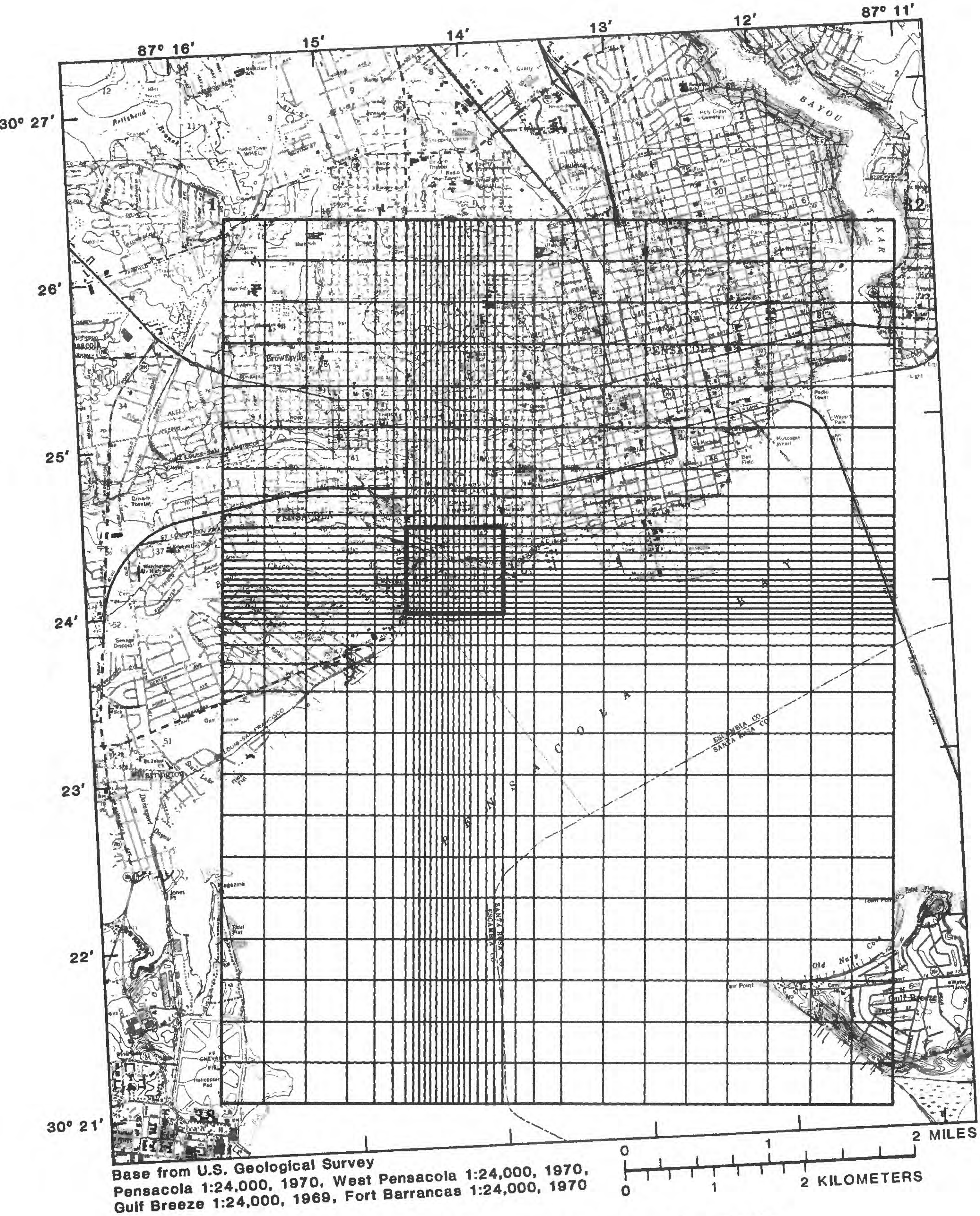

Figure 29.—Finite difference grid for the area of investigation.

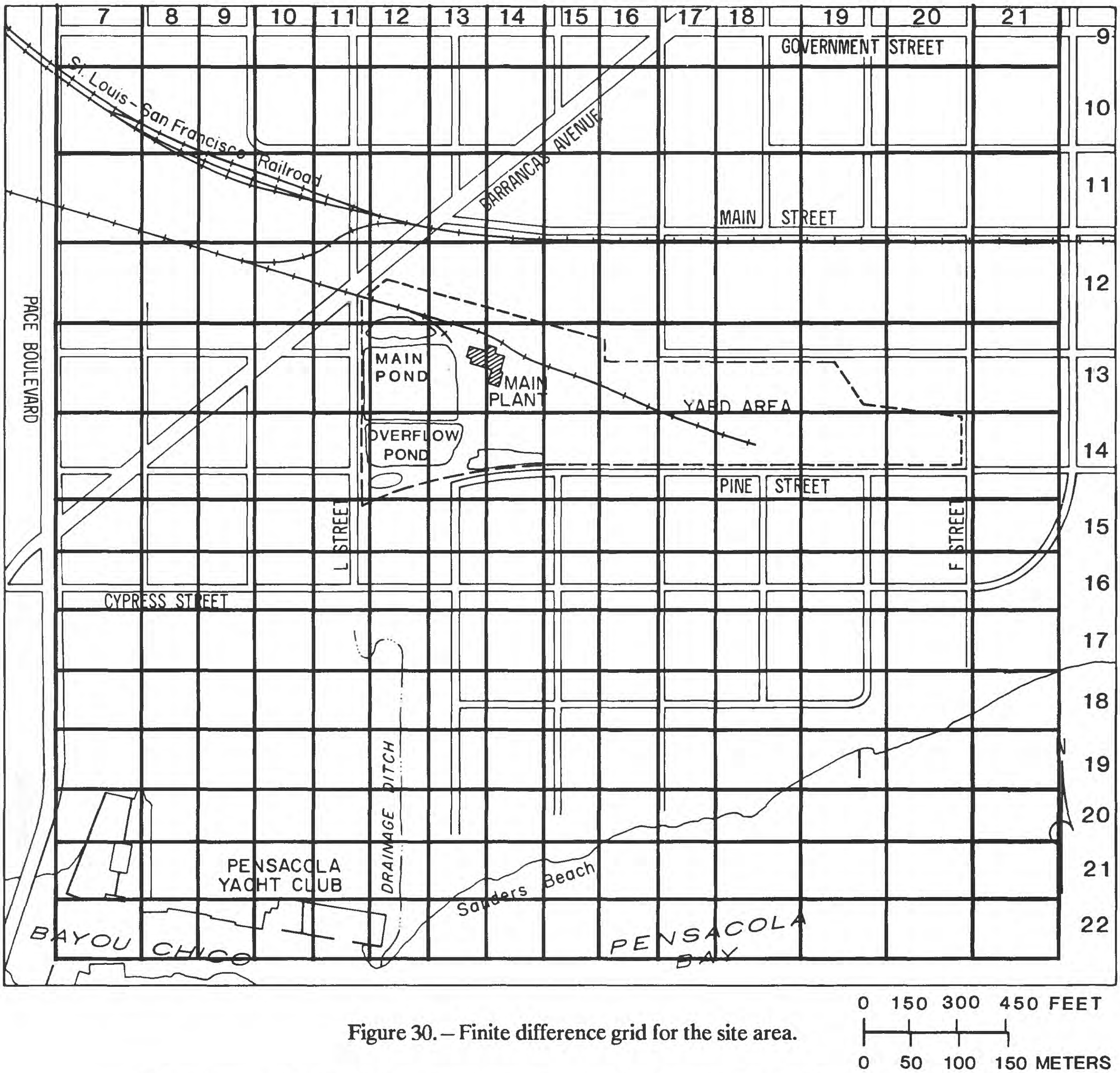

Figure 30. – Finite difference grid for the site area.

The best known data for all three layers, even in areas of the model with minimal data coverage, are the potentiometric surfaces. Lithologic data (tops, bases, and thicknesses of the layers) are also well defined. Other parameters (including hydraulic conductivity of layers 1 and 2, transmissivity of layer 3, and leakance between the permeable layers) were estimated based on minimal hydrologic data. These values were then refined by trial and error during model calibration. Calibration consists of comparing simulated heads, layer by layer, against observed heads (head distributions contoured from field measurements), and will be discussed in greater detail later in this report.

The minimal data available on the location of the freshwater-saltwater interface did not permit a definitive description of its location. The area of investigation chosen was sufficiently large to include an interface position as its southern, no flow, boundary. This boundary was chosen at a location near the estimated position of the interface. During model calibration, the southern model boundary was moved toward and away from the coast. There was no observable effect of the movement of the southern, no-flow boundary on the heads in site area.

Boundary Inflow

As discussed earlier, there are no nearby natural hydrologic boundaries to the north. It is thus necessary to estimate ground-water flow into each model layer based on an estimate of flow, node by node, using Darcy's Law, in the form:

$$Q = \frac{K\, b \Delta y \Delta h}{\Delta x} \qquad (2)$$

where

Q = flow (cubic meter per day);

K = hydraulic conductivity (meters per day);

b = thickness of aquifer layer (meters);

Δy = width of node rectangle, right angles to direction of flow (meters);

Δx = distance between boundary node and adjoining node used to determine external head (meters); and

Δh = difference in head between external and boundary node (meters).

Based on this equation, initial ground-water flow into each layer was calculated using the potentiometric surfaces shown in figures 20, 22, and 23.

Estimated flows across the northern boundary for each layer are 3,700 m^3/d (cubic meter per day) (layer 1), 7,100 m^3/d (layer 2), and 11,300 m^3/d (layer 3). These values are also calculated during the simulations, and are further discussed in an evaluation of the water budget for the entire flow simulation later in this report.

Recharge, Pumping, and Surface-Water Data

An initial uniform areal value of 20 cm/yr into layer 1 was used for recharge. The impoundments are estimated to contribute an average of 1.7 m^3/d directly into the aquifer, based on historical estimates described earlier. This input was evenly distributed into model nodes (13,12), (13,13), (14,12), and (14,13).

There are seven city wells in the area of investigation, but only three were actively pumping during the period of this investigation (city 4, 5, and 8 in fig. 6). Since the aquifer is believed to approach steady-state conditions within a few weeks of continuous pumping (Jacob and Cooper, 1940), average daily pumping rates were determined for the year prior to January 1986. These values of discharge are 7,400 m^3/d (city 4), 4,200 m^3/d (city 5), and 6,800 m^3/d (city 8).

A drainage ditch south of the impoundments at the creosote site also affects hydraulic head, primarily in layer 1. The effects of the ditch on the ground-water flow system were simulated. Required data input includes head (altitude) of the ditch along each node (reach), hydraulic conductance (C) of ditch bed material, and the altitude of the bottom of the ditch. Stage is an average value for all discharge measurements made.

$$\text{Conductance } C = \frac{KLW}{M} \qquad (3)$$

where

K = hydraulic conductivity of the riverbed (meters per day),

L = length of reach (meters),

W = width of ditch (meters), and

M = thickness of bed material of the ditch (meters).

Using this equation, average conductance was estimated to be:

$$C = \frac{4.6 \cdot 61 \cdot 3}{9} = 90 \ m^2/d$$

The hydraulic conductivity of 4.6 m/d was estimated based on analysis of sediment cores from the bed of the ditch.

Transmissivity and Hydraulic Conductivity

The transmissivity of layer 1 is a function of hydraulic conductivity and aquifer thickness, both of which vary throughout the area of investigation. Hydraulic conductivity, although variable over the area of investigation because of the highly heterogeneous nature of the sand and gravel aquifer, was initially assumed constant (and equal to 23 m/d). This assumed value was based on an evaluation of all available field and laboratory analyses presented earlier in this report. Inasmuch as the primary purpose for selecting the large area of investigation was to include significant geologic variations and hydrologic boundaries that would best define the regional flow in the aquifer, it was decided to simplify the initial value for hydraulic conductivity (and other parameters) where possible in order to improve our concept of the regional ground-water flow, at the possible expense of slightly reduced accuracy near the site.

Aquifer thickness is computed by the model, which subtracts the computed water-table head from the lithologically defined bottom of the layer (fig. 13). In general, the actual thickness of layer 1 was considered fairly uniform (about 15 m over much of the area of investigation), but the layer thins seaward (to about 8 m) as the underlying confining bed thickens.

The initial value for hydraulic conductivity was selected as 15 m/d in layer 2. Figure 14 was used to delineate the top of layer 2. The base of layer 2 was defined to be at 34 m below sea level throughout the area, primarily to simplify evaluation of the data below the contaminated part of the aquifer. The thin clay lens at this depth was observed in every lithologic log from wells in the site area and was confirmed in numerous other well logs in southern Escambia County (Jeffry Wagner, Northwest Florida Water Management District, written commun., 1985). Layer 2 is similar in configuration to layer 1, with a thickness of about 27 m in the north, gradually thinning to about 12 m in the southern parts of the area of investigation.

Initial transmissivity in layer 3 was set equal to 930 m^2/d. This value is representative of the main producing zone of the aquifer, based on available aquifer test analyses.

Leakance

Although the sand and gravel aquifer has been divided into three layers for simulation purposes, the entire system is hydraulically interconnected, with vertical flow both within and between layers. For this simulation, it is assumed that lateral flow dominates within each aquifer layer because of the greater transmissivity of the layers as compared to the intervening confining units. Vertical flow dominates in confining layers because of their comparatively low transmissivity. A leakance value was assigned for the confining units between layers 1 and 2, and also between layers 2 and 3. The former consists of an array which takes into account some of the known areal lithologic variability. Leakance is lowest in the northern nodes, and highest in the southern part of the modeled area. The clay is assumed to be present, although discontinuous, where data are not available offshore. The leakance between layers 2 and 3 is represented in the model by an areally uniform value because available data indicate that the confining clay unit between layers 2 and 3 is fairly uniform over the entire area of investigation.

Initial values for leakance were estimated from available confining unit hydraulic conductivity and thickness data. Leakance in the model is defined as the vertical hydraulic conductivity divided by the thickness of an intervening confining unit between two aquifers (McDonald and Harbaugh, 1984). The leakance between layers 1 and 2 was initially estimated to range between $1x10^{-4}$ (m/d)/m (meter per day per meter) where the confining unit is thick in the north, to $1x10^{-3}$ (m/d)/m for the remaining part of the area of investigation. Leakance between layers 2 and 3 was initially estimated to be $1x10^{-3}$ (m/d)/m throughout the area of investigation. These values correspond to a vertical hydraulic conductivity in the confining unit between layers 1 and 2 of 0.001 m/d, assuming an average clay thickness of 10 m and 1 m respectively; and in the confining unit between layers 2 and 3 of 0.003 m/d, assuming an average clay thickness of 3 m.

Model Calibration

To demonstrate that the simulation model is realistic, model computations must be compared with field observations. Calibration is the attempt to minimize differences between the observed and computed potentiometric surfaces by adjusting appropriate parameters. Although there are a large number of interrelated hydrologic variables affecting ground-water flow, which tend to make the calibration process a somewhat subjective experience, the degree of adjustment of any particular parameter is related to the uncertainty of its value. Values of relatively well-known parameters (like lithologic data, or pumping rates in city production wells) were not adjusted. Poorly known values (like recharge) were adjusted over their probable range.

The primary objective in the calibration procedure is to improve our conceptual model of the aquifer. Alternate concepts of steady-state flow conditions, such as different boundary conditions, were tested during calibration and were helpful in modifying and improving understanding of the ground-water flow system.

In order to evaluate these alternate concepts of the aquifer system, the remainder of this chapter is divided into three parts. First, a detailed description of adjustments of model input data is presented. This includes development of the present model from earlier versions by successive modifications of the conceptual model of the aquifer and consequent adjustments to the input data, as well as a description of criteria for calibration of the flow model. In the second part, calibrated simulations are presented, including comparisons of observed and simulated heads in each layer and mass balance in terms of water budget. Finally, sensitivity analyses of selected hydrologic parameters, namely recharge, hydraulic conductivity and transmissivity, and leakance, are presented.

Adjustments of Input Data

The calibration procedure is a series of attempts to improve the fit between observed and simulated steady-state heads by adjusting initial hydrologic input to reflect improving definition of the conceptual model of the aquifer. Because the observed aquifer contamination is confined to model layers 1 and 2 in part of the site area, and consequently most of the available data are there, much of the calibration effort centered on the hydrologic input parameters that most affected layers 1 and 2 in the site area.

A series of simulations were systematically conducted to determine the effects on the model from varying parameters that control flow. The model was calibrated using the following criteria:

- Observed and simulated potentiometric surfaces were compared. A general agreement between flow directions, as well as a reasonable matchup of observed and simulated potentiometric surfaces, was required.
- The differences between observed and simulated potentiometric surfaces would agree to within one-half of the contour interval. This corresponds to 1 m as represented on the area of investigation maps, and is a reasonable goal over much of the model area. Near the site, however, the residuals were minimized to 0.25 m, equal to one-half of the contour interval represented on the site maps. Comparisons between observed water-level measurement data (where available) and simulated heads at nodes were found to be more useful than a comparison of potentiometric surfaces, particularly in layer 1, because few data were available in the northern half of the area of investigation.
- The location of the transition between recharge and discharge areas in the simulations also had to agree with field observations. The known steady-state transition typically occurs about 300 m inland from the coast near row 16 in the site area. A model run was considered acceptable when the transition from recharge to discharge (as determined by direction of flow between model layers) occurred within one node (60 m) of row 16.
- Finally, the residuals for each layer and for the overall simulation were compared. Residuals are the differences between the observed and the simulated values, at each node, and are a measure of the relative error of the simulation. The run was considered acceptable if the number of positive residuals was within 25 percent of the number of negative residuals. If this criterion was not met, then the areal pattern of residuals would be mapped to analyze the source of error.

After the present boundary conditions were determined, adjustments were made to most of the aquifer parameters as part of the calibration procedure. Calibration of the three-dimensional model, however, required careful analysis of all results to determine all of the effects of varying a given parameter. For example, optimizing the composite effect of hydraulic conductivity did not result in minimizing the effect on each of the three layers individually. It was not uncommon, in fact, to minimize residuals in one layer at the expense of accuracy in another. Also, it was observed that the hydrologic parameters could be divided into two groups, as far as calibration criteria were concerned. The hydraulic conductivity of layers 1 and 2, and leakance between layers 1 and 2, were found to be the primary controls on shape of the simulated surfaces. Other parameters, including transmissivity of layer 3, recharge, and leakance between layers 2 and 3, were found to influence the overall range in residuals between surfaces rather than the shape of the surfaces. All of the latter parameters were treated as uniform areal values.

Recharge was varied over the entire range of reasonable rates, 18 to 39 cm/yr. No attempt was made to areally distribute recharge, because of the lack of information, and because such differentiation was not needed to adequately calibrate the model. The best fit in the calibration procedure was determined to be a recharge rate of 28 cm/yr. Simulations were found to be very sensitive to variations in recharge rate.

Hydraulic conductivity of both layers 1 and 2 was initially varied areally over the entire likely range of values, 9 to 27 m/d. The agreement between observed and simulated potentiometric surfaces was extremely poor, probably because of the failure of the model to consider known aquifer heterogeneities. Consequently, available lithologic data were used to define areal differences in the hydraulic conductivity for each of the layers. Two areas, in particular, are known from field data to be clay-rich, with consequent reduced hydraulic conductivity, in layers 1 and 2: the northeast corner of the area of investigation (fig. 9, cross section Y–Y′), and the coastal area within the site area (fig. 17). Sediments in layers 1 and 2 have a greater clay content at the site and in other areas near the coast than the equivalent surficial aquifer sediments farther north. The best fit for layer 1 is for hydraulic conductivity ranging from 18 m/d over much of the area to as low as 2.0 m/d in the clay-rich northeastern section of the area (fig. 31). In layer 2, the optimal values for hydraulic conductivity range from 23 m/d over most of the area to a low of 8 m/d in the sediments near the site (fig. 32).

While testing variations in hydraulic conductivity, the model was found to be extremely sensitive to leakance between layers 1 and 2. An array of leakance (between layers 1 and 2) values was constructed similar to the array for hydraulic conductivity for layer 1 (fig. 33). Because the leakance was one of the least-known parameters, it was extensively adjusted during the calibration process. The resulting calibrated values vary from a maximum of $1x10^{-3}$ (m/d)/m which exists over most of the area to a minimum of $2x10^{-4}$ (m/d)/m in the northern six rows of the model, where shallow confining units are typically thicker and more extensive than elsewhere in the area (section Y-Y′, fig. 9). These leakance values correspond to a vertical hydraulic conductivity ranging between $1x10^{-3}$ m/d in the northern nodes to $2x10^{-3}$ m/d over most of the model area. These values are very similar to the initial estimates for vertical hydraulic conductivity.

Leakance between layers 2 and 3 was treated as areally uniform because lithologic data indicated that the confining clay unit is fairly continuous. Because of the lack of detailed field data at depth in the aquifer, leakance between layers 2 and 3 was varied extensively during the calibration process over similar ranges as the leakance between layers 1 and 2. A value of leakance between layers 2 and 3 of $1x10^{-3}$ (m/d)/m was found to result in the best simulation, indicating that the confining beds at depth are comparable in leakance to the more shallow clays. This value corresponds to a vertical hydraulic conductivity of $3x10^{-3}$ m/d, which is identical to the initial estimate. This value is quite similar to the value of $1.86x10^{-3}$ (m/d)/m used in earlier simulations (Trapp and Geiger, 1986) for part of their model corresponding to the northern half of this study.

Variations in values of transmissivity for layer 3 used in the simulations did not significantly affect the calibrations. Transmissivity was varied between 560 and 1,100 m^2/d, corresponding to the range reported in the area by Trapp and Geiger (1986) in their model calibration. The initially determined value of 930 m^2/d was considered appropriate in the calibrated model. Given an effective thickness of 30 m for layer 3, this corresponds to a hydraulic conductivity in layer 3 of about 30 m/d. The calibrated hydraulic conductivity data for the sand and gravel aquifer thus agrees with the geologic observation that the aquifer is vertically stratified overall, with the shallow zones (layers 1 and 2) somewhat greater in clay content and consequently of slightly lesser hydraulic conductivity than the deeper parts of the aquifer (layer 3).

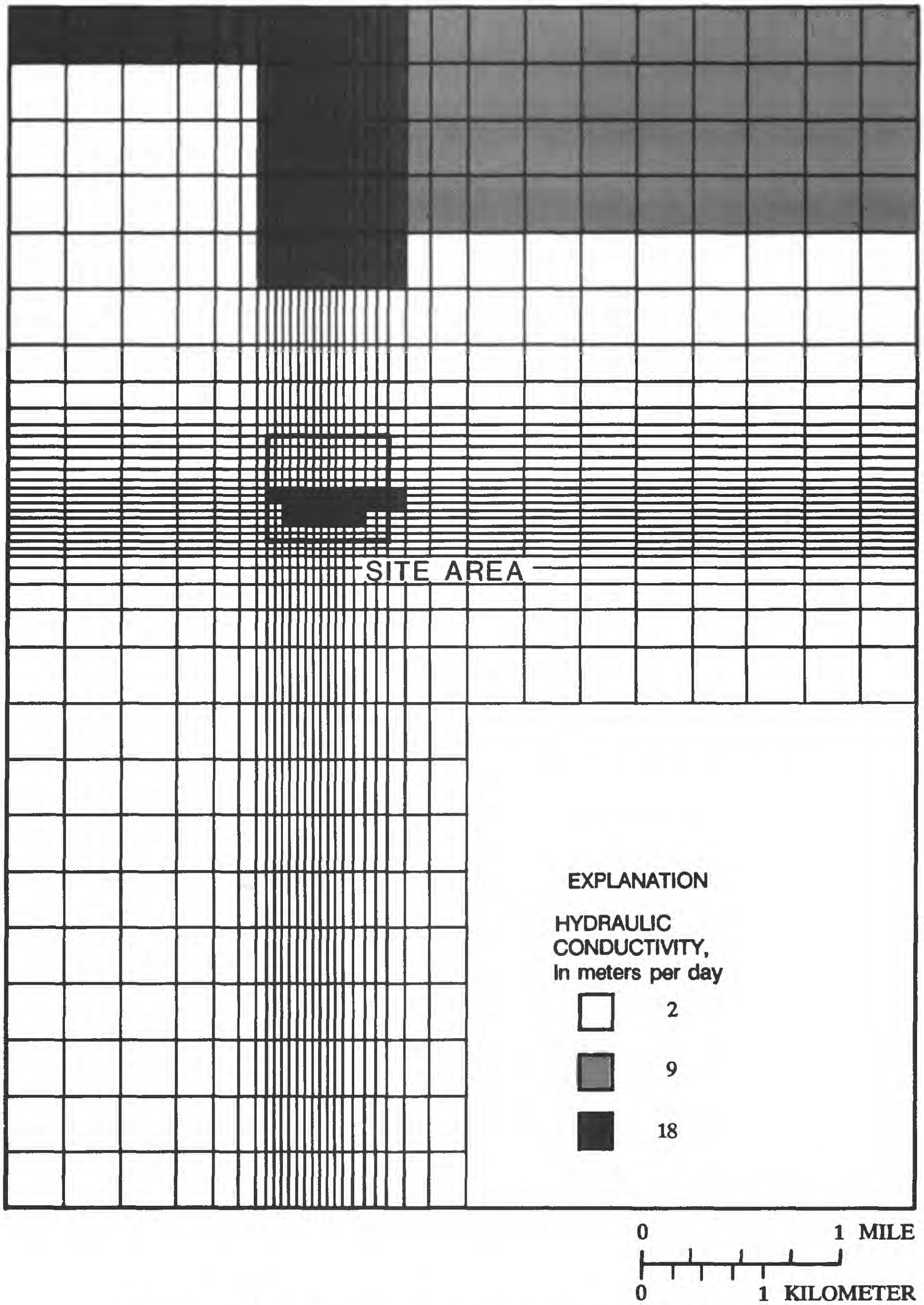

Figure 31.—Distribution of hydraulic conductivity of layer 1.

Results

When calibration of the steady-state model was judged to be complete, the absolute error was 0.37 m overall. Within each layer, the residual was 0.40 m (layer 1), 0.34 m (layer 2), and 0.37 m (layer 3). Overall, the criteria listed earlier for defining calibration were met. Calibration within the site area was good. Some of the anomalies include a relatively poor agreement between observed and simulated heads in the northeastern part of layer 1, slightly excessive simulated heads in the northern half of layer 2, and lower simulated heads near

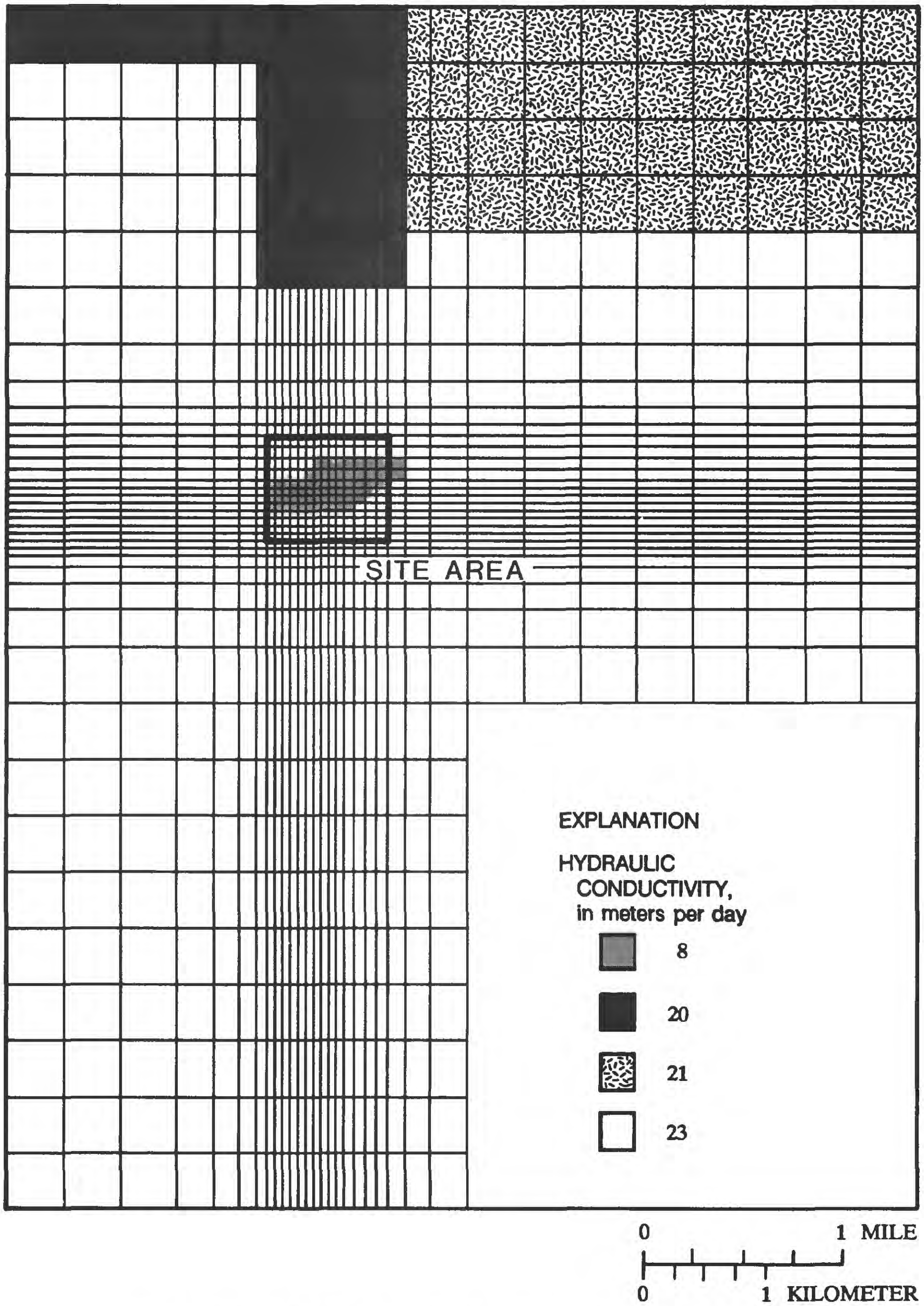

Figure 32.—Distribution of hydraulic conductivity of layer 2.

each of the city production wells in layer 3. Comparisons between observed and simulated heads will be discussed separately by layer, after a description of the overall calibration and water budget.

One criterion of calibration discussed earlier involved a check on the location of the transition between recharge and discharge areas. The calibrated model properly represents this transition, as can be seen on a north-south cross section

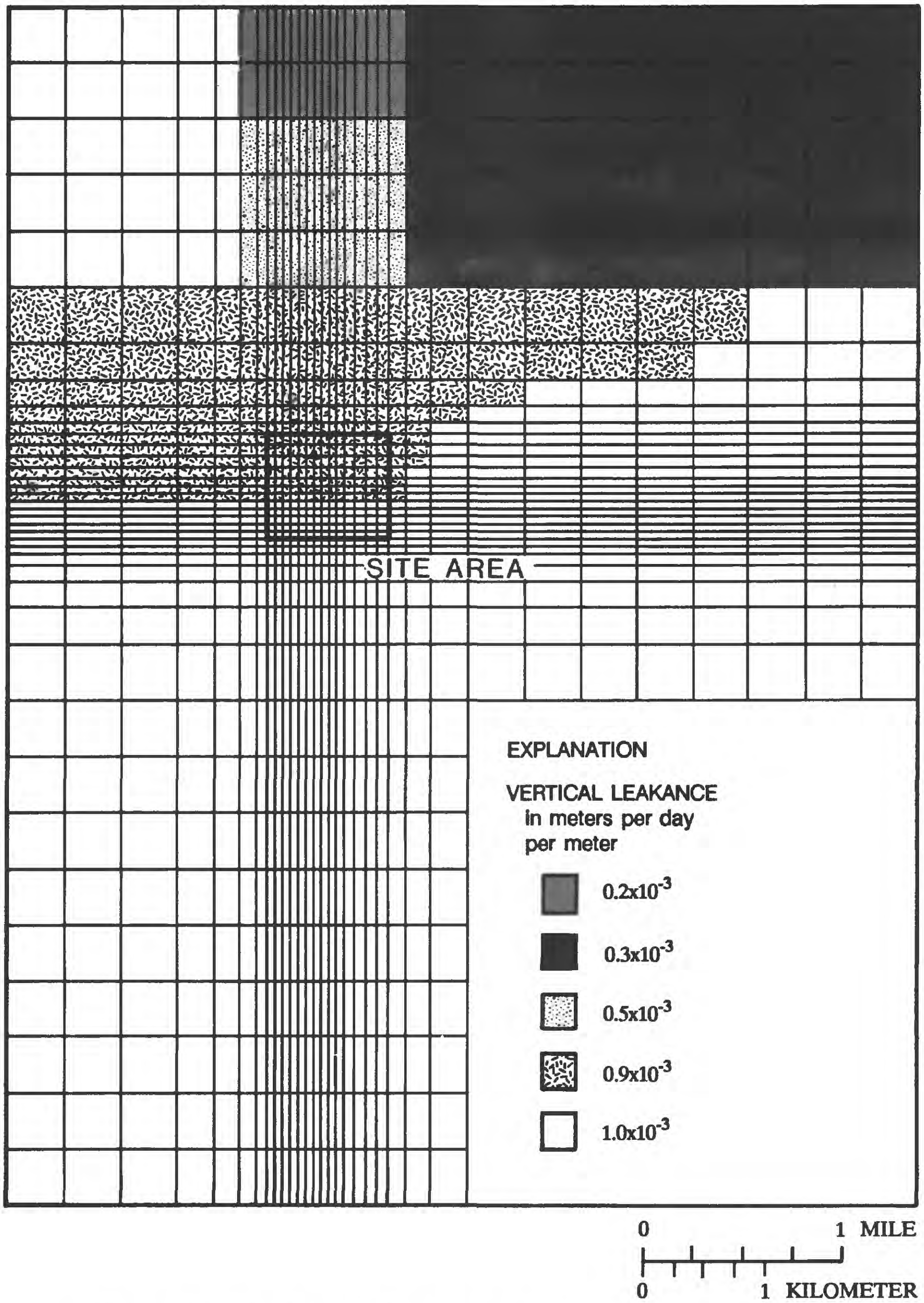

Figure 33. – Distribution of vertical leakance between layers 1 and 2.

located approximately midway in the area of investigation (fig. 34). Both observed and simulated potentiometric surfaces indicate that the transition between recharge and discharge occurs near row 16 in this part of the area, typically about 300 m inland from the coastline, at about 4,000 m on the profiles. It is evident that the hydrologic gradient in each layer is fairly smooth over most of the area, flattening out near the coastline. It should also be noted that the maximum downward vertical gradient occurs in the northern four rows, in the northern highlands, with a head difference

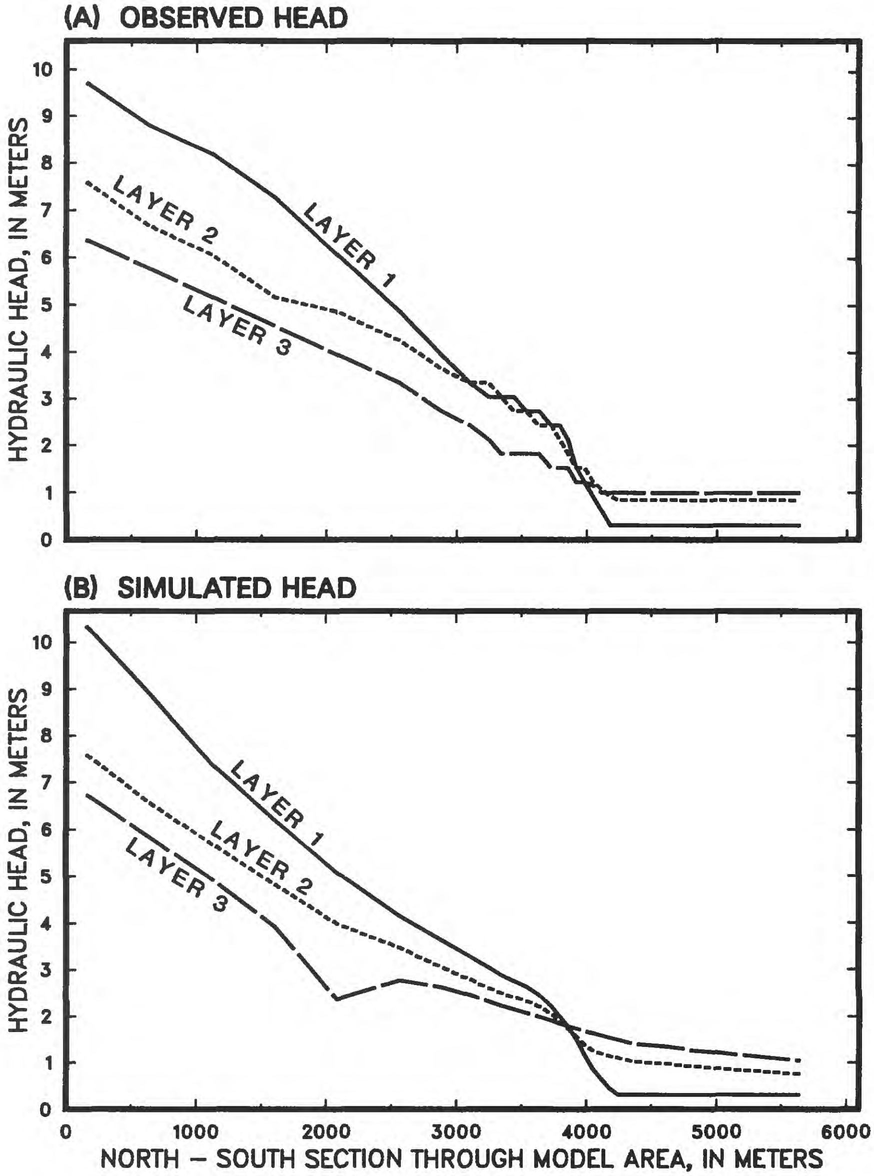

Figure 34.—Head gradients between model layers along column 15 for (a) observed heads and (b) simulated heads.

between layers 1 and 3 of between 3 and 3.7 m, and the maximum upward vertical gradients occur beneath Pensacola Bay.

The wide transition zone in the observed data between 3,200 and 4,000 m on the profile is probably a result of rounding errors in discretizing the potentiometric surfaces for the separate layers. Finally, the depression in simulated head at 2,300 m in layer 3 is a result of intersecting the cone of depression of a city production well. Observed data were insufficient to identify cones of depression from pumping wells.

A mass balance (water budget) was calculated to check the numerical accuracy of the solution and as a quantitative evaluation of the flow system (fig. 35). As part of the calculations, the net flux contributed by each part of the model was computed to determine a net hydrologic budget for the

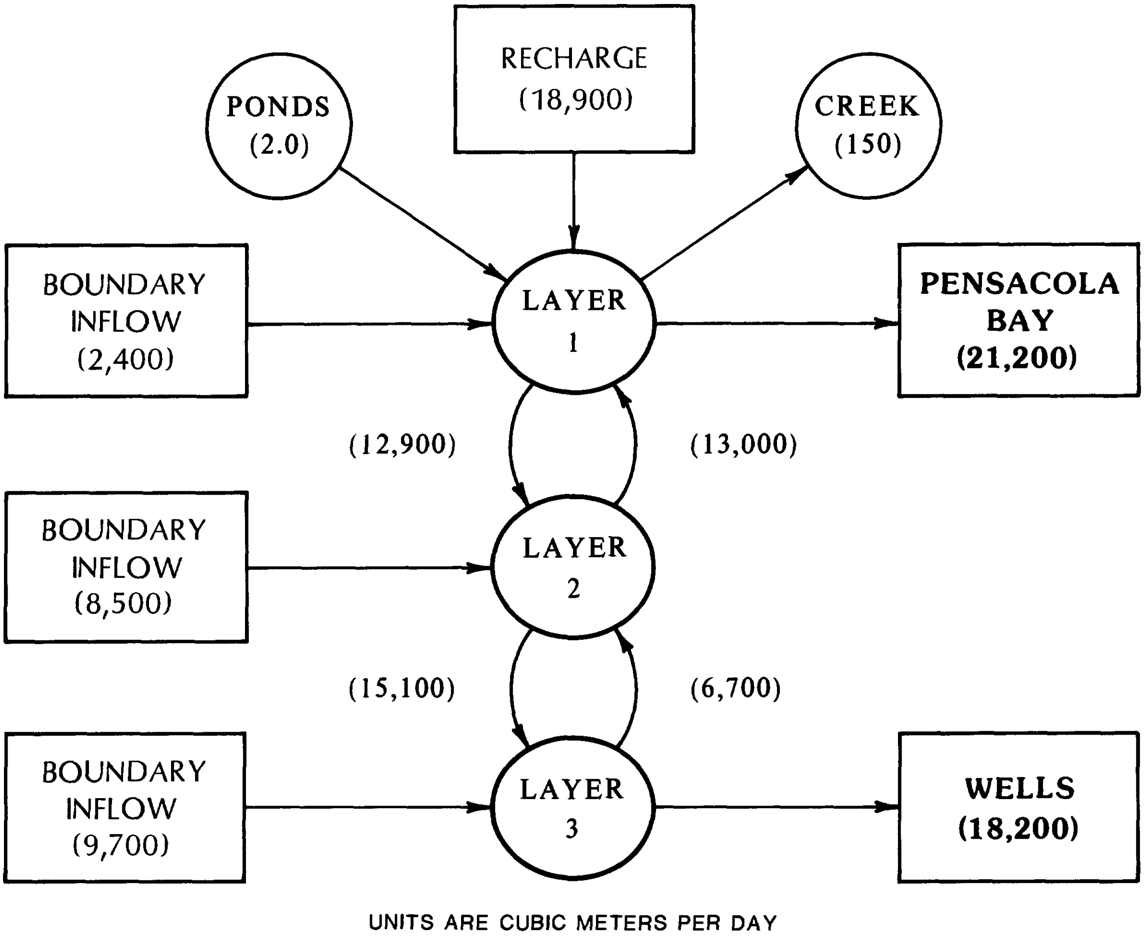

Figure 35.—Schematic water budget for the calibrated simulation.

aquifer. The mass balance shown identifies the contribution of each source and the withdrawal by each sink. It is evident that the amount of water calculated from recharge rates is comparable in volume to that calculated to enter the aquifer from boundary inflow. Also, large volumes of water flow vertically between layers in the aquifer, according to the simulation results. Although a volume of water equal to about 1.4 times the estimated recharge flows between layers 1 and 2, the net flux between those two layers is virtually zero. On the other hand, over twice as much water flows down into layer 3 than up into layer 2, primarily because of the pumping effects of the three municipal wells in the northern part of the area of investigation, which together are estimated to withdraw a volume comparable to the recharge inflow. At present there is no mechanism to verify these calculations of steady-state vertical leakage. Although these flows are the result of a calibration based on our best understanding of the flow system, the accuracy of these values is uncertain.

The simulated boundary inflow rates agree with the estimates based on calculations made from the observed potentiometric surfaces:

	Calculated, in m^3/d	Percent of total	Simulated, in m^3/d	Percent of total
Layer 1	3,700	(0.17)	2,400	(0.12)
Layer 2	7,100	(0.32)	8,500	(0.41)
Layer 3	11,300	(0.51)	9,700	(0.47)

Simulated flows into layers 1 and 3 are slightly less than the observed estimates, whereas flow into layer 2 is somewhat greater than estimated. These differences could be a result of numerous hydrologic variables, with variations in areal recharge as one likely possibility. Although recharge was treated as areally uniform, it is likely that recharge is actually greater in the less developed northern part of the area of investigation (upper 6–8 rows) than farther south in the more urbanized part of the area. Such a possibility was not considered in the model simulations.

Layer 1

A comparison between observed and simulated steady-state water-table surfaces is presented in figure 36. The residuals for this layer are 0.4 m, and there is excellent balance (within 10 percent) between positive and negative residuals. Also, the general fit of the water-table surfaces is good in

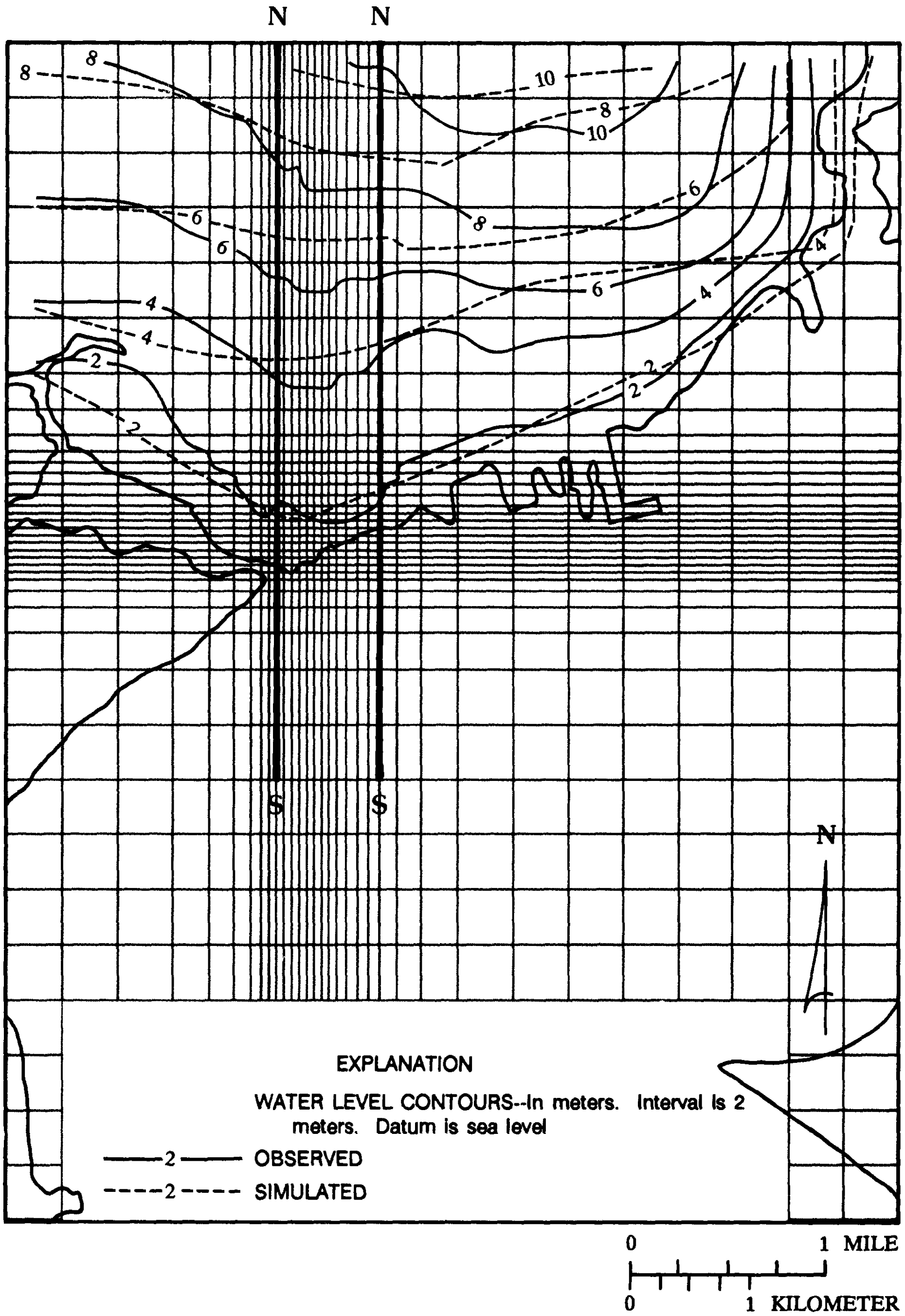

Figure 36. – Comparison between observed and simulated water-table surfaces for layer 1.

the site area and in the northwestern part of the area of investigation. Unfortunately, there are major discrepancies between the observed and simulated surfaces in the northeast and west-central model areas. These anomalies are in areas where data are minimal, and may suggest misconceptions in the assumed shape of the water-table surface in those areas. As discussed earlier, head in the upper part of the aquifer is locally variable, with sporadic perched water tables caused by local confining units.

Simulated head is generally 1.5 to 3.0 m lower in the northeast (rows 1–4, columns 21–30) than on the observed surface. Although the latter head surface is based on the best information available, the only data points in the area are actually north and west of the area of investigation (fig. 20). Extrapolation of the head surface to the area of investigation was based primarily on interpretation of topographic features. Although both observed and simulated surfaces along the west banks of Bayou Texar on the east boundary of the area indicate the occurrence of steep gradients in head, the large grid-block size in the area (460 m^2) limited the ability of the simulation to fit the observed data.

In the west-central area (rows 6–8, columns 1–4), the problem is similar, although simulated heads in this section are typically 0.9 to 1.5 m higher than observed values. The simulation has not adequately accounted for the effects of Bayou Chico on the heads.

In both areas, the paucity of data is the primary problem. Because the problem areas are well outside of the area of contamination and do not appear to have any significant effect on simulated heads in the site area, it was determined to be outside of the scope of this investigation to further evaluate which of the two water-table surfaces is more representative of field conditions.

As a further check on the validity of the calibration on layer 1, three other comparisons of the data are presented. First, to demonstrate the general fit between observed and simulated surfaces, two north-south cross sections of columns 9 and 21 were chosen (fig. 37). These columns were chosen because they border the site area, respectively, to the west and east, and include the entire contaminated area between them. The site area is located between 3,400 and 4,300 m on the profile, and is characterized by steep horizontal hydraulic gradients, relative to the remainder of the section, with a match generally within 0.25 m between the observed and simulated surfaces. The northern 6 rows are typified by a somewhat flatter head gradient and a match of no worse than 0.8 m. The simulated heads in the north are generally lower than observed heads, perhaps as a result of areal variations in recharge, discussed earlier.

The other two calibration tests involve direct correlation between observed heads and simulated results. There were 50 observed values of head available in the area of investigation. Each measurement was subtracted from the simulated head in the appropriate node to determine the residual. The mean absolute residual was 0.29 m, with a standard deviation of 0.27 m, near the desired criterion of 0.25 m. To further document the data fit, a map depicting observed water levels and the simulated water-table surface in the site area is presented (fig. 38). For 73 percent of the observed heads, the water level was within 0.25 m of the simulated head at that node. Only four of the observed heads were outside of two standard deviations removed, with residuals between 0.94 to 1.04 m in all. Two of these four wells are outside of the site area and do not affect interpretations near the site. Locations of the other two wells, in the recharge-discharge transition zone, indicate that local aquifer heterogeneities not accounted for in the simulation probably control heads in those areas.

Layer 2

A comparison between observed and simulated potentiometric surfaces for layer 2 is presented in figure 39. There is an excellent match of contours, with shapes virtually identical except for a few nodes near Bayou Chico in the west-central area which are probably affected by problems with the fit in layer 1. The residuals for this layer are 0.34 m, for the best fit of any layer. The match between positive and negative residuals is off more than 50 percent, however, with observed data generally greater than simulated. This is exemplified by looking at selected cross sections (fig. 40), the choice of which was

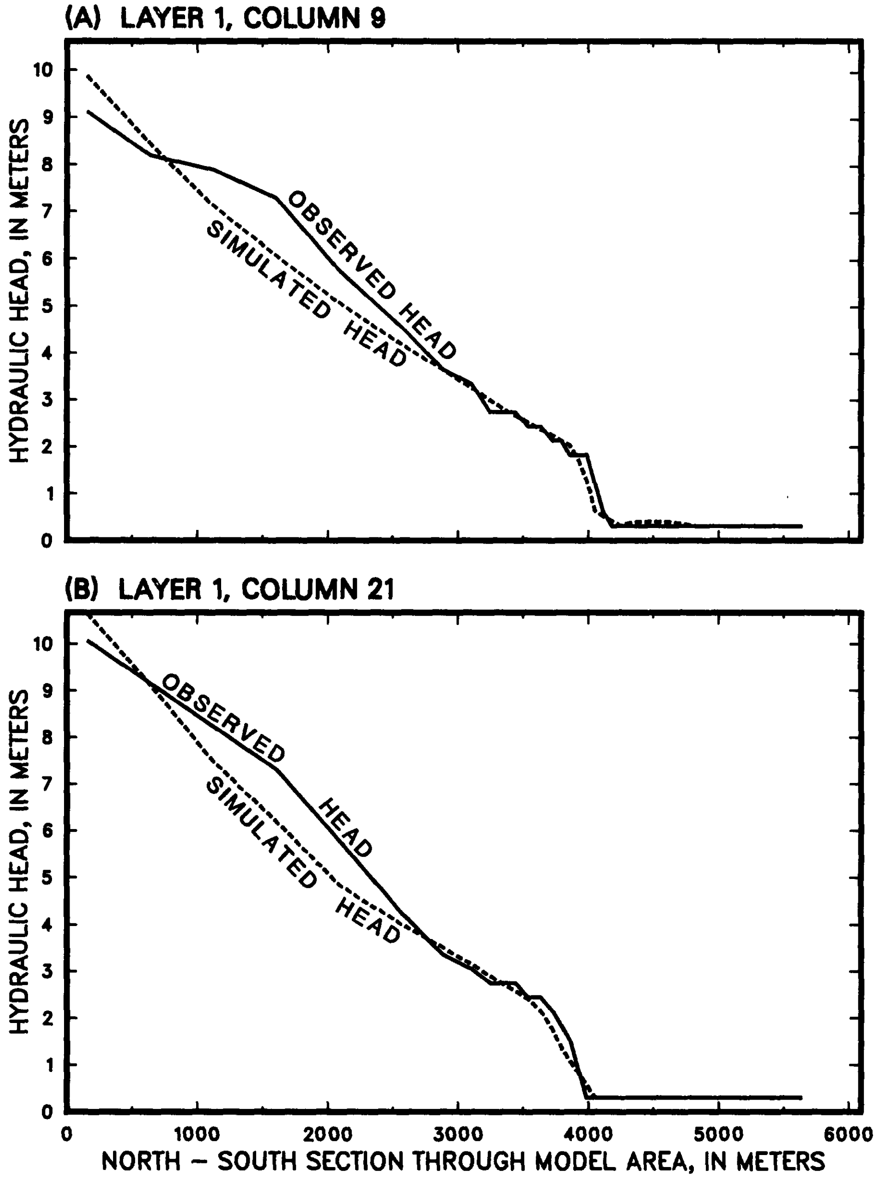

Figure 37.—North-south sections comparing observed and simulated water-level surfaces for layer 1: (a) column 9, and (b) column 21.

described for layer 1. Overall, the shape and gradient of the head surface are well reproduced, especially near the site. But simulated heads in the northern 8–10 rows, although well within the calibration criterion of 1.0 m, are uniformly lower than observed heads. Because these data are well north of the site area, and because no calibration adjustment improved the calibration without creating an even poorer fit in another parameter, the fit was accepted as part of the best calibration.

As with layer 1, an attempt was made to directly correlate observed and simulated heads in layer 2. On comparison of the 21 observed values of head available in the area of investigation with simulated heads in each node, the mean residual was 0.25 m, meeting the 0.25 m criterion. Standard deviation was 0.15 m. The data can be further evaluated by comparing observed water levels and the simulated potentiometric contours in the site area (fig. 41). The simulated water

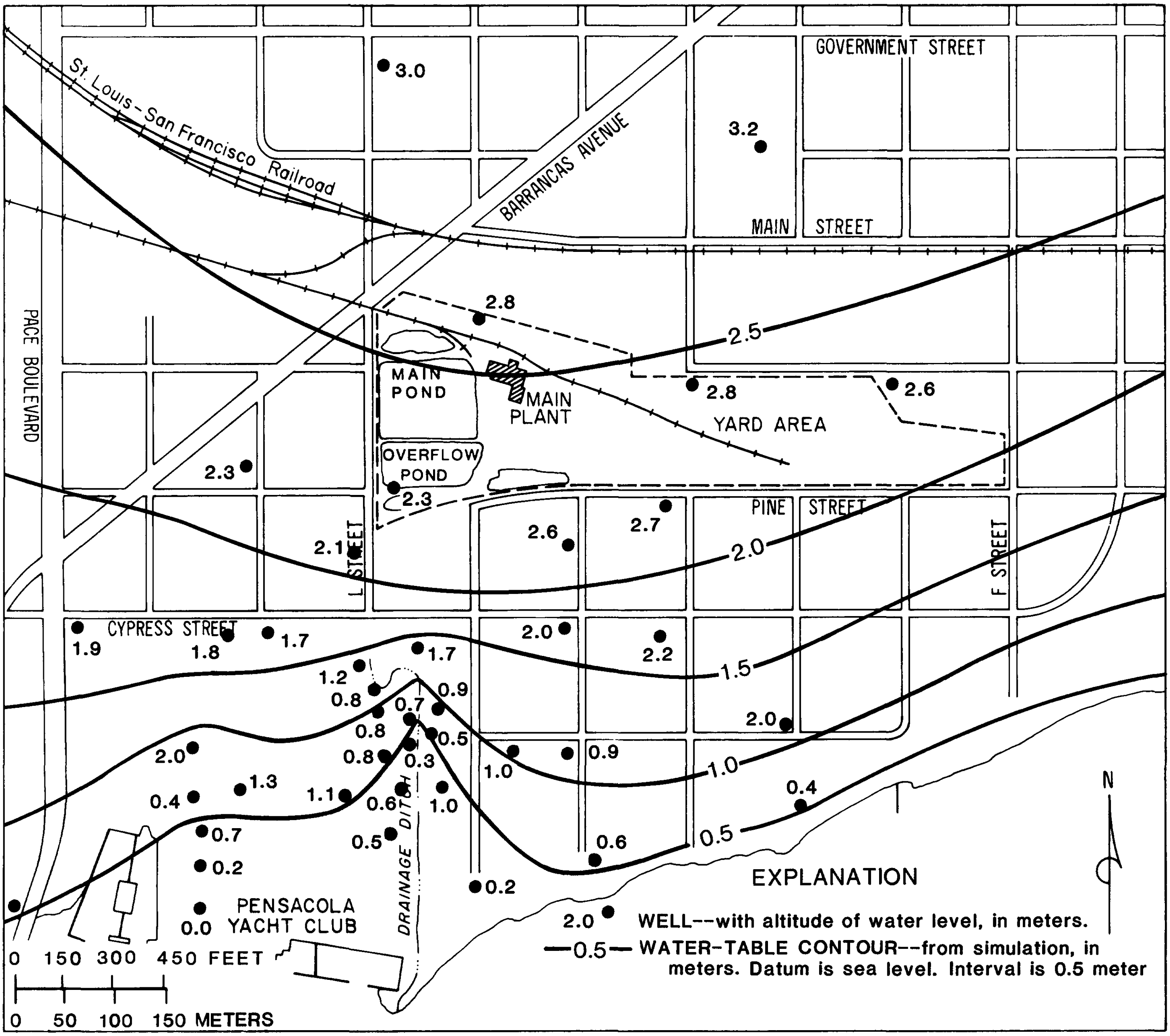

Figure 38.—Comparison between simulated water-table surface and observed water levels in layer 1, January 1986.

levels were within 0.25 m of the measured head in 83 percent of the wells, with all of the data within two standard deviations of the mean. The maximum difference of 0.55 m occurred in a well located at row 6, column 6, far north of the site area.

Layer 3

Comparison between observed and simulated potentiometric surfaces for layer 3 is shown in figure 42. In general, the contours match quite well, with the obvious exceptions of three areas of

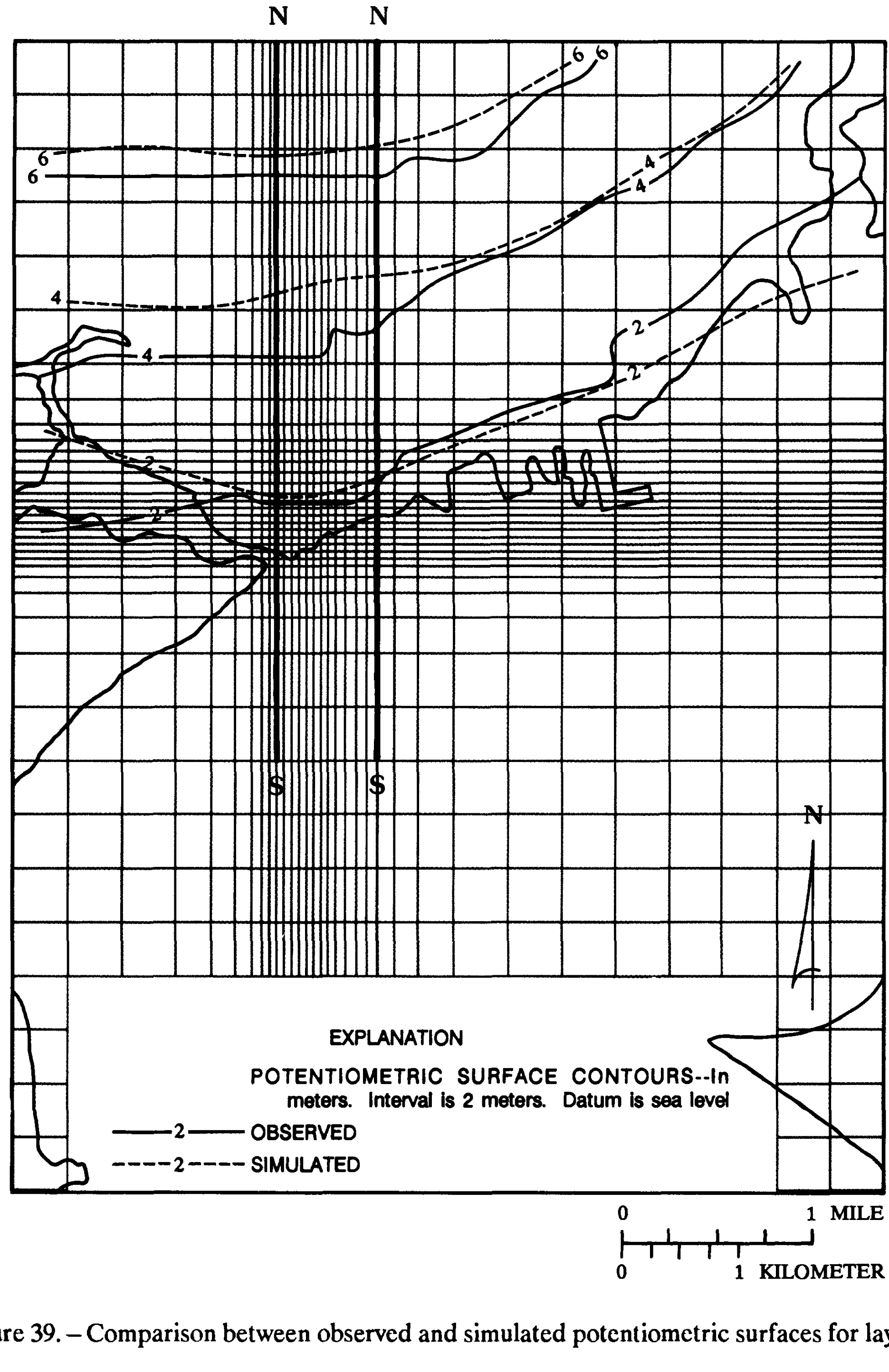

Figure 39. – Comparison between observed and simulated potentiometric surfaces for layer 2.

lower simulated heads which correspond to locations of the municipal pumping wells. The mean residual for layer 3 is 0.37 m, well within the accuracy acceptable for calibration of this layer. The match between positive and negative residuals is also excellent, within 15 percent.

Pumping from the municipal wells, although far north of the site area, was shown to be a major factor in defining the water budget for the system (fig. 35). Simulated heads in layer 3 are affected within a 1/2-mile radius about each well, which includes only two nodes in the northern parts of the

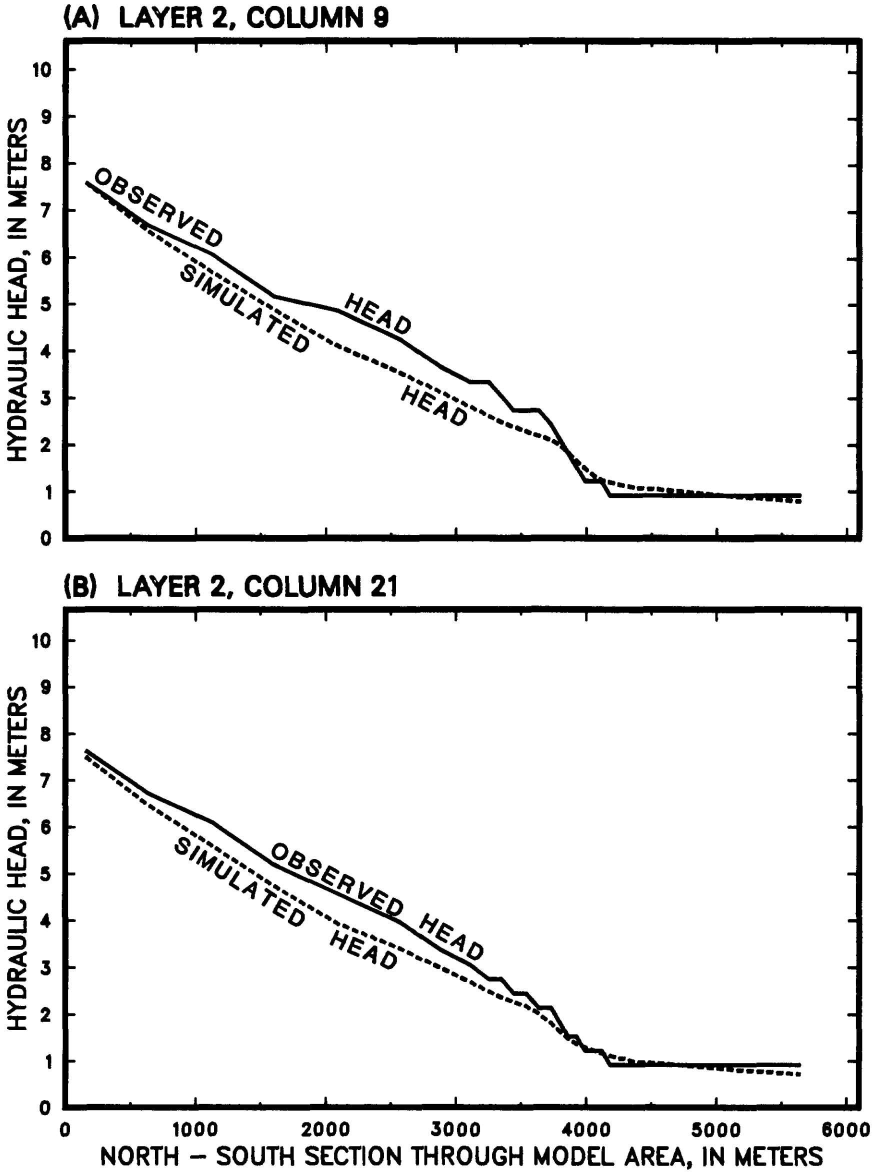

Figure 40.—North-south sections comparing observed and simulated potentiometric surfaces for layer 2: (a) column 9, and (b) column 21.

area of investigation. Because it can be shown that the effects of pumping do not affect hydraulic heads in the site area, which is far outside of the zone of influence of their individual cones of depression, the local errors in the simulated potentiometric surface were considered acceptable. It should also be observed that heads in both layers 1 and 2 show subdued reflections of the pumping effects of the municipal wells, with slightly lower heads in the nodes affected by pumping than in the surrounding nodes.

As with the other two layers, selected cross sections demonstrate the typical fit between observed and simulated surfaces (fig. 43). Simulated heads are within the calibration criterion of 1.0 m, with the hydraulic gradients reasonably well reproduced. Because understanding layer 3 was not a major objective of this investigation, these data were considered acceptable. The lower simulated water level at 2,300 m is a result of a municipal well located midway between columns 9 and 21. This section intersects part of the cone of depression of the pumping well.

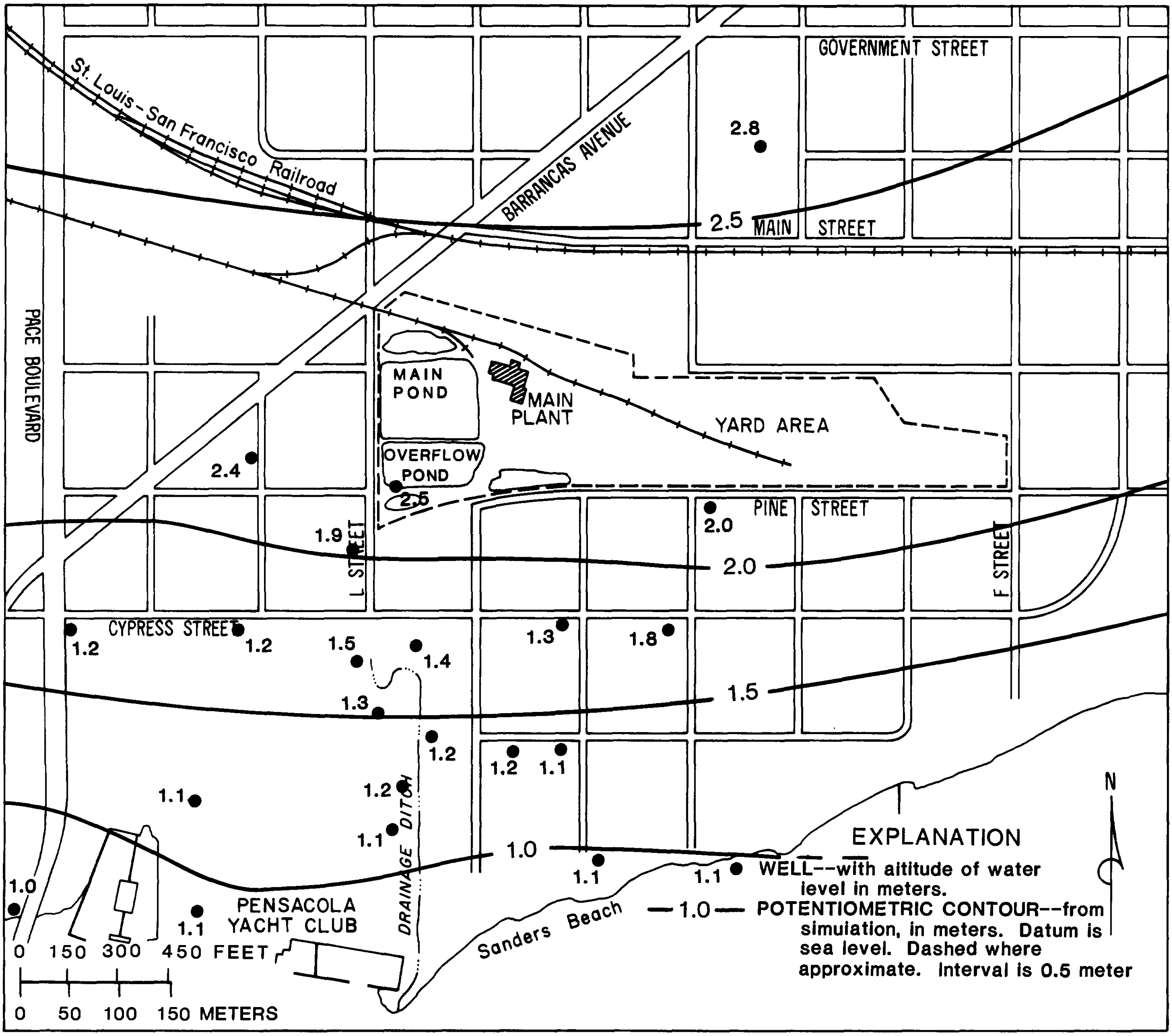

Figure 41.—Comparison between simulated potentiometric surface and observed water levels in layer 2, January 1986.

All available observed heads were compared with results of the simulation. There are only five observed values of head in the area of investigation. The mean residual at these nodes was 0.4 m, with a standard deviation of 0.21 m.

Sensitivity Analysis

The final result of model calibration is a definition of the aquifer system that incorporates the best defined hydrologic data with the adjusted estimates of the most poorly known parameters. Be-

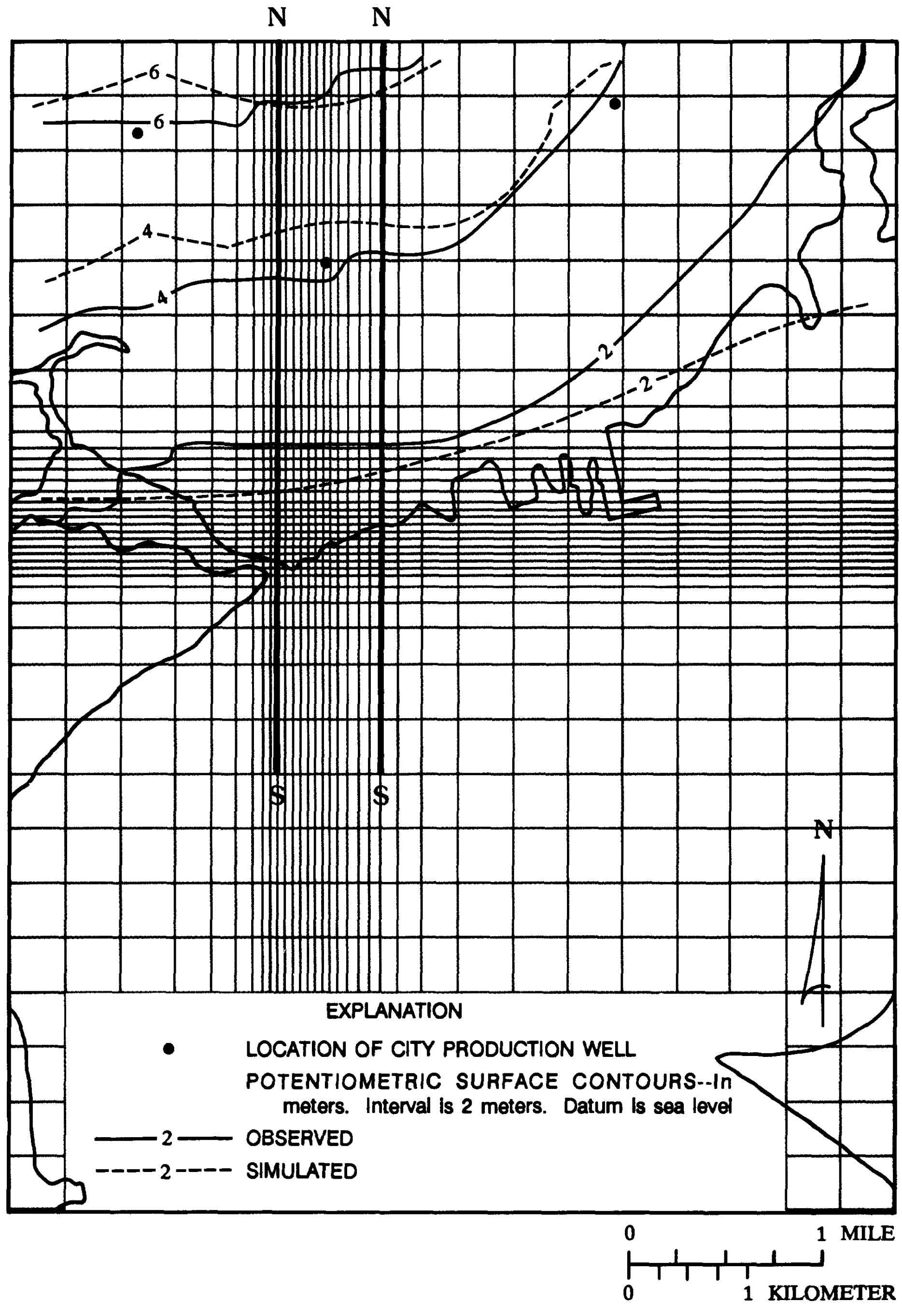

Figure 42.—Comparison between observed and simulated potentiometric surfaces for layer 3.

cause this study started with more than one poorly defined parameter, as many hydrologic investigations do, the solution is not unique. The purpose of sensitivity analysis is to determine to what degree model calibration is affected by varying each parameter over its probable range of values in an effort to ascertain that the described solution is, at minimum, reasonable for the given hydrologic variables. From sensitivity analyses, we can determine which factors have the greatest or least effect

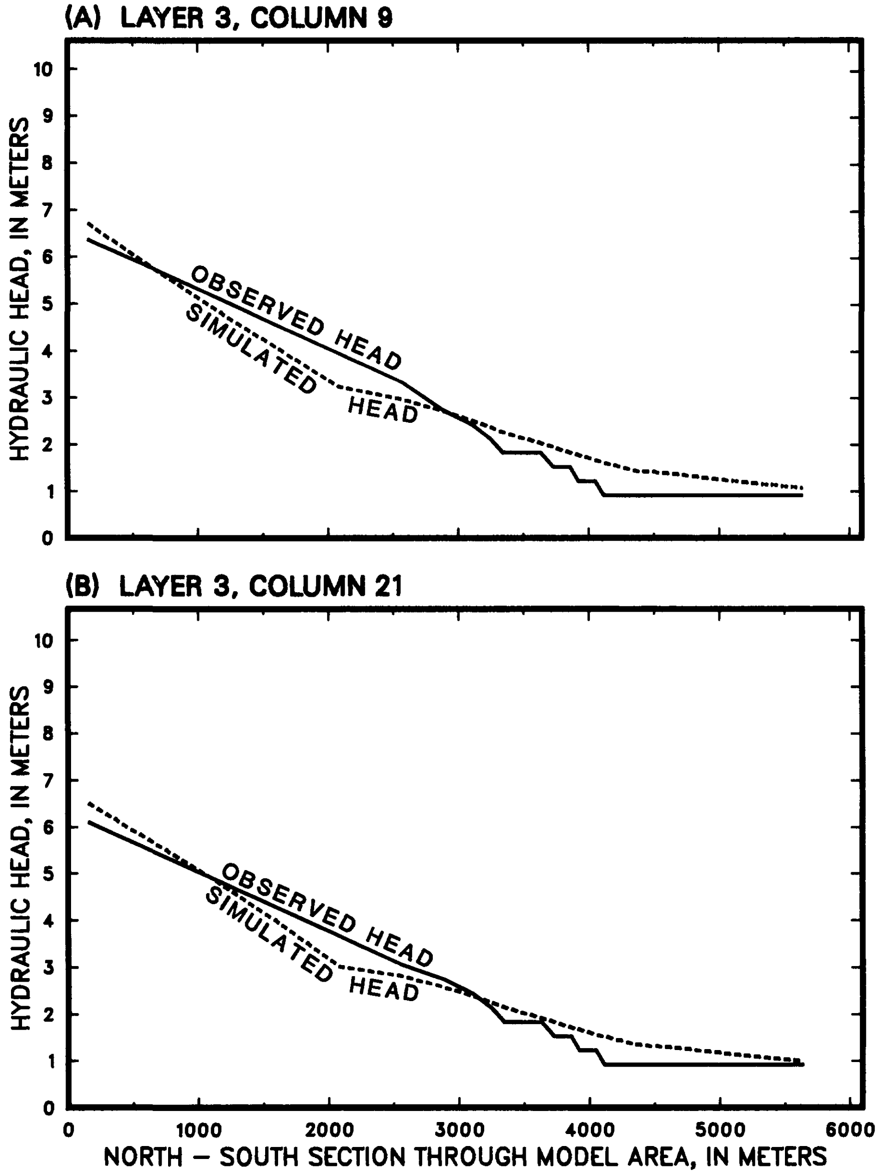

Figure 43.—North-south sections comparing observed and simulated potentiometric surfaces for layer 3: (a) column 9, and (b) column 21.

on the system. These conclusions can, in turn, help determine which data must be defined more accurately and which are already adequately defined.

One of the simplest methods of model sensitivity analysis is to uniformly vary a parameter, run the model, and observe the difference between observed and simulated head values. This technique was applied, in turn, for recharge, hydraulic conductivity of layers 1 and 2, transmissivity of layer 3, and leakance between layers 1 and 2 and also between layers 2 and 3. Beginning with the values for each parameter used to produce the best fit between observed and simulated data during the calibration process, each parameter was increased by 50 and 100 percent, and also decreased by 50 and 90 percent of the calibrated value. Leakance was also evaluated at an increase of 1,000 percent, inasmuch as its determination was more uncertain than that of any other parameter. In all cases, except perhaps leakance, the percentage changes during sensitivity analysis exceeded the range in values for the parameters based on our understanding of the hydrogeologic system. Results of these sensitivity runs are shown by graphing the average absolute error, defined as the difference between observed and simulated heads, versus the percentage change in simulated parameters, first for the composite simulated results and then for each of the three layers in turn (fig. 44).

Two general factors are obvious in looking at the plots. First, the overall maximum sensitivity of the model to reasonable adjustments of simulated parameters is less than 0.6 m (fig. 44a). This probably results from gradients in the system being quite low and fixed heads upgradient and at the seaward boundary. It is thus necessary to look at residuals in each layer as appropriate. Second, the system is primarily sensitive to changes in recharge and leakance between layers 1 and 2. Effects of these same parameters are accentuated in all three layers, with maximum effect on layer 1.

The composite plot suggests that not much information is obtained by lumping calibration data from all three model layers together. There is minimal overall sensitivity to most of the hydrologic parameters. Only recharge and leakance between layers 1 and 2 significantly affect composite statistics, although the calibrated value is at a minimum for each of the six parameters.

Layer 1, as expected, is the most affected by variations in several of the parameters (fig. 44b). Varying recharge, leakance between layers 1 and 2, and hydraulic conductivity of layer 1 all had major effects on calculated heads. Heads in layer 1, on the other hand, were fairly insensitive to changes in the other hydrologic parameters.

Recharge and leakance values were also the most significant in affecting layer 2 results (fig. 44c), although somewhat differently from layer 1. The slightly lower average absolute error at a recharge of 50 percent over the calibrated value suggests that calibration of layer 2 might be improved by increasing recharge. Based on an evaluation of the few data available for recharge and evapotranspiration in the area, calibration at a larger value for recharge was not considered. Similar analysis suggests that a slightly smaller value than the calibration value for hydraulic conductivity in layer 1 might improve the residual in layer 2. Although it was possible to slightly improve the fit in layer 2 with these changes, the overall effect on the system was minimal, as can be seen on the composite plot. Attempting these changes during calibration, however, increased the simulated heads in layer 1 and required major adjustments and recalibration of leakance and hydraulic conductivity. Consequently, the slightly larger difference in layer 2 was considered acceptable. One anomaly occurred when leakance between layers 1 and 2 was decreased 90 percent. This was the only sensitivity run for any parameter which improved heads relative to the model runs with a 50 percent decrease from calibrated data. Since field determinations of leakance are sparse, it is impossible at this time to determine a reasonable explanation for this observation.

Variations in layer 3 parameters are perhaps the most significant in evaluating the validity of the calibration, because the residuals are not distributed uniformly about the calibrated values. Contrary to the data from layer 2, a slightly lower value of recharge would appear to improve the fit of head in layer 3. Most interesting is probably the sensitivity of head in layer 3 to changes in leakance. Although the model is insensitive to increases in leakance between layers 1 and 2, it is extremely sensitive to decreases in leakance between the upper two layers. The opposite is true for leakance between layers 2 and 3. Although mildly sensitive to decreases in leakance between layers 2 and 3, heads in layer 3 are very much affected by increases in leakance between the lower two layers. These observations suggest not only that the calibrated value for recharge is a reasonable maximum but also that the gradient between the upper two layers has a significant effect on heads in layer 3.

Evaluation of Simulation Results

The purpose of three-dimensional simulations of the ground-water flow system is to improve our concept of the aquifer system and possibly to suggest alternate interpretations of the hydrogeologic picture which we have developed. This report documents our understanding of the existing hydrogeologic framework, the improved concept of the ground-water system provided by the model simulations, and inadequacies of the assumptions used in the model.

The most significant assumption is that heads in the aquifer can be considered to be under steady-state conditions and, in fact, that the

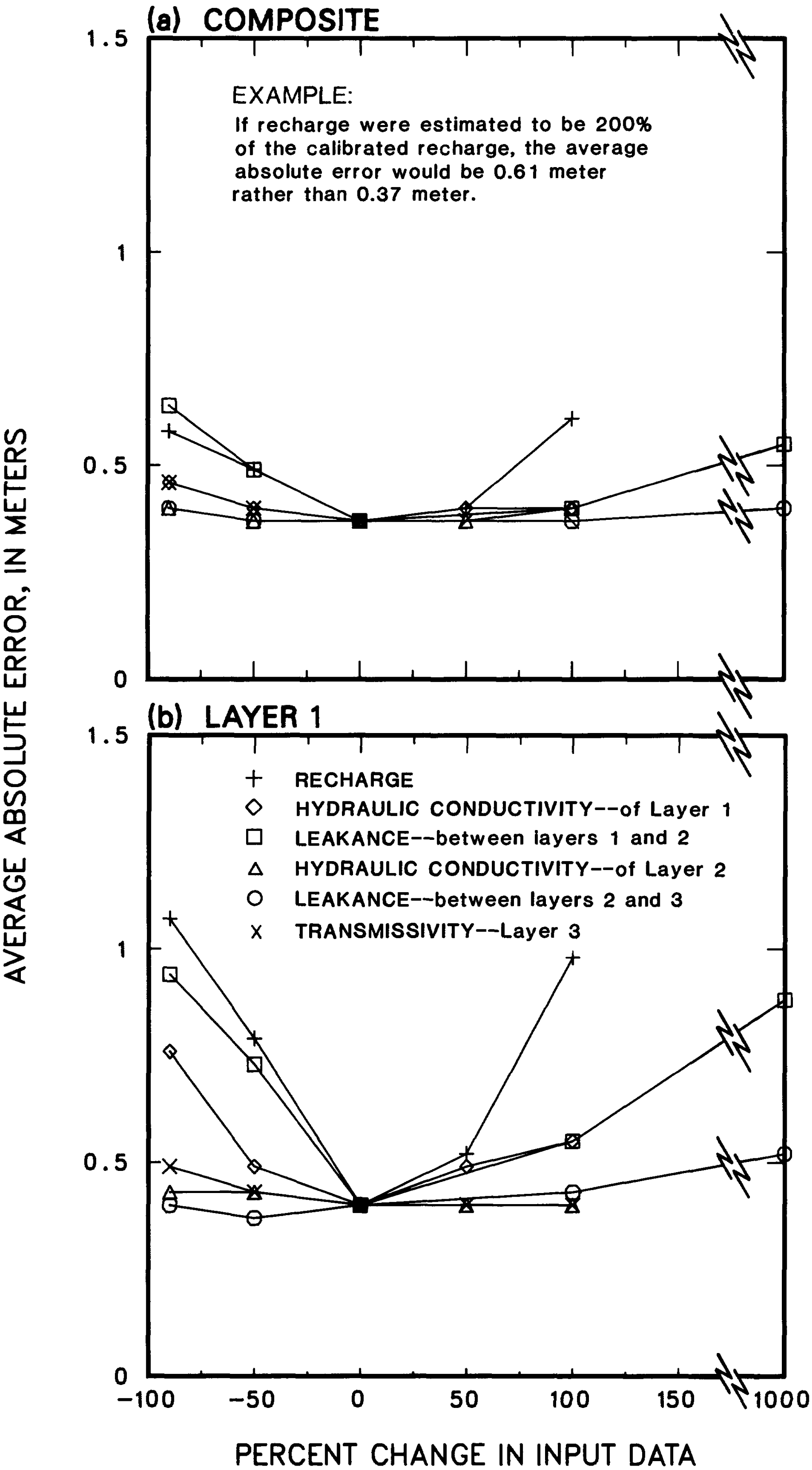

Figure 44.—Relation between average absolute error per grid block and changes in magnitude of input parameters for: (a) composite, (b) layer 1, (c) layer 2, and (d) layer 3.

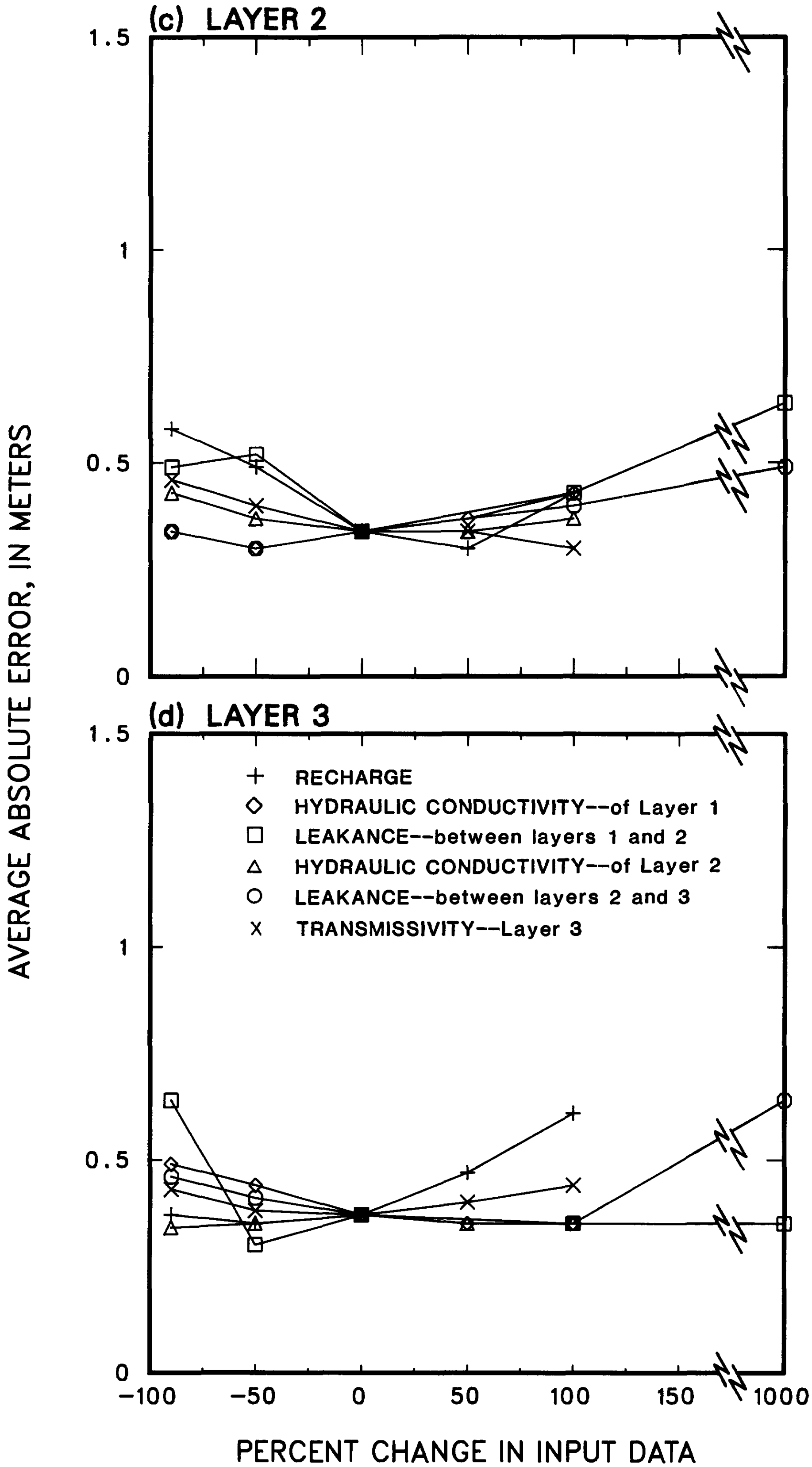

Figure 44.—Relation between average absolute error per grid block and changes in magnitude of input parameters for: (a) composite, (b) layer 1, (c) layer 2, and (d) layer 3.—Continued

January 1986 measured field values represent long-term steady-state equilibrium for the aquifer system. Earlier discussions concluded that the system is now at steady state. Water levels in layers 1 and 2 probably represent both a present-day steady-state condition and an "average" long-term steady state. Observed heads in some parts of layer 3 may not be as well represented by the assumption of steady state. Pumpage over the area of investigation has actually fluctuated considerably throughout the past 80 years, largely as a result of varying industrial and municipal pumping. For example, withdrawal rates at an industrial site near Bayou Chico have ranged from more than 30,000 m^3/d in the 1930's (Jacob and Cooper, 1940, p. 60) to the present day minimum of 1,700 m^3/d (Leach, 1984). Jacob and Cooper, in fact, conclude that extensive industrial water use was responsible for downward vertical gradients in the (normally discharge) area along the coast. It is conceivable that some of the uncertainty in the model calibration in all layers could be accounted for by transient simulations which take into account known historical variations in pumpage.

A second major uncertainty in our understanding of the aquifer involves the stated assumption that flow is only horizontal (no vertical flow) within each of the three model layers. The aquifer is three dimensional, and the model layers are a simplification of the hydrologic reality. Especially near the coast in the shallow parts of the aquifer, the vertical hydraulic gradients are steep compared to the average gradients over the area of investigation. This is especially true in layer 1 along the coast above the shallow confining clay lens separating layers 1 and 2. Also, the observation that values of vertical leakage between layers are significant implies that there must be vertical gradients of flow within each layer, at least near the contacts with adjacent layers. In other words, vertical flow is occurring locally within model layers, and may contribute significantly to errors in model calibration and sensitivity. In order to further define the effects of vertical flow, it would be necessary to subdivide the present model into more (and thinner) layers, based on increased field definition of vertical head gradients.

Another possible advantage of further discretization of the simulations into more layers involves the more general problem of aquifer heterogeneity. As summarized by Fogg (1986, p. 679), "Many so-called sandstone aquifers are actually multiple-aquifer systems consisting of discontinuous sand bodies distributed complexly in a matrix of lower-permeability silts and clays. The arrangement and interconnectedness of these various lithofacies strongly influence spatial patterns of hydraulic conductivity and, in turn, groundwater flow and mass transport." This caveat also applies equally to unconsolidated, but analogous, sand-silt-clay mixtures as found in the sand and gravel aquifer in the area of investigation. Recognizing that the heterogeneous distributions of aquifer materials will strongly affect not only fluid circulation paths and velocities but also contaminant transport in the subsurface, it is necessary to consider the fact that hydraulic head may not be very sensitive to microvariations in aquifer properties caused by varying interconnectedness. In other words, a reasonably well calibrated model of ground-water flow might poorly simulate the local velocity flow field. On this smaller scale, it would also be useful to simulate the aquifer in three dimensions with a fairly uniform density of field data to minimize interpreting results biased by lack of data in parts of the model area. The basic conclusion seems to be that if results from the calibrated three-dimensional ground-water flow model presented here are to be used in simulation of contaminant transport, it may be critical to further subdivide the contaminated area into unit dimensions capable of incorporating local details of aquifer heterogeneity. This would require both a much smaller node dimension and far more sublayers than were needed for calibration of the ground-water flow system itself.

SUMMARY AND CONCLUSIONS

Problems of ground-water contamination from leaking surface impoundments are common in surficial aquifers. As part of our understanding of the processes affecting transport of contaminants in the subsurface, it is necessary to investigate the hydrogeology and ground-water flow of such systems.

This study is part of an interdisciplinary investigation of a contaminated ground-water site in

Pensacola, Escambia County, Fla. The study site is underlain by surficial deposits of the sand and gravel aquifer, which consist of nonhomogeneous fine-to-coarse grained, locally well-sorted fluvial and deltaic sediments. The dominantly quartz sands and gravels are locally interbedded with discontinuous silt and clay lenses. The aquifer can be divided into three distinct but interconnected zones – a surficial (water-table) zone, a low-permeability intermediate zone, and a main producing zone. These generalized zones were confirmed in detail to occur in the site area.

Although the aquifer is divided into three distinct permeable zones, all zones are hydraulically interconnected. The primary sources of flow into the system are areal recharge and boundary inflow from areas upgradient of the area of investigation. A small source of flow is leakage from the impoundments in the site area into the aquifer. The principal discharge of water from the system is to Pensacola Bay and to municipal pumping wells in the northern part of the area of investigation in layer 3. A minor discharge is to the small drainage ditch in the site area. Within the aquifer, there is significant vertical leakage between zones. Water flows generally from north to south in the study area.

In order to synthesize the available hydrogeologic data, a three-dimensional ground-water flow model was developed to simulate flow in the area of investigation. Simplifying assumptions include that hydraulic heads in the aquifer can be considered to be at steady state and that the aquifer can be treated as multilayered and isotropic, with water moving only in a horizontal plane within each layer, and only vertically between layers. Layer 1 represents the surficial, water table, part of the system; layer 2 the intermediate zone; and layer 3, the deepest part of the aquifer, the main producing zone.

The ground-water flow model was calibrated for steady-state conditions as represented by January 1986 field measurements. Simulated water levels met most defined calibration criteria in successfully matching field measurements. Calibrated hydrologic parameters include recharge (28 cm/yr), hydraulic conductivity (0.3 to 23 m/d), vertical leakance ($3x10^{-4}$ to $1x10^{-3}$ (m/d)/m), and boundary inflow ($2.6x10^{4}$ m^{3}/d). Sensitivity analysis showed that the aquifer simulations were most sensitive to changes in recharge and decreases in the vertical leakance of the confining unit between layers 1 and 2, and relatively insensitive to changes in hydraulic conductivity and transmissivity and to other changes in vertical leakance. A mass balance including a water budget was calculated to quantitatively evaluate the flow system. Major inflows to the model included boundary inflow ($2.6x10^{4}$ m^{3}/d) and recharge ($1.9x10^{4}$ m^{3}/d). Major outflows from the model included discharge to Pensacola Bay ($2.1x10^{4}$ m^{3}/d) and to pumping wells ($1.8x10^{4}$ m^{3}/d).

The three-dimensional simulations were invaluable in improving our understanding of the ground-water flow system in the area of investigation. Reevaluation of our understanding of the ranges and significance of selected hydrologic parameters will be useful in further investigations of contaminant transport in the site area. Applications of the results of this calibrated flow model in evaluation of solute transport will require further subdivision of the contaminated area into much smaller grid-block dimensions and more sublayers than were needed for calibration of the ground-water flow system itself.

SELECTED REFERENCES

Barr, D.E., Maristany, Agustin, and Kwader, Thomas, 1981, Water resources of southern Okaloosa and Walton Counties, northwest Florida – Summary of investigation: Northwest Florida Water Management District Water Resources Assessment 81–1, 41 p.

Barraclough, J.T., 1967, Ground-water features in Escambia and Santa Rosa Counties, Florida: Florida Division of Geology Map Series 26, 1 sheet.

Barraclough, J.T., and Marsh, O.T., 1962, Aquifers and quality of ground water along the Gulf Coast of western Florida: Florida Geological Survey Report of Investigations 29, 28 p.

Bodine, M.W., Jr., in press, Clay mineralogy of sediments associated with a plume of creosote-contaminated ground water, *in* Ragone, S.E., ed., U.S. Geological Survey Toxic Waste – Ground-Water Contamination Program – Fiscal Year 1986: Program overview and selected abstracts presented at the Toxic Waste Program technical meeting, Cape Cod, Mass., October 21–25, 1985: U.S. Geological Survey Open-File Report 86–481.

Camp, Dresser, and McKee, Inc., 1983, Remedial action master plan for the American Creosote Works, Inc., site: Prepared for the U.S. Environmental Protection Agency, Project no. W–54936.A2.

Cushman-Roisin, Mary, and Franks, B.J., 1982, Sand-and-gravel aquifer, *in* Franks, B.J., ed., Principal aquifers in Florida: U.S. Geological Survey Water-Resources Investigations Open-File Report 82–255, 4 sheets.

Dohrenweld, R.E., 1976, A first order evaluation of evapotranspiration patterns in the State of Florida: Gainesville, University of Florida, School of Forest Resources and Conservation Evapotranspiration Map 15.

Dysart, J.E., Pascale, C.E., and Trapp, Henry, Jr., 1977, Water resources inventory of northwest Florida: U.S. Geological Survey Water-Resources Investigation 77–84, 114 p.

Ecology and Environment, Inc., 1986, Assessment of the remedial investigation and draft feasibility for the American Creosote Works site, Pensacola, Florida: Prepared for Florida Department of Environmental Regulation, Tallahassee, Fla.

Fogg, G.E., 1986, Groundwater flow and sand body interconnectedness in a thick, multiple aquifer system: Water Resources Research, v. 22, no. 5, p. 679–694.

Franks, B.J., ed., 1987, U.S. Geological Survey Program on Toxic Waste—Ground-Water Contamination: Proceedings of the third technical meeting, Pensacola, Florida, March 23–27, 1987: U.S. Geological Survey Open-File Report 87–109, 226 p.

Franks, B.J., Goerlitz, D.F., and Baedecker, M.J., 1986, Defining a contaminant plume using on-site analytical techniques, *in* Petroleum hydrocarbons and organic chemicals in ground water: Prevention, detection, restoration (Second annual conference, November 1985, Houston, Tex.).

Goerlitz, D.F., Troutman, D.E., Godsy, E.M., and Franks, B.J., 1985, Migration of wood-preserving chemicals in contaminated ground water in a sand aquifer at Pensacola, Florida: Environmental Science and Technology, v. 19, no. 10, p. 955–961.

Heath, R.C., and Clark, W.E., 1951, Potential yield of ground water on the Fair Point Peninsula, Santa Rosa County, Florida: Florida Geological Survey Report of Investigations 7, 56 p.

Hughes, G.H., 1978, Runoff from hydrologic units in Florida: Florida Bureau of Geology Map Series 81, 1 sheet.

Jacob, C.E., and Cooper, H.H., Jr., 1940, Report on the ground-water resources of the Pensacola area in Escambia County, Florida: U.S. Geological Survey Open-File Report FL–40001, 89 p.

Leach, S.D., 1984, Projected public supply and rural water use in Florida through year 2020: Florida Bureau of Geology Map Series 108, 1 sheet.

MacFarlane, D.S., Cherry, J.A., Gillham, R.W., and Sudicky, E.A., 1983, Migration of contaminants in ground water at a landfill: a case study—1. Groundwater flow and plume delineation: Journal of Hydrology, v. 63, p. 1–29.

Marsh, O.T., 1966, Geology of Escambia and Santa Rosa Counties, western Florida Panhandle: Florida Division of Geology Bulletin 46, 140 p.

Matson, G.C., and Sanford, Samuel, 1913, Geology and ground waters of Florida: U.S. Geological Survey Water-Supply Paper 319, 445 p.

Mattraw, H.C., Jr., and Franks, B.J., eds., 1986, Movement and fate of creosote waste in ground water, Pensacola, Florida: U.S. Geological Survey Toxic Waste—Ground-water Contamination Program: U.S. Geological Survey Water-Supply Paper 2285, 63 p.

McDonald, M.G., and Harbaugh, A.W., 1984, A modular three-dimensional finite-difference ground-water model: U.S. Geological Survey Open-File Report 83–875, 528 p.

Musgrove, R.H., Barraclough, J.R., and Grantham, R.G., 1965, Water-resources of Escambia and Santa Rosa Counties, Florida: Florida Geological Survey Report of Investigations 40, 102 p.

– – –1966, Water-resources records of Escambia and Santa Rosa Counties, Florida: Florida Geological Survey Information Circular 50, 106 p.

Musgrove, R.H., Barraclough, J.T., and Marsh, O.T., 1961, Interim report on the water resources of Escambia and Santa Rosa Counties, Florida: Florida Geological Survey Information Circular 30, 89 p.

National Oceanic and Atmospheric Administration, 1982, Monthly normals of temperature, precipitation, and heating and cooling degree days 1951–80, Florida: Climatography of the United States no. 81, 14 p.

NUS Corporation, 1984, Remedial investigation report, American Creosote Works, Inc., site, Pensacola, Florida: Prepared for the U.S. Environmental Protection Agency, Work assignment no. 30-4L45, Contract no. 68-01-6699, 2 volumes.

– – –1985, Feasibility study of alternatives, American Creosote Works, Inc., site, Pensacola, Florida: Prepared for the U.S. Environmental Protection Agency, Work assignment no. 30–4L45, Contract no. 68–01–6699.

Olhoeft, G.R., 1986, Toxic waste geophysics: Proceedings of the American Society for Testing Materials Annual Meeting, February 1986.

Ragone, S.E., ed., in press, U.S. Geological Survey Toxic Waste – Ground-water Contamination Program – Fiscal Year 1986: Program overview and selected abstracts presented at the Toxic Waste Program technical meeting, Cape Cod, Mass., October 21–25, 1985: U.S. Geological Survey Open-File Report 86–481.

Trapp, Henry, Jr., 1972, Availability of ground water for public-water supply in the Pensacola area, Florida: U.S. Geological Survey Open-File Report 72002, 56 p.

– – –1973, Availability of ground water in central and southern Escambia County, Florida, Interim Report, July 1972: U.S. Geological Survey Open-File Report 72029, 40 p.

– – –1975, Hydrology of the sand-and-gravel aquifer in central and southern Escambia County, Florida: U.S. Geological Survey Open-File Report 74027, 37 p.

– – –1978, Preliminary hydrologic budget of the sand-and-gravel aquifer under unstressed conditions, with a section on water-quality monitoring, Pensacola, Florida: U.S. Geological Survey Water-Resources Investigations 77–96, 57 p.

Trapp, Henry, Jr., and Geiger, L.H., 1986, Three-dimensional steady-state simulation of flow in the sand-and-gravel aquifer, southern Escambia County, Florida: U.S. Geological Survey Water-Resources Investigations 85–4278, 149 p.

Troutman, D.E., Godsy, E.M., Goerlitz, D.F., and Ehrlich, G.G., 1984, Phenolic contamination in the sand-and-gravel aquifer from a surface impoundment of wood treatment wastes, Pensacola, Florida: Region IV, Environmental Services Division, Project no. 83–016.

U.S. Department of Agriculture, 1981, The biologic and economic assessment of pentachlorophenol, inorganic arsenicals, creosote, Volume 1, Wood preservatives: U.S. Department of Agriculture Technical Bulletin 1658–I, 435 p.

U.S. Environmental Protection Agency, 1983, Hazardous waste site investigation, American Creosote Works, Inc., Pensacola, Florida: Region IV, Environmental Services Division, Project no. 83–016.

U.S. Geological Survey, 1975, Hydrology of the sand and gravel aquifer in central and southern Escambia County: U.S. Geological Survey Professional Paper 975, p. 91.

———1979, Geological Survey Research 1979: U.S. Geological Survey Professional Paper 1150, p. 114.

Visher, F.N., and Hughes, G.H., 1975 (2d ed.), The difference between rainfall and potential evaporation in Florida: Florida Bureau of Geology Map Series 32, 1 sheet.

von Rumker, Rosmarie, Lawless, E.W., and Meiners, A.F., 1975, Production, distribution, and environmental impact potential of selected pesticides: U.S. Environmental Protection Agency EPA 540/1-74-001, 439 p.

Wilkins, K.T., Wagner, J.R., and Allen T.W., 1985, Hydrogeologic data for the sand-and-gravel aquifer in southern Escambia County, Florida: Northwest Florida Water Management District Technical File Report 85-2, 153 p.

☆U.S. GOVERNMENT PRINTING OFFICE: 1988-530-101/ 80005